

12-1-2013

Criticality and Characteristic Neutronic Analysis of a Transient-State Shockwave in a Pulsed Spherical Gaseous Uranium-Hexafluoride Reactor

Jeremiah Boles

University of Nevada, Las Vegas, jtboles2010@gmail.com

Follow this and additional works at: <https://digitalscholarship.unlv.edu/thesesdissertations>



Part of the [Nuclear Commons](#), [Nuclear Engineering Commons](#), and the [Oil, Gas, and Energy Commons](#)

Repository Citation

Boles, Jeremiah, "Criticality and Characteristic Neutronic Analysis of a Transient-State Shockwave in a Pulsed Spherical Gaseous Uranium-Hexafluoride Reactor" (2013). *UNLV Theses, Dissertations, Professional Papers, and Capstones*. 1977.

<https://digitalscholarship.unlv.edu/thesesdissertations/1977>

This Thesis is protected by copyright and/or related rights. It has been brought to you by Digital Scholarship@UNLV with permission from the rights-holder(s). You are free to use this Thesis in any way that is permitted by the copyright and related rights legislation that applies to your use. For other uses you need to obtain permission from the rights-holder(s) directly, unless additional rights are indicated by a Creative Commons license in the record and/or on the work itself.

This Thesis has been accepted for inclusion in UNLV Theses, Dissertations, Professional Papers, and Capstones by an authorized administrator of Digital Scholarship@UNLV. For more information, please contact digitalscholarship@unlv.edu.

CRITICALITY AND CHARACTERISTIC NEUTRONIC ANALYSIS OF A
TRANSIENT-STATE SHOCKWAVE IN A PULSED SPHERICAL GASEOUS
URANIUM-HEXAFLUORIDE REACTOR

By

Jeremiah Thomas Boles

Bachelors of Science in Mechanical Engineering

University of Nevada, Las Vegas

2012

A thesis submitted in partial fulfillment
of the requirements for the

Masters of Science - Materials and Nuclear Engineering

Department of Mechanical Engineering

Howard R. Hughes College of Engineering

The Graduate College

University of Nevada, Las Vegas

December 2013



THE GRADUATE COLLEGE

We recommend the thesis prepared under our supervision by

Jeremiah Boles

entitled

Criticality and Characteristic Neutronic Analysis of a Transient-State Shockwave in a Pulsed Spherical Gaseous Uranium-Hexafluoride Reactor

is approved in partial fulfillment of the requirements for the degree of

**Master of Science - Materials and Nuclear Engineering
Department of Mechanical Engineering**

William G. Culbreth, Ph.D., Committee Chair

Charlotta E. Sanders, Ph.D., Committee Member

Alexander Barzilov, Ph.D., Committee Member

Hualiang Teng, Ph.D., Graduate College Representative

Kathryn Hausbeck Korgan, Ph.D., Interim Dean of the Graduate College

December 2013

ABSTRACT

The purpose of this study is to analyze the theoretical criticality of a spherical uranium-hexafluoride reactor with a transient, pulsed shockwave emanating from the center of the sphere in an outward-radial direction. This novel nuclear reactor design, based upon pulsed fission in a spherical enclosure is proposed for possible use in direct energy conversion, where the energy from fission products is captured through the use of electrostatic fields or through induction. An analysis of the dynamic behavior of the shockwave in this reactor is the subject of this thesis. As a shockwave travels through a fluid medium, the characteristics of the medium will change across the shockwave boundary. Pressure, temperature, and density are all affected by the shockwave. Changes in these parameters will affect the neutronic characteristics of a fissile medium. If the system is initially in a subcritical state, the increases in pressure, temperature, and density, all brought about by the introduction of the shockwave, will increase the reactivity of the nuclear system, creating a brief super critical state that will return to a subcritical state after the shockwave dissipates.

Two major problems are required to be solved for this system. One is the effects of the shockwave on the gas, and the second is the resulting effects on system criticality. These problems are coupled due to the unique nature of the speed of the expanding shockwave in the uranium-hexafluoride medium and the energy imparted to the system by the shockwave with respect to the fissile uranium-hexafluoride. Using compressible flow and shockwave theories, this study determines the properties of the gaseous medium for reference points before, during, and behind the shockwave as it passes through the fissile medium. These properties include pressure changes, temperature changes, and density changes that occur to the system. Using the parameters calculated from the

shockwave, the neutron transport equation is solved with the appropriate boundary conditions to identify system criticality, neutron flux, and the appropriate changes to system variables such as buckling, and migration length. The analytical solution is then verified using MCNPX, a Monte Carlo method for computational analysis of the neutron transport equation. Through manipulation of the initial pressure of the system, which is intrinsically linked to the density of the system by the ideal gas Equation of State, neutron and flux multiplication trends are corroborated.

The results show that both compressible flow theory and shockwave theory are in relatively close agreement for parameter changes across, after, and along the shockwave expansion. The solution to the analytical transport equation is in good agreement with the results from MCNPX. The change in the effective multiplication factor is similar between both the analytical solution and the computational solution. Furthermore, a new method for determining the transient effective multiplication factor is devised. These results show the maximum criticality of the reactor is at the initiation of the shockwave. The shockwave creates a local supercriticality until the wave dissipates below Mach 1.

Several tools and methods are employed in this study, including the use of Monte Carlo numerical methods, Euler method solutions, and computer programs, such as MCNP, MATLAB, and Mathcad, which provide necessary the necessary computational abilities to understand the mathematical model of the system.

ACKNOWLEDGMENTS

The spherical shockwave reactor has been a subject of great interest to me for the better part of the last 2 years. After the idea was originally proposed, I immediately saw the potential in a unique and novel idea such as this. To me personally, this concept has the ability to be a breakthrough concept and push the bounds of nuclear science and engineering back into a realm of social and publically favorable research.

I would like to thank Dr. Bill Culbreth, my advisor for this thesis and one of the few individuals who has inspired me to push back against the conventional thought of making money and to instead pursue my wildest aspirations. You have helped guide me through some of the more difficult mathematics I have ever seen, and what's more, I always learn something new and I never feel intimidated or bothered when asking for help. It has been a true delight to listen to some of your quirky anecdotes on a range of issues beyond the classroom, from politics to social media. Even in those off-topic asides, you still managed to relate everything back to the subject at hand. As my advisor on this project, every meeting would leave me wanting to spend more time on the project and to make it become a reality. Thus, for the inspiration to follow my dream and push myself beyond what I thought I was capable of, I thank you.

I would also like to thank Dr. Charlotta Sanders and Dr. Denis Beller. As the leaders of the Nuclear Criticality Safety Engineering program, I would not be writing this paper without their guidance, mentorship, and friendship. To Dr. Beller, who placed his faith in me as a graduate research assistant, I owe a debt of gratitude for your guidance and mentorship as I learned about MCNP and the practicalities of real world nuclear engineering. To Dr. Sanders, I will always appreciate your friendship and support to help

make nuclear criticality a common phrase in my vernacular. Additionally, the academic opportunities you have presented to me have brought a wealth of joy and pride, as well as a little angst, into my wonderful experience at UNLV. To both of you, I thank you and if there is ever any help I can give to you guys, it would be my honor.

Finally, to my dearest Tracy, you have stuck by my side for better and worse. You have witnessed the good, the bad, and sometimes the downright ugly sides of me through the college experience. Without you, this degree, this research, and my overall success for the past 6 years would not have been possible. It is on your strengths of dedication and support that I have stood and I look forward to returning that same level of dedication and support. I will always love you.

TABLE OF CONTENTS

ABSTRACT	iii
ACKNOWLEDGMENTS	v
TABLE OF CONTENTS.....	vii
LIST OF TABLES	ix
LIST OF FIGURES	x
CHAPTER 1 – INTRODUCTION.....	1
Why Do We Need Nuclear Power?.....	4
CHAPTER 2 – REVIEW OF PREVIOUS WORK	7
CHAPTER 3 – THEORETICAL REVIEW	10
The Theory of Fission.....	10
Nuclear Criticality (The Chain Reaction)	13
Criticality Controls	18
Compressible Flow	19
Shockwaves and Explosive Events	23
Proposed Reactor Design.....	26
CHAPTER 4 – METHODOLOGY	31
Transport Theory	31
Monte Carlo N-Particle Transport Code.....	36
CHAPTER 5 – REACTOR ANALYSIS.....	40
Analysis of Compressible Flow versus Shockwave Theory	40
One-Group Theory (Steady State) Analytical Analysis	41
Transient Reactor Analysis via MCNPX.....	44

Spherical Shockwave Reactor Parameter Analysis	48
MCNPX Input Decks	52
CHAPTER 6 – RESULTS	55
Compressible Flow Results	55
Shockwave and Explosive Events Results	61
Analytical Neutron Transport Results	64
MCNPX Results	71
Variation of Parameters	76
Design Cost	81
CHAPTER 7 – CONCLUSIONS	84
Final Reactor Design as Proposed	84
Summary of Results	86
Recommendations for Future Work	91
APPENDIX	93
MATLAB Results	93
Mathcad Results	99
Numerical Results	111
Example Input File	117
Example Output File	121
Schematics	143
WORKS CITED	146
CURRICULUM VITAE	149

LIST OF TABLES

Table 1 - Binding Energy and Critical Energy of Fissions	12
Table 2 - Selected Isotope Cross Sections (Korea Atomic Energy Research Institute (KAERI)).....	15
Table 3 - List of Materials and Functions in Spherical Gaseous Shockwave Reactor Design.....	30
Table 4 - Energy Bins for use in MCNPX Computational Analysis.....	46
Table 5 - Temperature Library Profile for MCNPX Input Cards	54
Table 6 - Atomic Weights of Atoms, Isotopes, Molecules, and Mixture	55
Table 7 - Specific Heats of the Reactor Medium Components.....	55
Table 8 - Additional Constants and Initial Derived Parameters	55
Table 9 - Composition Parameters for Nuclear Variable Determinations.....	64
Table 10 - Atomic Number Densities Corresponding to Composition Paramaters	64
Table 11 - Microscopic Cross-Section Data from ENDF/B Nuclear Data Library	65
Table 12 - Calculated Macroscopic Cross-Sections for UF ₆	65
Table 13 - Material Constants in Undisturbed Region of the Reactor Medium	65
Table 14 - Calculation of k_{inf} for the Reactor Medium in an Undisturbed State	66
Table 15 - Criticality Value with Standard Deviation as Determined in MCNPX	72
Table 16 - Select Values to the Computational Solution to Transient Region M^{\wedge}	73

LIST OF FIGURES

Figure 1 - Spherical Gaseous Shockwave Reactor Problem.....	1
Figure 2 - Simple Fission Chain Reaction for Uranium-235	13
Figure 3 - Explosive Shockwave Event.....	23
Figure 4 - Schematic of Spherical Gaseous Shockwave Reactor.....	30
Figure 5 - Single-Parameter Limit Curve for ²³⁵ U Metal-Water Mixtures.....	52
Figure 6 - Shockwave Mach Number in an Infinite Reactor Medium	56
Figure 7 - Maximum Shockwave Density in an Infinite Reactor Medium	57
Figure 8 - Maximum Shockwave Pressure in an Infinite Reactor Medium	57
Figure 9 - Shockwave Radius and Shockwave Speeds in an Infinite Reactor Medium....	58
Figure 10 - Actual Shockwave Mach Number in the Reactor Medium	59
Figure 11 - Maximum Shockwave Density in the Reactor Medium as Bounded by Mach Number.....	59
Figure 12 - Maximum Shockwave Pressure in the Reactor Medium as Bounded by Mach Number.....	60
Figure 13 - Actual Radius of Shockwave Expansion in the Reactor Medium as Bounded by Mach Number	60
Figure 14 - Non-Dimensional Shockwave Curves as Determined for an Arbitrary Shockwave Radius (R).....	62
Figure 15 - Maximum Shockwave Pressure as Determined by Taylor Similarity Methods	63
Figure 16 - Diffusion Constant (D) within the Transient Reactor Region	67
Figure 17 - Diffusion Length (L) within the Transient Reactor Region	67

Figure 18 - Material Buckling (B_m^2) within the Transient Reactor Region.....	68
Figure 19 - Migration Length (M^2) within the Transient Reactor Region.....	68
Figure 20 - Analytical Solution to Transient Region k_{eff}	69
Figure 21 - Neutron Flux in the Undisturbed Region of the Reactor Medium.....	70
Figure 22 - Neutron Flux in the Transient Region of the Reactor Medium	70
Figure 23 - Computational Solution to Transient Region M^{\wedge}	73
Figure 24 - Local Shockwave M^* as a Function of Radius	74
Figure 25 - Cellular Flux by Track Length as Determined by MCNPX for Radial-Time Steps by Energy Bin	75
Figure 26 - Contoured Results for k_{eff} for the Undisturbed Reactor Configuration Analyzing Enrichment and Concentration	76
Figure 27 - Variation of Nominal k_{eff} Based on Changes in Pressure.....	77
Figure 28 - Variation of Nominal k_{eff} Based on Changes in Concentration.....	78
Figure 29 - Computational Solution to Transient Region M^{\wedge} for Nominal Atmospheric Reactor Pressure	79
Figure 30 - Shockwave M^* as a Function of Radius for Nominal Atmospheric Reactor Pressure	80
Figure 31 - Cellular Flux by Track Length as Determined by MCNPX for Radial-Time Steps by Energy Bin for Nominal Atmospheric Reactor Pressure	81
Figure 32 - SWU Cost Curve Results for Enrichment of UF_6	82
Figure 33 - Final Design of the Transient-State Pulsed Spherical Uranium-Hexafluoride Reactor	86

CHAPTER 1 – INTRODUCTION

In recent years, America has been clamoring for a new, clean, and green energy resource. The spherical gaseous shockwave reactor analysis in this study proposes to fill this need and provide a new direction for energy research and investigation for the near and foreseeable future. The physics of this reactor proposal are complex as shown in Fig. 1.

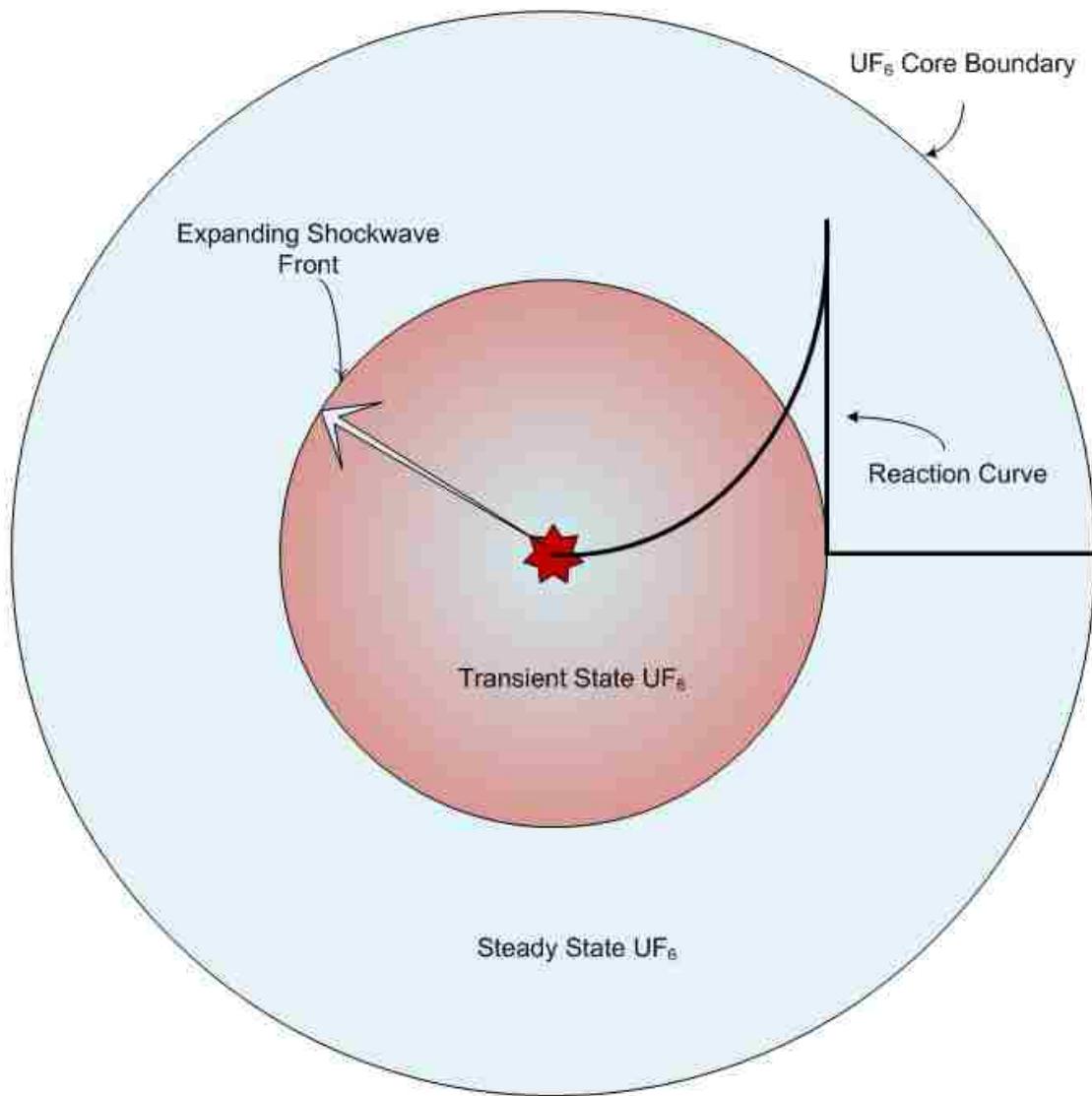


Figure 1 - Spherical Gaseous Shockwave Reactor Problem

The history of atomic science has traditionally focused on two applications of nuclear physics; control of atomic reactions or creating as large of a reaction as possible. The latter is obviously the study of atomic weapons, but the former is a well-studied problem in engineering and the basic concept of all nuclear power plants. The concept of using heat energy to create useful work is also a well-studied engineering problem. In 1823, Nicolas Lèonard Sadi Carnot derived the limitations for the maximum amount of useful work that can be converted from heat energy. This ceiling is known as the Carnot Cycle. The basis for this ceiling is the minimum and maximum temperature reservoirs that exist in the system. Mathematically, the amount of useful work that can be achieved is determined from (Cengel and Boles):

$$W = \oint PdV = (T_H - T_C)(S_B - S_A) \quad [1-1]$$

where S_B and S_A represent the maximum and minimum system entropies, respectively, and T_H and T_C represent the maximum and minimum temperature reservoirs, respectively.

This limit has plagued the nuclear power industry for decades because most nuclear power operations are not trying to actively create new temperature reservoirs, but rather push the boundaries of the existing temperature reservoirs and the efficiency of conversion equipment. While optimization of currently existing systems is a necessary and remarkable achievement, new systems should look for ways to circumvent the limitations of the Carnot cycle. Direct energy conversion is one of these ways. Energy does not exist in a single form; thus, instead of using heat energy converted to useful work, kinetic energy can be used for useful energy conversions. The basis for the gaseous spherical shockwave reactor presented in this study is the utilization of fission kinetic

energy to induce a voltage potential and flow of electrons to produce electricity. By scaling the size of a reactor to create a system that employs direct energy conversion, many extraneous systems that are found in current systems can be removed. Systems such as turbine loops and tertiary cooling loops would have no useful meaning in a direct energy conversion system. This presents another opportunity; a reactor of the size presented in this study, without copious extra systems coupled to it, could be used to create small modular power stations or power generators. Given the size of the atom, the number of atoms with kinetic energy in a system like this is sufficiently large to make theoretical sense.

A direct energy conversion reactor, such as the one proposed herewithin can have a multitude of applications. One such application could be the generation of electricity for deep space missions. Solar powered craft, such as the Martian rovers *Spirit* and *Opportunity*, or the *Juno* spacecraft that recently launched in 2011 to study Jupiter, have an effective limit to the distance they can travel into the solar system. A spacecraft powered with a spherical pulsed reactor could create electricity for the expected lifetime of the craft and still provide enough power to run all of the vital scientific instrumentation that will be aboard. Closer to home, a reactor of this type would be invaluable for remote research locations such as polar explorations or deep jungle investigations. One user group that could benefit tremendously from this vital research would be the military. Our fighting forces are often required to travel to locations without utility infrastructure support and survive for extended periods. Given the dependency of today's technology on electricity, these reactor systems would require only a handful of people to operate or maintain and could greatly contribute to a reduction of fuel resupplies that are common

with current fossil fuel based generators. This could save both human lives and machinery in hostile combat situations. Finally, the general public is one of the largest consumers of electrical energy. The mobility of American society and commerce is intrinsically linked to our economic power. If a single reactor is configured to power a vehicle, the results could be extraordinary in terms of impact on the amount of non-renewable imports that are consumed each year.

Why Do We Need Nuclear Power?

Atomic interactions are one of the fundamental natural interactions between matter in the universe. Stars utilize fusion in order to create heavier isotopes and ions as well as a host of other particles. These particles interact to form molecules and compounds, and eventually the macroscopic life that we see around us today. Some of the macroscopic universe that we see today, however, is unstable. Very heavy metals are unstable due to their large atomic size and abundance of neutrons. The quantum forces within the atom are striving for a stable configuration, therefore these atoms decay by releasing energy and nucleons in the form of neutrons, protons, or alpha particles. The release of energy is a vitally important commodity for our energy "consuming" society. The United States is the global economic leader, but the cost of this status is that we are also the largest consumer of global energy demands. Previous technologies have sought to harness the heat given off from the chemical interactions of molecules and then convert that heat into useful work; this is the premise of coal and natural gas electricity plants. The newer "green-energy" technologies are attempting to exploit natural processes through innovative techniques that maximize some of the unique energy transfer methods

nature has devised for molecular and physical stability. Nuclear fission is the ultimate "green-energy" technology in that it attempts to exploit the largest energy-releasing process that is found in nature. No carbon-based pollution occurs as a byproduct of fission. There is no need to destroy huge tracts of land for solar panel emplacements. There will not be an "ugly" skyline, as far as the eye can see, full of 50-foot-tall wind fans. There will not be an economically unfriendly balance between the cost of the technology and the energy return such as is the case with geothermal or tidal electricity production methods. Nuclear fission is a well-researched phenomenon for a technology that is only 70 years old.

Unfortunate events such as Chernobyl, Three Mile Island, and most recently, Fukushima Daiichi have created a stigmatic perception of nuclear power in public circles. Many people misunderstand the dangers associated with nuclear power and nuclear research believing that radioactive effects are widespread and cannot be stopped. Furthermore, many of those who misunderstand the dangers of nuclear physics also believe that the danger of nuclear power is inherent from flaws in scientific knowledge rather than human error. The culmination of these accidents, nuclear weapons, nuclear testing from the 1950's to the 1990's, and a lack of positively reinforcing dialog in the scientific community has led to a culture of distrust and condemnation for nuclear research. It is true, as this paper will show, there is a level of uncertainty concerning the ability to definitively control and calculate many specifics of nuclear reactions. Atomic reactions are violent in the microscopic sense. However, they are also a very common fundamental process of nature and the universe.

This study will add to the knowledge that has been gained over the course of the past 70 years by increasing our understanding of neutronics and nuclear engineering. Static system and quasi-static systems are fairly well understood in the context of nuclear power plants and solid metal systems. If the neutrons are the only particles in motion, it makes it very easy to track the interactions and reactions. A gaseous system, such as the one proposed here, has all particles in motion by the very nature of the system being a gas. Furthermore, variation of the critical parameters that will be discussed later complicates the problem and begins to move it beyond the well-understood atomic physics realm. Additionally, another benefit of this research is to initiate further study into direct energy conversion. While the limitations and possibilities of the Carnot cycle have already been discussed, an important discussion needs to be brought forth about the necessity to diversify our energy cycles. The main cycles, Otto, Rankine, Diesel, and Brayton, as well as their variations, are limited by Carnot efficiency. These cycles comprise and influence every profitable electricity production method. Currently, every electricity production method will reach a point where it will become impossible to meet the demand for energy production. By directly understanding how to create electricity from atomic kinetic energy, it will be possible to expand on this idea and one-day transform energy directly from accelerators, or lasers, or even galactic solar winds. Determining the neutron flux and effective multiplication factor of the shockwave as a function of time and shockwave radius, as this study intends to solve, is a small piece in the puzzle in making the transient-state pulsed spherical uranium-hexafluoride reactor one of the solutions to our future energy production systems.

CHAPTER 2 – REVIEW OF PREVIOUS WORK

The design concept proposed in this study is a complex weave of several different research subjects. No single study has been published regarding the neutronics of a spherical shockwave reactor. The most relevant publication study was conducted in 1969 by Walter Podney, Harold Smith, and A. Oppenheim, on the subject of generating a fissioning plasma within a linear tube due to the introduction of a shockwave (Podney, Smith and Oppenheim). Variation of local state properties, across and after a shockwave has passed, is the crux of the spherical shockwave reactor design concept. Analysis of the change in properties across and behind the shockwave front was released for publication in 1950 after Sir Geoffrey Taylor did the initial studies during the lead up to the atomic test in New Mexico (Taylor, The Formation of a Blast Wave by a Very Intense Explosion II. The Atomic Explosion of 1945). Understanding what is happening within the working fluid medium is essential to the analysis of the spherical shockwave reactor concept; however, in order to understand and propose a viable design, the initial state of uranium-hexafluoride (UF_6) must be understood. The UF_6 equations of state have been assessed in a study conducted in 2009 at the Lawrence Livermore National Laboratory by Phil Brady, et. al, and determined the gas properties at room temperature and nominal room pressures (Brady, Chand and Warren). Using these three studies as the basis for the analysis of the spherical gaseous shockwave reactor, a design concept is proposed in Chapter 3.

The article “Generation of a Fissioning Plasma in a Shock Tube” details an experimental method to study high-temperature, fissioning gas dynamics in a controlled environment (Podney, Smith and Oppenheim). The experiment utilized a linear reflecting

tube of pure deuterium, with a deuterium reflector cap at one end, and a pure $^{235}\text{UF}_6$ medium influenced by a shock of Mach 2. The experiment assumes ideal gas properties, constant speed of the shockwave throughout the experiment, and the reflection of the shockwave leaves the compressed gas behind it at rest. The primary conclusion determined by the experiment is that a period of approximately 0.2 seconds exists before fission-fragment energy expands the gas by 1%, however, this period of time is highly dependent upon the speed of the incident shock.

Sir Geoffrey Taylor published a set of papers in 1950 relating to a theoretical study of large explosions that was conducted several years earlier. The original studies “The Formation of a Blast Wave by a Very Intense Explosion. I. Theoretical Discussion & II. The Atomic Explosion of 1945” were commissioned during the height of WWII and subsequently classified for several years until after the Allied victory. The results of this study yielded the approximate behavior of density, velocity, and pressure as functions of the radial fraction of an unbounded explosion in an infinite air medium. Taylor utilized the Rankine-Hugoniot relations as the boundary conditions for the shockwave front. From these relations, it is possible to determine the kinetic and heat energy of the disturbance and the temperature profile through the shockwave (Taylor, The Formation of a Blast Wave by a Very Intense Explosion I. Theoretical Discussion). A more rigorous analysis of the parameter equations will be covered in Chapter 3.

The final previous study of importance is the “Assessment of the UF_6 Equation of State” by Phil Brady, Kyle Chand, Dave Warren, and Jennifer Vandersall. This study determined the validity of the ideal gas assumption for UF_6 for Mach numbers between 1 and 7. They determined the ideal gas assumption was valid for Mach numbers less than 4,

however, for greater Mach numbers, error between ideal and non-ideal assumptions increased to as much as 6%. Furthermore, this study found that treating specific heats as a constant, rather than a true variable that is a function of temperature, results in differences that are statistically insignificant (Brady, Chand and Warren).

CHAPTER 3 – THEORETICAL REVIEW

The basic composition of the atom was unknown until 1938. For several decades before this, scientists knew some elements were radioactive, however, they did not understand why. Since then, we have been studying the properties of the atom with great curiosity and passion. Once the basic building blocks of the atom were known, it did not take long for us to discover natural atomic processes and how to artificially recreate them. As science learned how to split the atom and recreate atomic decay, many new questions arose such as why materials behaved the way they did in the presence of energetic neutrons. In answering these questions, the study of nuclear engineering took root. As we will see in this chapter, many different parameters affect how a material will respond to collisions and mass/energy transfer on the atomic scale.

The Theory of Fission

The essence of nuclear engineering is the ability to create a fission chain reaction that will throw off heat as a by-product. This heat is then used to create a phase change in a secondary material, usually water into steam, and then changes back to its original phase after passing through a turbine and transferring the energy to the turbine system for electricity production. The efficiency of this process is limited to a maximum that is governed by the Carnot cycle as we have previously discussed. However, what does it really take to create a chain reaction? Scientists struggled with this problem for several years and it is still a concept that is understood in the most fundamental of senses. Some isotopes will readily fission, whereas others will not. The difference is not necessarily in more or less neutrons, but rather the quantum state of the isotope. Certain elemental

isotopes, chiefly Uranium isotopes 235 and 233 (^{235}U , ^{233}U), and Plutonium isotopes 239 and 241 (^{239}Pu , ^{241}Pu) have quantum configurations that make them relatively accepting of thermal neutrons and result in a fission event. This is due to the binding energy of the isotope. Binding energy is quantity of energy required to split the atom into individual parts. This concept is also closely related to the neutron separation energy, which is the energy required to separate a single neutron from the atom. The concept of neutron separation energy, however, is generally more applicable to a quantum study of isotopes, rather than the general nuclear engineering study. For this study, it will be important to be able to calculate the binding energy of the last neutron, which will be expressed simply as the binding energy. Mathematically, this is shown as the difference between the mass of the incident neutron and target isotope, minus the mass of the excited nucleus multiplied by the velocity constant squared. Most people recognize this equation from Einstein's special theory of relativity, or $E = mc^2$. In the case of binding energy, the equation now becomes:

$$E_b = (M_n + M_0 - M_e) * c^2 \quad [3-1]$$

where M_0 is the original mass of the nucleus, M_n is the mass of the neutron, M_e is the mass of the excited nucleus, and c^2 is the relativity constant (Krane).

The binding energies of the isotopes can be compared to the critical energy of fission that is calculated from the semi-empirical mass formula and reaction energies. If the binding energy is greater than the critical energy, an instantaneous fission is highly probable. If the binding energy is less than the critical energy, incident neutrons must carry a quantity of kinetic energy that is equal or greater than the difference between the two for fission to occur. The binding energies for Uranium and Plutonium have been

thoroughly investigated and can be found in tabulations (Lamarsh and Baratta). Table 1 shows a sample of the binding and critical energies of ^{235}U and ^{238}U (Lamarsh and Baratta).

Table 1 - Binding Energy and Critical Energy of Fissions

<i>Isotope</i>	<i>Critical Energy</i>	<i>Binding Energy</i>	<i>Energy Difference</i>	<i>Fission from Thermal Neutron</i>
Uranium 235	5.3 MeV	6.545 MeV	1.245 MeV	Yes
Uranium 238	5.5 MeV	4.806 MeV	-0.694 MeV	No

For years, scientists have been splitting the ^{235}U isotope and studying the reaction. Careful analysis of the data has shown the approximate yield of neutrons in a thermal fission event is $\nu=2.4$. That is, between 2 and 3 neutrons are the product of a fission occurring at room temperature energies, along with two fission product isotopes and energy in the form of gamma rays and neutrinos. Given the physicality of a non-integer yield of neutrons, it can also be expected that this number may change. In fact, it is a variable related to the energy input by the incident neutron and the impacted isotope. A fast neutron, carrying approximately 10MeV kinetic energy may result in as many as 4 or 5 neutrons separating during the fission event. Between 2 and 3 neutrons, however, is the practical lower limit because thermal neutrons; those travelling at room temperature energy, carry with them 0.0253 eV kinetic energy (Lamarsh and Baratta).

Nuclear Criticality (The Chain Reaction)

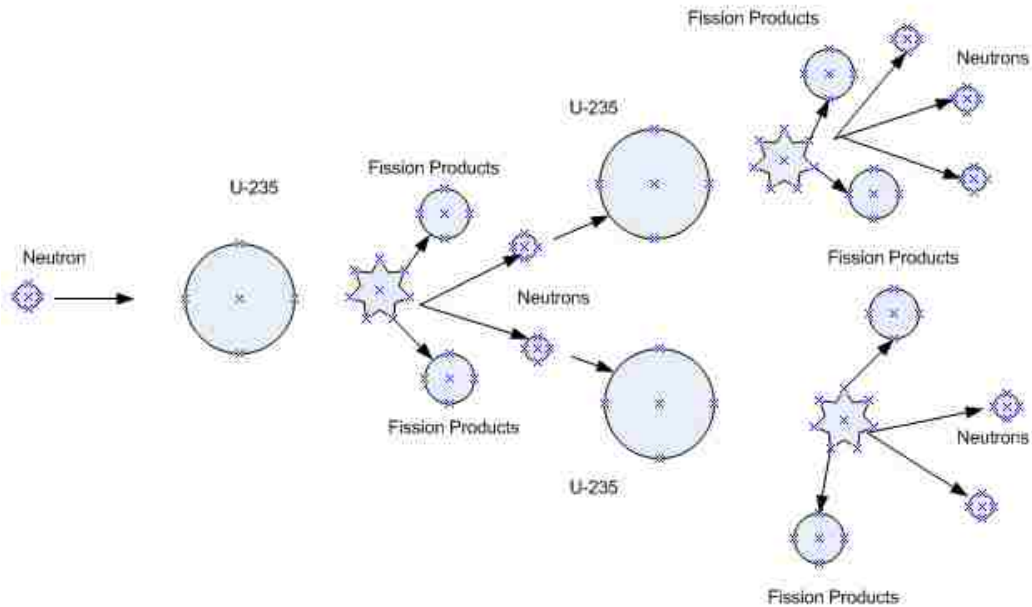


Figure 2 - Simple Fission Chain Reaction for Uranium-235

Getting an isotope to fission is only the first step in the process sustaining a chain reaction. Once the fission neutrons are released, at least one neutron must impact another nucleus and result in another fission, as shown in Fig. 2. In simplest terms, criticality is the accepted term for yielding one new fission per one (previous) fission. If several new fissions occur from a single instigating fission, this is known as being supercritical and it is the basis for weapons technology. If less than one new fission occurs for every instigating fission, this is known as being subcritical and it is the basis for all current nuclear material testing in nations that abide by the nuclear test ban treaties. In subcritical systems, it is important to reiterate; a chain reaction is not sustained. Criticality is readily calculated in nuclear engineering. For an infinitely large system, a bounding calculation

is performed and known as the 4-factor formula (k_{∞}). This calculation determines the reactivity of the system if there is no loss of neutrons due to leakage. More practically, however, reactivity is calculated from the 6-factor formula (k_{eff}). This formula is a simplification of the Boltzmann transport equation, which describes the kinetic theory of gas mixtures, which will be presented in detail in Chapter 4 (Duderstadt and Hamilton). The 4-factor and 6-factor formulas are shown as (Duderstadt and Hamilton):

$$k_{\infty} = \eta f \varepsilon p \quad [3-2]$$

$$k_{\text{eff}} = \eta f \varepsilon p P_{FNL} P_{TNL} \quad [3-3]$$

The variables in [3-2] and [3-3] have specific meaning. η is the reproduction factor; the expected number of neutrons produced from a thermal absorption in fuel. This factor is dependent upon the fuel type and the number of neutrons produced during fission. f is the thermal utilization factor, which is the probability a thermal neutron will be absorbed in the fuel before leaking from the system. This factor is dependent upon the cross-sections, number density of the atoms, and geometric configuration of the system. ε is the fast fission factor, which is generally about 1.02 for thermal systems. This factor is dependent upon the number of ^{238}U atoms in the system and the kinetic energy of the neutrons. p is the resonance escape probability. It is a function of the cross-sections of the atoms and the material composition of the system. Finally, P_{TNL} is the probability for thermal non-leakage, and P_{FNL} is the probability for fast non-leakage. The non-leakage probabilities are both function of the geometries of the system and differ only by the energy of the free neutrons.

The probability of an event occurring is known as the cross-section or reaction probability. There are many different cross-section values, depending chiefly on the

reaction type. A few of the most popular cross-sections are the scattering, fission, and capture cross-sections. The fission and capture cross-sections are collectively known as the absorption cross-section, and conversely, the scattering cross-section is comprised of both elastic and inelastic scattering cross-sections. Table 2 shows some of the common cross-section values for ^{235}U and ^{238}U . These values are available in the Evaluated Nuclear Data Files (ENDF), and specifically, the ENDF/B.VII cross-section data library that is available with the different computational software programs. The units of cross-sections are commonly given or listed in Barns. One Barn is the equivalent to 10^{-24} cm^2 . Several trends can be observed in different cross-sections. For example, in the absorption cross-section, good neutron absorbing materials exhibit a $1/v$ behavior in thermal energy ranges ($< 1 \text{ eV}$). v is the corresponding velocity of an atom at the specific energy. Generally, the lowest absorption cross-section values correspond to the average "birth" energy of a neutron, or about 2 MeV. Scattering cross-sections, by contrast, remain relatively flat across the energy spectrum (Brookhaven National Laboratory).

Table 2 - Selected Isotope Cross Sections (Korea Atomic Energy Research Institute (KAERI))

<i>Thermal Reaction Probabilities</i>		
<i>Type</i>	<i>Uranium 235 (barns)</i>	<i>Uranium 238 (barns)</i>
Elastic Scattering	15.04	9.360
Radiative Capture	98.81	2.717
Fission	584.4	11.77 E-06

The energy spectrum for the birth of new neutrons is dependent upon several variables including nuclear isotope, incident neutron energy, and whether or not new neutrons are prompt or delayed. Experiments and studies have shown the average energy of new neutrons is approximately 2MeV. However, a relatively simple relationship

defines the probability that a neutron will be born at a particular energy. This equation, for ^{235}U , is (Lamarsh and Baratta):

$$\chi(E) = 0.453e^{-1.036E} \sinh \sqrt{2.29E} \quad [3-4]$$

where E is the probable energy of the new neutron. While this equation is relatively accurate, it does have its limitations; especially for the study of ^{235}U . Many years of research and experimentation have led to very detailed probabilities for discrete energy bins, which are cataloged in the Evaluated Nuclear Data Files.

Temperature also has an important effect on cross-section values. All atoms have resonance peaks that are characterized by sharp increases in the cross-section value across small energy windows. As the temperature, or thermal motion, of the atoms increases, the cross-section peaks flatten and expand in range in an effect known as Doppler-broadening (Duderstadt and Hamilton). The impact of this phenomenon is that it will be more difficult and result in a lower probability that a neutron will scatter through the resonance cross-section region of an atom and achieve thermal energies.

Another important concept that is required for calculating criticality in nuclear engineering is known as the mean free path. The mean free path is the average distance a neutron will travel before encountering a reaction. This number is largely dependent upon the energy of a neutron and the number density of atoms in the surrounding medium. The number density can be readily calculated for a given medium. In volumetric terms, it is shown to be (Lamarsh and Baratta):

$$N_d = \rho * \frac{A_v}{A_w} \quad [3-5]$$

where ρ is the mass density of the material. A_v is Avogadro's number, and A_w is the atomic weight of the material. By converting between barns and square-centimeters, the

atom density can be shown as barn/cm. Additionally, by multiplying the number density by the molar fraction of the isotopes and elements in the mixture, the specific mole-fraction and weight percent can be derived.

Given these terms, we can now show how each factor affects criticality. In the 6-factor formula (Duderstadt and Hamilton):

$$\eta = \frac{\nu \Sigma_f^{fuel}}{\Sigma_a^{fuel}} \quad [3-6]$$

$$f = \frac{\Sigma_a^{fuel}}{\Sigma_a^M} \quad [3-7]$$

$$p = \exp \left[-\frac{N^{fuel} V^{fuel} I}{\zeta^M \Sigma_S^M V^M} \right] \quad [3-8]$$

$$\varepsilon = \frac{P_{NL} p f \nu P_F + P_{FNL} P_{FF} \nu (1-p)}{P_{NL} f \nu P_F} \quad [3-9]$$

$$P_{NL} = P_{FNL} P_{TNL} = \frac{1}{1 + L^2 B_g^2} \quad [3-10]$$

In the above equations, the superscript M denotes the entire material including fuel and non-fuel. I is the resonance integral, V is the volume, P_{NL} is the total non-leakage probability, P_F is the probability that a thermal absorption will cause a fission, while P_{FF} is the probability that a fast absorption will cause a fission. L and B are the diffusion length and geometric buckling, respectively, which will be described in further detail in Chapter 4. The parameters p and ε are shown as analytical equations here, however, it should be noted that experimental data is available and extrapolated from the ENDF data libraries, which are much more accurate and the preferred method for obtaining these values.

The most general definition of macroscopic cross-sections is to multiply the number density by the microscopic cross-section. Thus:

$$\Sigma_i = N_d \sigma_i \quad [3-11]$$

where i represents the generic type of reaction cross-section, being absorption, scattering, or fission as a few examples (Duderstadt and Hamilton).

Criticality Controls

In addition to the energy spectrum variables and the different types of multiplication factors to consider, nine fundamental parameters must be accounted for to determine the magnitude of criticality. These parameters are sometimes known as *MAGIC MERV* and stand for Mass, Absorption, Geometry, Interaction, Concentration, Moderation, Enrichment, Reflection, and Volume (Knief). Several of these parameters are very influential in the design proposed here; and several of these parameters are intrinsically dependent upon each other. Beginning with the mass of ^{235}U contained in the system, greater mass allows for lower enrichment levels. Absorption parameters include specific isotopes that readily absorb free neutrons. Common absorbers include boron, cadmium, hafnium, and gadolinium. None of these absorbers will be utilized in the proposed design. Geometry is one of the largest contributors to critically favorable configurations. Geometry dictates the magnitude of leakage from the system. A sphere has the smallest surface area to volume ratio, which minimizes the number of neutrons that leak from the system. Therefore, this system maximizes the number of neutrons in the system at any given time. Interaction is the parameter given to control the number of neutrons entering the system from outside sources. Since there are no outside sources and all neutrons are born within the system, there is no interaction parameter of concern. Concentration, in the context of this reactor, is the ratio of UF_6 to Helium gas as a

moderator. Greater concentrations do not necessarily equate to greater reactivity, there is an optimal concentration value. The optimal concentration of UF₆ to Helium is between 50% and 80%. Moderation is inherently dependent upon the concentration in this gaseous system, greater concentration relates to less moderation. Helium is used as a moderator because of low molecular weight. Enrichment dictates the quantity of ²³⁵U mass in the system. Enrichment is also a fundamental parameter that relates financial cost of the system to its reactivity. Higher enrichment relates to larger costs and a more reactive system. Optimal enrichment for this system varies depending on concentration and moderation. Reflection is an additional parameter that keeps neutrons from leaking out of the system. This is accomplished by utilizing materials that do not absorb neutrons, but rather scatter neutrons with relatively little energy transfer. Beryllium and hydrocarbons are examples of excellent neutron reflectors. Beryllium is the material that will be utilized as a reflector in the design proposed here. Finally, the volume of the system is a parameter that is dependent upon several other parameters. As vital controls such as concentration, moderation, and enrichment are varied, the volume should be manipulated to keep the overall state of the system in adherence to the double contingency principle. The design presented in this study utilizes a static volume in order to allow state properties such as pressure and temperature to fluctuate without egregious changes in criticality parameters.

Compressible Flow

The basis for the macroscopic physics of the reactor design proposed here is studied from the theory of compressible flow. The concepts of compressible flow are well

studied and can be found in many different academic textbooks. Relationships such as the ratio of specific heats for the mixture, speed of sound in the mixture, Mach number, and parameter effects caused by a shockwave discontinuity can be studied and estimated (Anderson). It will be shown in subsequent subchapters, how the parameter variables change within the shockwave, therefore, the equations presented here will show how these variable change with respect to the speed of the shockwave, or specifically the Mach number of the shockwave.

The ratio of specific heats for the mixture is a basic parameter that governs many of the variations in parameters. This parameter is commonly identified as γ and is calculated by:

$$\gamma_i = \frac{c_p}{c_v} \quad [3-12]$$

For a mixture, such as the two-component gaseous mixture in this reactor;

$$\gamma = (1 - N_{He})\gamma_{UF6} + N_{He}\gamma_{He} \quad [3-13]$$

where N_{He} is the fraction of Helium gas in the mixture.

The speed of sound in the mixture can now be calculated as:

$$a_0 = \sqrt{\gamma R_{mix} T_0} \quad [3-14]$$

where R_{mix} is the gas constant of the mixture, which is

$$R_{mix} = \frac{R_{Universal}}{Atomic\ Composition} \quad [3-15]$$

Additionally, the nominal density can be calculated using the ideal gas equation and solving for density.

$$\rho_0 = \frac{p_0}{R_{mix} T_0} \quad [3-16]$$

A constant was determined to be necessary based on the relationships between kinetic energy and time rate of change in the size of the shock. This constant A is calculated from the equation for kinetic energy, integrated with respect to radius and time, and given as (Taylor, The Formation of a Blast Wave by a Very Intense Explosion I. Theoretical Discussion):

$$A = \sqrt{\frac{3E_0}{2\pi\rho_0}} \quad [3-17]$$

The radial size of the shockwave can then be calculated as a function of time, where $R(t)$ is the radius of an unconfined shock:

$$R(t) = A^{2/5} * t^{2/5} \quad [3-18]$$

Thus, the speed of the shockwave can then be calculated as the derivative of the radius:

$$W(t) = A^{2/5} * \frac{2}{5} t^{-3/5} \quad [3-19]$$

The Mach number is simply the ratio of wave speed to the speed of sound in the medium:

$$M(t) = \frac{W(t)}{a_0} \quad [3-20]$$

The case of this analysis is unique because of the type of shock that exists. The initiating event is classified as a moving shock. The pressure ratio, as a function of the Mach number, across the shockwave is given as (Mourtos):

$$\frac{p_2}{p_1} = 1 + \frac{2\gamma}{\gamma+1} (M(t)^2 - 1) \quad [3-21]$$

Given the pressure ratio, and assuming the gas is calorically perfect, the temperature and density ratios can now be solved for (Mourtos):

$$\frac{T_2}{T_1} = \frac{p_2}{p_1} \left(\frac{\frac{\gamma+1+p_2}{\gamma-1+p_1}}{1+\frac{\gamma+1p_2}{\gamma-1p_1}} \right) \quad [3-22]$$

$$\frac{\rho_2}{\rho_1} = \frac{1 + \frac{\gamma+1}{\gamma-1} \left(\frac{p_2}{p_1}\right)}{\frac{\gamma+1}{\gamma-1} + \frac{p_2}{p_1}} \quad [3-23]$$

The relationships for pressure, temperature, and density satisfy the Navier-Stokes equations and obey continuity for conservation of mass, conservation of momentum, and conservation of energy (Mourtos).

- Continuity $\rho_1 W(t) = \rho_2 (W(t) - u_p)$ [3-24]

- Momentum $p_1 + \rho_1 W(t)^2 = p_2 + \rho_2 (W(t) - u_p)^2$ [3-25]

- Energy $e_2 - e_1 = \frac{p_1 + p_2}{2} (v_1 - v_2)$ [3-26]

where u_p represents the particle or surface velocity and is given as:

$$u_p = W(t) \left(1 - \frac{\rho_1}{\rho_2}\right) \quad [3-27]$$



Figure 3 - Explosive Shockwave Event¹

The shockwave discontinuity is the phenomenon that forces criticality to occur in the gaseous UF_6 medium. The strength of the shockwave depends on many different factors, including the specific heats of the medium, the initial pressure of the medium, and the energy associated with the initiating event. The physical effects of the shockwave create a small window with parameters that are favorable for criticality; such as a density change between 4 to 7 times the nominal density of the UF_6 mixture. The time duration of the discontinuity is very short, on the order of less than a single millisecond, which is one of the favorable parameters that keeps the criticality excursion from turning into an

¹ (Boles)

unintentional nuclear event. Other parameters that are expected to vary are the temperature and pressure.

The calculations for parameter changes across the shockwave were formulated by Taylor and assume the total energy of the event is constant but pressure, density, and radial velocity will vary (Taylor, The Formation of a Blast Wave by a Very Intense Explosion I. Theoretical Discussion). The solution to the shockwave is in the form of the ordinary differential equation, as expressed by Taylor:

$$f' \left\{ (\eta - \phi)^2 - \frac{f}{\psi} \right\} = f \left\{ -3\eta + \phi \left(3 + \frac{1}{2}\gamma \right) - \frac{2\gamma\phi^2}{\eta} \right\} \quad [3-28]$$

where γ is the ratio of specific heats, and η is the non-dimensional ratio of the radius of the shockwave to a point behind the shockwave. ϕ is the non-dimensional velocity of the shock as a function of η , f is the non-dimensional ratio between the speed of sound and the energy of the incident shock as a function of η , and ψ is the non-dimensional ratio of density across the shockwave as a function of η .

The Rankine-Hugoniot equations utilized as bounding conditions for the ODE are shown as:

$$\frac{\rho_1}{\rho_0} = \frac{\gamma - 1 + (\gamma + 1)y_1}{\gamma + 1 + (\gamma - 1)y_1} \quad [3-29]$$

$$\frac{U^2}{a^2} = \frac{1}{2\gamma} \{ \gamma - 1 + (\gamma + 1)y_1 \} \quad [3-30]$$

$$\frac{u_1}{U} = \frac{2(y_1 - 1)}{\gamma - 1 + (\gamma + 1)y_1} \quad [3-31]$$

where the subscript 1 represents the conditions directly behind the shockwave, y is the pressure ratio across the shockwave, and U represents the radial velocity of the shockwave.

Resolving these equations for the parameter changes at the discontinuity yield the relationships for ψ , f , and ϕ at their limits:

$$\psi = \frac{\gamma+1}{\gamma-1} \quad [3-32]$$

$$f = \frac{2\gamma}{\gamma+1} \quad [3-33]$$

$$\phi = \frac{2}{\gamma+1} \quad [3-34]$$

which are all functions of γ . Given these equations, The Euler Method can now be used to back-solve for ψ , f , and ϕ as functions of η for values between 1 and 0. That is:

$$0 < \eta \leq 1$$

The numerical solution is obtained by utilizing the Euler Method where;

$$f(\eta)_{i-1} = f(\eta)_i - \Delta\eta * df(\eta) \quad [3-35]$$

$$\phi(\eta)_{i-1} = \phi(\eta)_i - \Delta\eta * d\phi(\eta) \quad [3-36]$$

$$\psi(\eta)_{i-1} = \psi(\eta)_i - \Delta\eta * d\psi(\eta) \quad [3-37]$$

Such that:

$$df(\eta) = f * \frac{3\eta + \phi\left(3 + \frac{\gamma}{2}\right) - \frac{2\gamma\phi^2}{2}}{(\eta - \phi)^2 - \frac{f}{\psi}} \quad [3-38]$$

$$d\phi(\eta) = \frac{\left(\frac{1}{\gamma}\right) * \frac{df(\eta)}{\psi} - \frac{3}{2}\phi}{\eta - \phi} \quad [3-39]$$

$$d\psi(\eta) = \frac{\psi\left(d\phi(\eta) + \frac{2\phi}{\eta}\right)}{\eta - \phi} \quad [3-40]$$

Utilizing the numerical results for f and ψ , the temperature solution behind the shockwave can be readily calculated as a function of η .

$$\frac{T}{T_0} = \frac{f(\eta)}{\psi(\eta)} \quad [3-41]$$

Finally, the numerical results can also be used to predict the maximum pressures of the shockwave as a function of the radius R of the shockwave and the energy of the initiating event.

$$\frac{p_1}{p_0} = \frac{A^2}{a^2 R^3} * f_{\eta=1} \quad [3-42]$$

where A is from compressible flow theory and a^2 is:

$$a^2 = \frac{\gamma p_0}{\rho_0} \quad [3-43]$$

The accuracy of Taylors' calculations is relatively good for his time-period. With the advantage of advanced computational power, the solution to the ODE can be calculated using a much smaller step for η . Unfortunately, Taylor concludes that if the maximum pressure of the shockwave is less than 10 atmospheres, the accuracy of the solution deviates with relation to conservation of energy principles and the pressure ratio shown in [3-42] (Taylor, The Formation of a Blast Wave by a Very Intense Explosion I. Theoretical Discussion).

Proposed Reactor Design

Two major problems exist for this system. First; the effects of the shockwave on the gas, and second; the shockwave effects on system reactivity. The second problem is inherently dependent upon the conditions of the first. As discussed earlier in this Chapter, the characteristics of large, bounding shockwaves in air have been studied for many years (Taylor, The Formation of a Blast Wave by a Very Intense Explosion I. Theoretical Discussion). These studies show that normalized system parameters will approach an asymptotic value as the magnitude of the shockwave energy increases. The effects of a large shockwave in a UF_6 medium behave similarly to a large shockwave in air. The decrease of the characteristic parameter magnitudes as the

shockwave travels through air have also been studied for many years and are adequately defined by compressible flow theory (Mourtos).

The logical first step in reactor design is to determine the effects of the characteristic parameters that will define the operating boundaries of the reactor materials. Material requirements can be determined concurrently with the characteristic parameters in order to define the mechanical limits of the reactor design (Beer, Johnston and DeWolf).

In order to determine the maximum pressure the vessel can safely withstand, typical pressure vessel stress analysis is performed. The governing equation for stress is:

$$\sigma = P/A \quad [3-44]$$

Where P is the force and A is the cross-sectional area. This can be amended to account for pressure vessels, where the stress is shown to be:

$$\sigma = \frac{Pd}{4t} \quad [3-45]$$

Where d is the diameter of the vessel and t is the thickness of the vessel walls.

The highly theoretical nature of the proposed design dictates that caution should be taken to ensure safety in the mechanical design. This can be done by incorporating a Factor of Safety (FoS) into the mechanical design.

$$\sigma_{allow} = \frac{\text{Material Yield Strength}}{FoS} \quad [3-46]$$

The strain is calculated using assumptions. In this analysis, it is assumed that 1mm will be the maximum expansion of the vessel. The strain is then calculated as:

$$\delta = \frac{PL}{tE} \quad [3-47]$$

Where E is the modulus of elasticity and L is the maximum expansion length of the vessel.

The Beryllium reflector is the first material to be impacted by the effects of increased temperature due to the shockwave and fission effect. In this analysis of the gaseous shockwave reactor, it has been assumed that the temperature change due to fission will be negligible. The governing mode of temperature change will be from the shockwave.

Thermal stresses and strains can quickly cause a material to fatigue more rapidly than through normal mechanical impacts. Repeated shocking of the gaseous reactor medium may cause an accumulation of thermal effects. Therefore, it is important to consider thermal strain of the enclosing materials as given by:

$$\delta_T = \alpha(\Delta T)L \quad [3-48]$$

where α is the thermal expansion constant.

The proposed reactor design will experience operations at high pressure and high temperatures. A more rigorous analysis of the mechanical design is performed in Chapters 5 and 6. The physical dimensions of the reactor are detailed here to provide definitive context for calculation methodology and analysis that is presented in later Chapters. The maximum spherical volume for containment of the UF_6 is $65,450 \text{ cm}^3$, which corresponds to a radius of 25 cm. Due to the high neutron leakage probability, a pure Beryllium reflector is used to encompass the reactor area. The thickness of the reflector is 65 cm. The reflector is then surrounded by a safety pressure vessel made from AISI 302 Stainless Steel. The pressure vessel is 12.5 cm in thickness.

The non-physical parameters of the reactor are detailed here to provide context for the calculations and analysis that is presented in later Chapters. Additionally, Chapter 6 will also provide a thorough discussion on the effects of these parameters if they are

modified from the initial states that are presented here. Initial pressure of the UF₆ gas medium is 1000 kPa. The primary initiating event utilizes the equivalent of 12 grams of TNT to generate an energy discontinuity of 50,000 Joules. The initial enrichment of the UF₆ gas is 80%, which represents a non-ideal enrichment scenario and allows for a slightly elevated probability of fast fission reactions occurring through ²³⁸U reactions. ²³⁵U, however, does have a greater probability of fission when neutrons are in the thermal spectrum. To aid in moderation of the neutrons, Helium gas is also present in the gaseous medium and comprises 80% of the gas medium. A schematic of the proposed design is shown in Fig. 4 with the associated legend shown in Table 3.

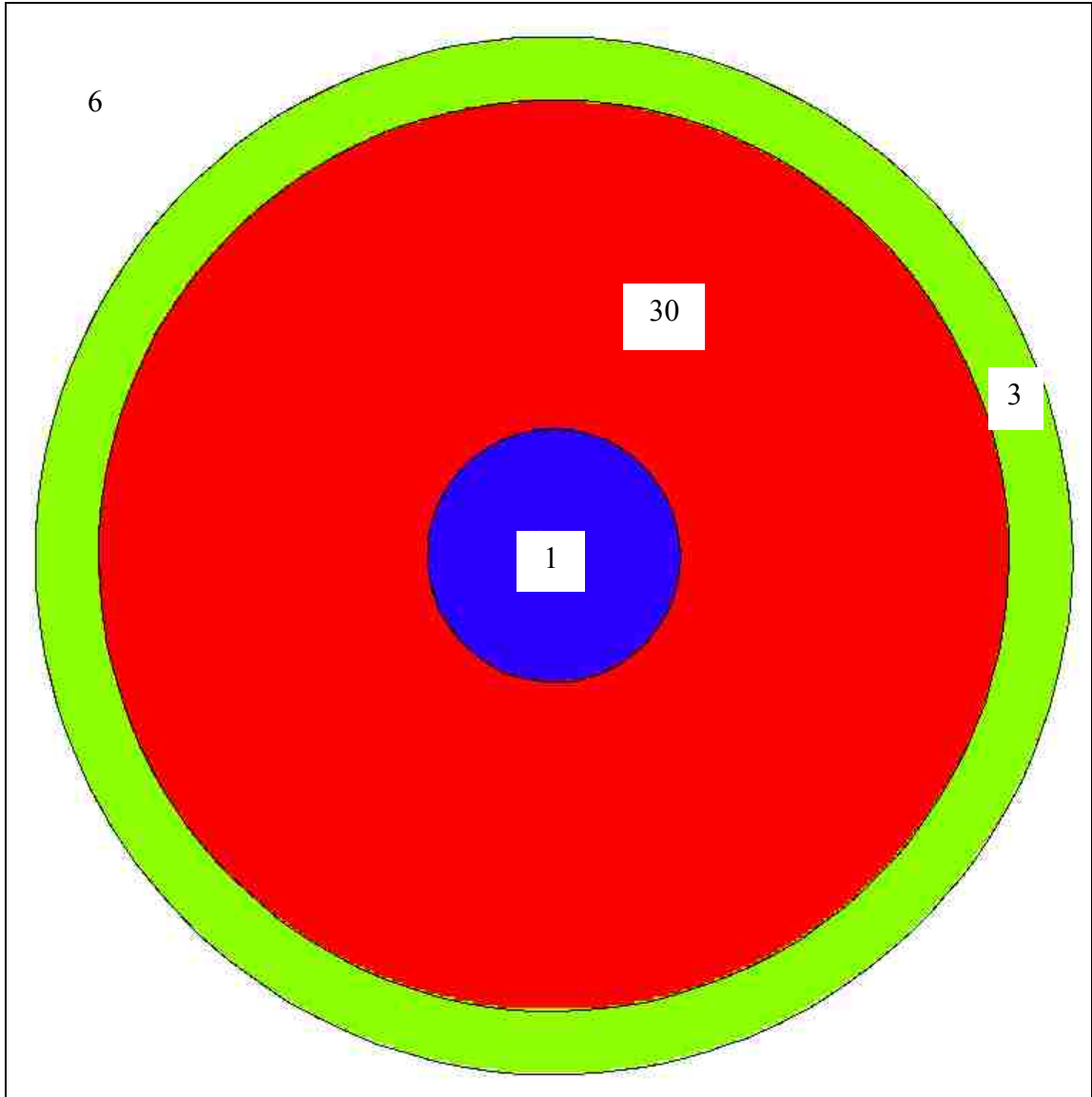


Figure 4 - Schematic of Spherical Gaseous Shockwave Reactor

Table 3 - List of Materials and Functions in Spherical Gaseous Shockwave Reactor Design

<i>Numbered Location</i>	<i>Functions</i>	<i>Material</i>	<i>Dimensions</i>
1	Reactor Core	UF ₆ -He Mixture	25cm – Radius
30	Reflector	Beryllium	65cm – Thickness
3	Pressure Vessel	S. Steel AISI 302	12.5cm – Thick
6	Void	Edge of Analysis Area	Infinite

CHAPTER 4 – METHODOLOGY

A major goal of this study is to advance the science of Nuclear Engineering as well as our understanding of neutronics in transient environments. Several tools and methods are necessary to analyze this problem, including the use of Monte Carlo numerical methods, and computer programs such as MCNP, MATLAB, and Mathcad, which will be necessary to understand the mathematical model of the system.

Transport Theory

The Boltzmann transport equation is a complicated partial differential equation. This fundamental equation is a complicated non-linear solution for gas dynamics and has been utilized for more than a century (Duderstadt and Hamilton). This equation led to the more recent development of the neutron transport equation, which is characterized by its linear partial differential equation distinction. The full equation is given as (Duderstadt and Hamilton):

$$\frac{1}{v} \frac{\partial \varphi}{\partial t} + \widehat{\Omega} \cdot \nabla \varphi + \Sigma_t(\mathbf{r}, E) \varphi(\mathbf{r}, E, \widehat{\Omega}, t) \quad [4-1a]$$

$$= \int_{4\pi} d\widehat{\Omega}' \int_0^\infty dE' \Sigma_s(E' \rightarrow E, \widehat{\Omega}' \rightarrow \widehat{\Omega}) \varphi(\mathbf{r}, E', \widehat{\Omega}', t) + s(\mathbf{r}, E, \widehat{\Omega}, t)$$

$$IC: \varphi(\mathbf{r}, E, \widehat{\Omega}, 0) = \varphi_0(\mathbf{r}, E, \widehat{\Omega}) \quad [4-1b]$$

$$BC: \varphi(\mathbf{r}_s, E, \widehat{\Omega}, t) = 0 \text{ if } \widehat{\Omega} \cdot \hat{e}_s < 0, \text{ all } \mathbf{r}_s \text{ on } S \quad [4-1c]$$

where the IC and BC equations represent the initial conditions and the boundary conditions of the solution. Many years of study, however, have seen simplifications and assumptions that will hold true for most solutions to this equation. In fact, some of these assumptions have already been studied in this analysis by describing the effect of

neutronic parameters on k_{eff} and k_{inf} . When the transport equation is analyzed, it is important to understand the different components of the equation, especially how they relate to the macroscopic effect of the neutron interactions. The transport equation is separated into five different "subjects"; the neutron population as a function of time, the production factor, the loss factor, the interaction factor, and the source term. Each of these "subjects" is complex on its own and has been the subject of much research for many years.

The most popular analog solution method for the transport equation is through One-group theory, where all of the neutrons are expected to be travelling at a single energy, usually in the thermal regime. This solution method is also known as One-speed theory or One-speed diffusion theory. While this theory is quite simplified, by which the expected results are not expected to be fully accurate, this method can be used to approximate preliminary design estimates (Duderstadt and Hamilton). The essence of this theory factors down to determining the time rate of change of the number of neutrons in the system. The production, loss, and leakage terms still exist, however, the production term is generally a function of the source term, the loss term is a function of the absorption cross-sections, and the leakage term is a function of the neutron current density. The beauty of this method is the neutron current density can often be simplified using Fick's Law of Diffusion: $\vec{j} = -D\vec{\nabla}\phi$. Thus, the neutron current is a function of the diffusion coefficient, D , of the medium, which is a material property. Time-dependent solutions may also be necessary in some calculations, depending entirely on the necessity of the engineer, and the importance of reactor period, or some other time parameter. The neutron transport equation for steady state kinetics simplifies to:

$$-D\nabla^2\phi(\mathbf{r}) + \Sigma_a\phi(\mathbf{r}) = S(\mathbf{r}) \quad [4-2]$$

while the time-dependent transport theory equation becomes a partial differential equation in the variables of space and time.

$$\frac{1}{v}\frac{\partial\phi}{\partial t} - D\nabla^2\phi(\mathbf{r}) + \Sigma_a\phi(\mathbf{r}) = S(\mathbf{r}) \quad [4-3]$$

in both [4-2] and [4-3], D is the diffusion coefficient, and the flux and source terms are functions in the spatial dimensions.

Reactor kinetics in a geometrically simple multiplying medium can readily be solved using basic calculus methods (Duderstadt and Hamilton). The general time-independent solution for a bare spherical reactor with no external influences, and homogeneous composition becomes:

$$\nabla^2\phi + B^2\phi = 0 \quad [4-4]$$

so that the solution to the problem becomes an eigenfunction solution:

$$\phi(r) = \phi_0 \frac{\sin(Br)}{Br} \quad [4-5]$$

The necessary boundary conditions applied to derive this solution are given such that the tilde operator denotes the extrapolated radius:

$$\phi(\tilde{r}) = 0 \quad [4-6a]$$

$$\phi(0) = \text{finite, such that } A_2 = \frac{\phi_0}{B} \quad [4-6b]$$

The eigenvalue conditions then shows:

$$B = \frac{n\pi}{\tilde{r}} \quad [4-7]$$

The case of the reflected reactor is much more complicated, however, the concept is similar to combining reactor kinetics solutions in multiplying mediums and non-multiplying mediums with continuity boundary conditions. Thus, the general equations

for a reflected spherical reactor can be described as follows with the subscripts 1 representing the core and 2 representing the reflecting blanket:

$$\nabla^2 \phi_1 + B_1^2 \phi_1 = 0 \quad [4-8a]$$

$$\nabla^2 \phi_2 - B_2^2 \phi_2 = 0 \quad [4-8b]$$

with continuity boundary conditions:

$$\phi_1(r = 0) = \text{finite} \quad [4-9a]$$

$$\phi_2(r = \tilde{r}) = 0 \quad [4-9b]$$

$$\phi_1(r = R) = \phi_2(r = R) \quad [4-9c]$$

$$-D_1 \left. \frac{\partial \phi_1}{\partial r} \right|_R = -D_2 \left. \frac{\partial \phi_2}{\partial r} \right|_R \quad [4-9d]$$

The purpose of the analytical solution to the transport equation is to efficiently solve for the eigenfunctions and eigenvalue solutions. The eigenvalue is the solution whereby the ordinary differential equation solution is correct. The eigenfunction is the set of equations that accurately describe the problem for given harmonics or series calculations. In spatial dimensions that are independent of time, the eigenvalue often relates to the geometric buckling solution when solving for the fundamental solution. The geometric buckling is shown as B^2 . Once the geometric buckling is obtained, it is customary to utilize this solution to determine the criticality condition of the problem. This is done by setting the geometric buckling equal to the material buckling, which is a function of the material composition of the reactor core (Duderstadt and Hamilton).

$$B_g^2 = B_m^2 = \frac{\nu \Sigma_f - \Sigma_a}{D} = \frac{k_\infty - 1}{L^2} \quad [4-10]$$

where ν is the number of new neutrons that are produced, Σ_f is the total fission cross-section, Σ_a is the total absorption cross-section, and D is the diffusion length. This is very

useful since the ratio of material to geometric buckling can give the engineer an idea of the criticality state of the reactor (Duderstadt and Hamilton).

$$B_g^2 = B_m^2 \Rightarrow \lambda = 0 \Rightarrow \textit{Critical State} \quad [4-11a]$$

$$B_g^2 < B_m^2 \Rightarrow \lambda < 0 \Rightarrow \textit{Supercritical State} \quad [4-11b]$$

$$B_g^2 > B_m^2 \Rightarrow \lambda > 0 \Rightarrow \textit{Subcritical State} \quad [4-11c]$$

where λ is an arbitrary constant related to the time eigenvalue.

Furthermore, the criticality state of the reactor can be related back to the equations for k_{inf} and k_{eff} that were shown in Chapter 3. This can be shown as:

$$\lambda = v\Sigma_a \left(1 + L^2 B_g^2\right) \left(1 - \frac{v\Sigma_f/\Sigma_a}{1+L^2 B_g^2}\right) \quad [4-12]$$

where L is the neutron diffusion length:

$$L \equiv \sqrt{D/\Sigma_a} \quad [4-13]$$

In order to increase accuracy in One-group theory calculations, temperature effects should be accounted for in the total absorption cross-section of [4-13]. This is done by taking the combined absorption cross-sections and multiplying them by a temperature factor.

$$\Sigma_a = \sum(N_i \sigma_{a(i)}) * \frac{\sqrt{\pi}}{2} \sqrt{\frac{293K}{T_0}} \quad [4-14]$$

where $\sigma_{a(i)}$ is the microscopic absorption cross-section for the i -th element or isotope.

From simplifications gathered in One-group theory, k_{eff} can also be calculated based on macroscopic cross-section data. The macroscopic transport cross section is needed, however, and can be calculated as:

$$\Sigma_{tr} = \sum \frac{2N_i \sigma_{s(i)}}{3A_i} \quad [4-15]$$

where $\sigma_{s(i)}$ is the scattering cross-section of a given isotope or element, and A_i is the atomic weight of that isotope or element.

Using these pertinent macroscopic cross-sections, the diffusion coefficient is calculated as:

$$D = \frac{1}{3\Sigma_{tr}} \quad [4-16]$$

The migration length is a commonly calculated or tabulated variable. This variable, when coupled with the material buckling, can directly relate k_{eff} and k_{inf} . The migration length is calculated as:

$$M^2 = L^2 + \frac{D}{\Sigma_a + \Sigma_{tr} + \Sigma_f} \quad [4-17]$$

The pertinent variables in [4-10] and [4-17] can now be used to with the calculated k_{inf} as described in [3-2] to determine k_{eff} (Knief):

$$k_{eff} = \frac{k_{inf}}{1 + B^2 M^2} \quad [4-18]$$

Monte Carlo N-Particle Transport Code

Current computational solution programs utilize Monte Carlo methods to solve the transport theory equation. These methods are especially well suited for solving complicated integral and multi-dimensional problems and have been found useful in a variety of fields, including Nuclear Engineering. Monte Carlo methods use random numbers in the course of statistical sampling experiments to determine the most likely convergence solution to the mathematical problem being analyzed.

In the field of Nuclear Engineering, one of the primary computational suites is the Monte Carlo N-Particle Transport Code or MCNP. MCNP utilizes geometric surfaces to

build a mathematical model of the problem. A series of particle interaction simulations are then performed, with variation in the simulations being introduced by the use of random numbers, which identifies the statistical solution to the model. The particular solutions to the problems are not straightforward, and most often, MCNP is used to calculate the eigenvalues for critical neutronic systems. MCNP can also be utilized to calculate photon, electron, or high-energy physics systems (X-5 Monte Carlo Team).

Efficient use of MCNP relies upon specified Data Libraries, such as ENDF/B.VII, to provide context to the interactions determined by random number generation. ENDF stands for Evaluated Nuclear Data File. The ENDF/B library is the official and verified U.S. database for neutron-isotopic interactions. Version VII is the most current version of the library in use. Several other nations have also developed libraries, and each is used for comparison and verification of the data in the different internationally available databases. The ENDF/B data library contains point data for virtually all isotope interaction possibilities for a range of energies spanning from thermal to 20 MeV. MCNP utilizes program subroutines to interpolate and extrapolate data and thus create continuous reaction probabilities.

One of the drawbacks of MCNP is that it relies on statistical solution methods that are best suited for static and quasi-static geometry and not a highly-transient geometry as proposed in the spherical shockwave reactor that is studied in this analysis. If there are multiple variables in the system parameters, MCNP lacks the capability and functionality to continuously update its geometry, density, or composition in a single input file. Furthermore, because it often takes millions of particle histories for the program to develop an accurate picture of the most likely neutron interactions and eigenvalue

solutions, small variations and changes in geometry, temperature, and density of a given input cell can radically alter the solution. The large numbers of particle histories are necessary and required in order to reduce the statistical error that is associated with the Monte Carlo method. The statistical error of this method is proportional to $1/\sqrt{N}$, where N is the number of particle histories, thus a very large number of particle histories is required for accurate analysis.

It is not possible to alter the physics of the reactor in order to allow for better computational analysis; however, there are a several options available to overcome the limitations of MCNP to accurately characterize the system. One possible option is to create quasi-static models of the shockwave conditions for analysis. The gaseous spherical shockwave reactor does have a steady-state conditions where the parameters can be easily calculated and built into a computational input file. This condition is the initial state of the reactor before the shockwave is introduced; henceforth known as the nominal configuration. This configuration can be utilized to study the effects of non-operational criticality of the system. It is important to understand the nominal configuration criticality in order to understand how operations, such as transportation, will affect the safety of the reactor.

MCNP computational models of the system will also be created in order to analyze the expansion of the shockwave as a function of time. These models will reflect discrete time steps throughout the spherical shockwave process. These models require manipulation of the input surfaces, input densities, and input temperatures. This method will allow a discrete approach to the actual physics of the process. The drawback with creating many interim state configurations for MCNP is that the computational program

is assuming a static reactor model, while the true physics of the reactor are a high-energy and fast moving fluid model, however, this will result in a general conclusion about the criticality of the system shockwave to be determined. The physics processes that will not be determined by using this quasi-static method are the effects of neutrons that scatter forward of the shockwave, scatter and thermalize in the undisturbed medium, and then re-enter back into the shockwave as the shockwave front radiates outward.

In this analysis of the gaseous spherical shockwave reactor, MCNPX is the Monte Carlo program that is used for calculations. MCNPX stands for Monte Carlo N-Particle Transport Code eXtended. MCNPX is used for this analysis because it is better suited for high-energy physics rather than MCNP5, a closely related version that is well suited for conventional thermal reactor analyses (D. B. Pelowitz). Use of additional codes, such as deterministic methodology codes were not utilized in this study primarily because MCNPX is one of the preferred Monte Carlo computational programs in the United States.

CHAPTER 5 – REACTOR ANALYSIS

Analysis of Compressible Flow versus Shockwave Theory

The spherical shockwave reactor proposed in this analysis is dependent upon the property changes of the gaseous medium as the shockwave passes through the reactor. There are two rates of change that must be considered that neither compressible flow theory nor shockwave theory consider together. The first is how the parameters of the shockwave change with respect to the expanding radius of the shockwave and the second is how the parameters of the shockwave change behind the shockwave front. Compressible flow theory handles the first of these problems adequately, while the explosive event shockwave theory adequately describes the second.

The different theories can be utilized in a straightforward manner to calculate the relative parameters such as pressure, density, and radius. Unfortunately, there is a slight disconnect between the two theories, as utilized in this analysis. Shockwave theory, as derived by Taylor, assumes the Mach speed of the shockwave is infinite, in accordance with the boundary conditions identified in equations [3-29] to [3-31]. This assumption is propagated throughout the event, regardless of radial size or time analysis from the event initiation. Additionally, compressible flow theory, as derived in Chapter 3, is primarily analyzed for shock tube applications, rather than unrestrained spherical shocks, therefore, the values of the parameters behind the discontinuity are poorly described.

To resolve the inconsistency accounting for density changes as the shockwave radiates outward, such that the pressure of the shockwave front decreases with distance from the initiation point, which causes the density of the shockwave front to also decrease with distance from the initiating point, a simple relationship is derived. This

relationship assumes that the parameters at all points behind the shockwave front behave the same as the ideal case, even though the peak of the parameter at the shockwave front is decreasing. The relationship is calculated as:

$$\rho_i = \frac{\rho_c^*}{\psi_1} \rho_0 \psi_i \quad [5-1]$$

where the subscript of i represents the radial/time step of the wave, ρ_c^* is the density ratio as calculated from compressible flow theory, and ψ is the density ratio from shockwave theory. The resulting incremental density outputs were then utilized to determine the appropriate shockwave shell densities in the MCNP input decks.

One-Group Theory (Steady State) Analytical Analysis

One-group theory analysis is an efficient way to understand the trends that can be realized by the shockwave. It is not very accurate for the problem presented by this reactor, however, it appropriate to show the derivation of the flux and buckling for later comparison in Chapter 6.

The initial problem is modeled without a reflector and as a two-zone region. Zone-1 is the undisturbed region, while Zone-2 is the transient region behind the shockwave. The general solutions are in the form of:

$$\nabla^2 \phi_1 + B_1^2 \phi_1 = 0 \quad [5-2a]$$

$$\nabla^2 \phi_2 + B_2^2 \phi_2 = 0 \quad [5-2b]$$

with the boundary conditions:

$$\phi_2(0) = \text{finite} \quad [5-3a]$$

$$\left. \frac{\partial \phi_1}{\partial r} \right|_{R_a} = 0 \quad [5-3b]$$

$$\phi_1(R) = \phi_2(R) \quad [5-3c]$$

$$-D_1 \left. \frac{\partial \phi_1}{\partial r} \right|_R = -D_2 \left. \frac{\partial \phi_2}{\partial r} \right|_R \quad [5-3d]$$

where R_a is the outermost boundary of the reactor and representative of a perfect reflecting surface, while R is the instantaneous radius of the shockwave. The perfect reflecting surface boundary condition, shown in [5-3b], is chosen for this analysis rather than the extrapolation distance boundary, because of the actual reactor will have a thick Beryllium reflector at the boundary of the reactor volume. Furthermore, the focus of this study is to analyze the flux of the shockwave. Therefore, the flux at the boundary of the reactor, which based on diffusion theory, is not a valid representation of the flux, is not analyzed for the spherical shockwave reactor.

The exact solution in steady state is then:

$$\phi_1(r) = A_1 \left(\frac{\sin(B_1 r)}{r} \right) + A_2 \left(\frac{\cos(B_1 r)}{r} \right) \quad [5-4a]$$

$$\phi_2(r) = C_1 \left(\frac{\sin(B_2 r)}{r} \right) + C_2 \left(\frac{\cos(B_2 r)}{r} \right) \quad [5-4b]$$

where A and C are arbitrary constants. Next, to apply boundary conditions as defined in equations [5-3a] through [5-3d].

Applying [5-3a] to [5-4b] and using L'Hospitals Rule:

$$\phi_2(r) = C_1 \left(\frac{\sin(B_2 r)}{r} \right) + C_2 \left(\frac{\cos(B_2 r)}{r} \right) = \text{finite} \quad [5-5a]$$

$$C_1 = \frac{\phi_0}{B_2}, \text{ therefore, } \phi_2(r) = \frac{\phi_0}{B_2} \left(\frac{\sin(B_2 r)}{r} \right) + C_2 \left(\frac{\cos(B_2 r)}{r} \right) \quad [5-5b]$$

Applying [5-3b] to [5-4a]:

$$\frac{\partial \phi_1}{\partial r} (R_a) = \frac{A_1 B_1 \cos(B_1 R_a)}{R_a} - \frac{A_1 \sin(B_1 R_a)}{R_a^2} - \frac{A_2 B_1 \cos(B_1 R_a)}{R_a} - \frac{A_2 \cos(B_1 R_a)}{R_a^2} = 0 \quad [5-6a]$$

reducing [5-6a] and combining like terms:

$$A_2 = A_1 \left(\frac{B_1 R_a + \tan(B_1 R_a)}{1 + B_1 R_a \tan(B_1 R_a)} \right) \quad [5-6b]$$

then simplifying such that:

$$K_1 = \frac{B_1 R_a + \tan(B_1 R_a)}{1 + B_1 R_a \tan(B_1 R_a)} \quad [5-6c]$$

So:
$$A_2 = A_1 K_1 \quad [5-6d]$$

And:

$$\phi_1(r) = A_1 \left[\left(\frac{\sin(B_1 r)}{r} \right) + K_1 \left(\frac{\cos(B_1 r)}{r} \right) \right] \quad [5-6e]$$

Applying [5-3c] to [5-5b] and [5-6e] and solving for the undetermined constants:

$$C_2 = A_1 \left(\frac{\sin(B_1 R) + K_1 \cos(B_1 R)}{\cos(B_2 R)} \right) - \frac{\phi_0 \tan(B_2 R)}{B_2} \quad [5-7a]$$

such that:

$$K_2 = \frac{\sin(B_1 R) + K_1 \cos(B_1 R)}{\cos(B_2 R)} \quad [5-7b]$$

which leads to:

$$\phi_1(r) = A_1 \left[\left(\frac{\sin(B_1 r)}{r} \right) + K_1 \left(\frac{\cos(B_1 r)}{r} \right) \right] \quad [5-7c]$$

$$\phi_2(r) = \frac{\phi_0 \sin(B_2 r)}{B_2 r} + \frac{\cos(B_2 r)}{r} \left(A_1 K_2 - \frac{\phi_0 \tan(B_2 r)}{B_2} \right) \quad [5-7d]$$

Finally, applying [5-3d] to [5-7c] and [5-7d] reveals, after simplifying and combining like terms, the solution to the neutron flux:

$$\phi_1(R) = \frac{A_1}{R} (\sin(B_1 R) + K_1 \cos(B_1 R)) \quad [5-8a]$$

$$\phi_2(R) = \frac{\phi_0}{R B_2} \{ \sin(B_2 R) - \tan(B_2 R) \cos(B_2 R) \} + \frac{A_1 K_1 \cos(B_2 R)}{R} \quad [5-8b]$$

$$A_1 = \frac{\phi_0 R D_2 \cos(B_2 R) (1 + \tan^2(B_2 R))}{D_1 \cos(B_1 R) \{ B_1 R + \tan(B_1 R) + K_1 B_1 R \tan(B_1 R) + K_1 \} + D_2 K_2 \cos(B_2 R) \{ B_2 R \tan(B_2 R) + 1 \}} \quad [5-8c]$$

With the solutions for ϕ solved in equations [5-8a] and [5-8b], including the

constant of integration in [5-8c], the flux, as a function of radius can be determined analytically, provided the initial flux value is known. The buckling values are determined by manipulating [5-8a] and [5-8b] to solve for B_i .

Additionally, the buckling ratio can also be determined as:

$$\frac{B_2}{B_1} = \left(\frac{\rho_2}{\rho_1}\right)^2 \quad [5-9]$$

Given that the density ratio is calculated from compressible flow and shockwave theory and the undisturbed buckling value approximation is calculated shown in [4-10], the buckling value in the transient reactor state can easily be calculated from [5-9].

Transient Reactor Analysis via MCNPX

Transient reactor behavior is not directly calculated in MCNPX. Analysis of the reactor is accomplished by deriving results from the computational outputs. As stated in Chapter 4, MCNPX relies on numerical methods that assume the system is in steady-state. The standard computational method of MCNPX requires using millions of neutron histories and following these histories until they result in a definitive termination. Furthermore, as discussed in Chapter 4, these histories are followed independent of time. The spherical shockwave reactor presented in this analysis has an effective outward cycle of 2.9×10^{-4} seconds before the shockwave event has receded below Mach 1. This cycle time is approaching the same order of magnitude as the prompt fission lifetime. The increased density and short time scale of the shockwave does not necessarily allow time for neutrons to thermalize. Furthermore, events such as delayed neutron fissions can occur many seconds after the absorption event, in which case, the shockwave has long passed and the nominal reactor properties either have or are returning to original states.

It will be shown in Chapter 6 that modeling the reactor in MCNPX, as it would be physically, does not accurately capture the local effects of the shockwave in terms of reactivity and neutron production. The quasi-static modeling approach of the reactor is accomplished by creating several models of the shockwave that capture the shockwave as a standing wave. If both the transient-state medium and undisturbed medium are modeled in MCNPX, the MCNPX simulations create conditions where neutrons escape from the shockwave and then populate in the much larger, by volume, undisturbed UF₆ medium. Thus in all criticality calculations, MCNP defaults to, and is influenced heavily by the undisturbed UF₆ medium. Simple scrutiny of the output data shows the number of reactions in the undisturbed medium to be approximately 300 times the number of reactions in the shockwave medium of concern. To eliminate this error, the quasi-static models were created using just the shockwave and the transient medium behind the shockwave with vacuum boundary conditions outside the shockwave front. Unfortunately, the size of the shockwave and intense compaction of materials into the outermost 0.01% of the transient medium at the shockwave front, inhibit traditional criticality analysis by kcode inputs because not enough material is available for neutron thermalization analysis. Therefore, a new method is needed for describing the effects of localized changes in reactivity that cannot be captured by macroscopic analysis of the reactor as a whole. The approach to understanding criticality and neutronic analysis presented in this study is to calculate and examine the multiplication factors in terms of neutron production rate and the instantaneous neutron population. Analytically, this is approach is derived as:

$$M = \frac{\int_{Vol} \int_0^t v \Sigma_f \phi(r) dt}{\int_{Vol} \int_0^t S(r) dt} \quad [5-10]$$

Five energy bins, as shown in Table 4, are specified for analysis of the cell flux in MCNPX. Each energy bin is averaged, and the total width of the energy bin is determined for computational analysis. The energy bin spectrums were chosen in order to accurately capture the Watt Spectrum as described in Chapter 3.

Table 4 - Energy Bins for use in MCNPX Computational Analysis

<i>Energy Spectrum by MCNPX Bin</i>		
Energy Bin (E_i)	Avg. E_i	dE_i
0-0.5 MeV	0.25	0.5
0.5-1MeV	0.75	0.5
1-2MeV	1.5	1
2-4MeV	3	2
4-20MeV	12	16

Using the mass of the neutron, in MeV/c^2 , and the MCNPX cell flux output, the flux per source particle per radius is determined by:

$$\frac{\phi(r,t)}{\text{neutron}} = \sum \left(\frac{\phi_{\text{MCNPX}} dE_i}{\sqrt{2E_i/m_n}} \right) \quad [5-11]$$

where i is the energy bin of interest and summed over the entire set of bins. The neutron flux per radius is then determined by factoring in the source term by multiplying [5-10] by the number of initiating source particles, as defined in the input deck.

The number of neutrons as a function of time is determined by multiplying the differential area of the shockwave by the flux as a function of radius and time:

$$\# \text{ Neutron}_l(t) = \phi(r, t) * 4\pi r^2 dr_l \quad [5-12]$$

where the subscript l is the radial expansion distance over the time step.

Using the results of [5-11] and dividing it by the time averaged source output of MCNPX, the multiplication factor for neutron production rates at a specific time step can be determined. This factor is called \widehat{M}_l .

$$\widehat{M}_l = \frac{\# Neutron_l(t)}{\# Source Neutron(t)} \quad [5-13]$$

The summation of \widehat{M}_l represents the cumulative effects of source particle generation as the shockwave expands out through the undisturbed reactor medium.

$$\widehat{M} = \sum \widehat{M}_l \quad [5-14]$$

\widehat{M} is the expected multiplication value of the shockwave as a whole and considered in this analysis to be representative of criticality of the system induced by the shockwave.

Analysis of the instantaneous neutron population is approached with the same method as shown in [5-10] through [5-12]. For each time step, [5-12] is divided by the time interval of analysis, a Δt . This results in the number of neutrons in the system that are created by the shockwave.

$$\# Neutron_l = \frac{\# Neutron(t)}{\Delta t_l} \quad [5-15]$$

Determination of the instantaneous neutron population multiplication ratio is accomplished by removing the source term from the result of [5-15].

$$M^* = \frac{\# Neutron_l}{\# Source Neutron} \quad [5-16]$$

M^* represents a time-independent snapshot of the number of neutrons generated by the shockwave front while the shockwave is expanding through the undisturbed medium. Plotting M^* against the shockwave radius shows how the intensity of the shockwave can be related to the number of neutrons generated by the shockwave.

Spherical Shockwave Reactor Parameter Analysis

The specific nominal condition parameters of this reactor create ideal conditions that help propagate reactivity in the reactor system in a controlled manner. A nominally critical reactor will quickly lead to an uncontrolled supercritical event when an increase of density is applied. Conversely, if the nominal condition parameters result in a reactor that is very subcritical, there is a reduced likelihood of the system output being substantial enough to justify its operations. The inherent difficulty with defining the nominal conditions is that small changes in one parameter affect several other parameters. The ideal gas relationship of the gaseous medium dictates that changes in pressure result in additional changes in density and temperature, which affects the ability of free neutrons to interact with the gas and the probability of a specific reaction occurring based on cross-section changes due to Doppler broadening. Intrinsic parameters of the system, such as initial energy source, reflector type, and volume of the reactor affect the intensity of the shockwave and leakage probabilities of the system.

Some parameters with direct impact on the reactivity of the system can be manipulated to efficiently produce critical systems. The quickest method for achieving a reactive system is to increase the concentration of the gaseous UF_6 medium, favouring higher quantities of UF_6 . As we will see in Chapter 6, the reactor proposed in this design is safe by design, meaning that with almost no Helium concentration, and design basis pressure and enrichment, the reactor will barely reach the estimated critical reactivity point. The drawback to reducing the concentration of Helium in the reactor medium is the loss of moderating abilities. The Helium atom, is comparable to the size and mass of the

neutron travelling with kinetic energy. This allows for the ability to thermalize the neutrons in a manner that is not available in a 100% UF₆ medium. The UF₆ molecule is incredibly large, based on size and mass, in comparison to the neutron, therefore, the transfer of energy from the neutron to the UF₆ molecule is small, which will result in larger mean free path values and longer mean neutron lifetimes.

Increasing the enrichment is also an incredibly effective method of achieving a critical state. ²³⁵U can readily fission at all energies and the number of new neutrons produced per fission increases proportionally to the increase in incident neutron energy. Therefore, it is readily apparent that increases in the number of ²³⁵U atoms in the reactor medium will result in higher reactivity. This option, however, is much more costly than using a moderated system. UF₆ is currently a staple commodity in the nuclear industry and many studies have been done to relate the costs of enrichment to the cost of the enriched material. The common terminology used to describe this relationship is called the SWU, or Separative Work Unit. The SWU is calculated as:

$$SWU = M_p(V_p - V_T) - M_F(V_F - V_T) \quad [5-17a]$$

$$V_i = (1 - 2x_i) \ln\left(\frac{1-x_i}{x}\right) \quad [5-17b]$$

where M is the mass of the product, and V is an enrichment conversion factor based on gaseous diffusion thermodynamics, x is the percent enrichment, and the subscripts represent the *Product*, *Feed*, or *Tails*, respectively, with i being the indiscriminate of those three parameters.

Finally, one of the most pertinent parameters to the spherical shockwave reactor is the nominal pressure of the system. The 1MPa nominal pressure of the reactor is chosen specifically to aid in the control of criticality in this study. Changes in nominal pressure

help to control the intensity, speed, and radial distance the shockwave will travel.

Increases in the pressure are directly proportional to the density and temperature of the system. As further discussed in Chapter 6, the given nominal pressure limits the distance the supersonic portion of the wave will travel to approximately two-thirds the radial diameter of the reactor, thus allowing a small distance for energy dissipation and reduce effects of wave reflection.

The intrinsic parameters, such as the energy of the initiating event can directly affect how the fluid medium will react. The initiating starting event for the design proposed in this study allows a good mix of wave-speed and wave-pressure. Larger events were considered analytically and the effects on the reactor become quickly apparent. Increasing the imparted energy by approximately one order of magnitude increases the wave-speed to a value that is faster than thermal neutrons speeds.

Additionally, the instantaneous Mach number of the shockwave as $t \rightarrow 0$ theoretically rises towards infinity. With higher energy initiating events, the wave travels farther in the medium and may quickly reach a point where reflection effects must be accounted for in analytical and computational analyses. Taylor utilized an infinite wave speed in his studies of atomic explosions, hence the reliance on compressible flow is necessary for the analysis of the spherical shockwave reactor as described here (Taylor, The Formation of a Blast Wave by a Very Intense Explosion I. Theoretical Discussion).

The Beryllium reflector chosen for this reactor is chosen to maximize the compromises between material strength and material reaction probabilities. Beryllium is a commonly used metal reflector, will help to bound free neutrons within the system, reduce leakage, and thus increases k_{eff} . The thickness of the reflector, as modelled in this

study is chosen so that unknown, long-term effects of the reactor can be contained within a relatively broad margin of safety. Some of the long-term effects of the reactor include temperature rate-of-rise with regards to both fission and explosive events. Cooling time of the reactor is also unknown; therefore, if the reactor-metal surface does not have sufficient internal convective properties, or lacks the appropriate conductive temperature gradient from the internal metal side to the outer steel surface, the reactor may be prone to temperature failure. Beryllium is slightly softer than steel, based on the Mohr hardness scale, therefore, the effects of the pressure wave and pressure differentials will be absorbed more readily with thicker reflector material, but the cyclical rate of pressure induced forces on the metal are undetermined.

Finally, the last intrinsic parameter of this reactor is the volume size of the reactor. While volume is one of the parameters used to control criticality, as discussed in Chapter 3, it is a very hard parameter to manipulate after the design constructed. The volume of the spherical shockwave reactor was initially explored based on single-parameter limits for metal units and water reflection as shown in Fig.5. This method was used to determine bounding case volume and would be considered very conservative because the single-parameter limits for mass are different for the gaseous mixtures, such as the UF_6 and He mixture that is utilized in the spherical shockwave reactor. Additionally, many issues arose relating to chemical interactions between water and UF_6 that developed unintended reactions and impurities in the reactor, both of which inhibit reactor applicability. However, for this initial analysis, this limit does provide a reasonable estimate of the critical mass of UF_6 required. The spherical volume for the

containment of UF₆ in this design analysis, is 65,450 cm³, which corresponds to a reactor radius of 25 cm.

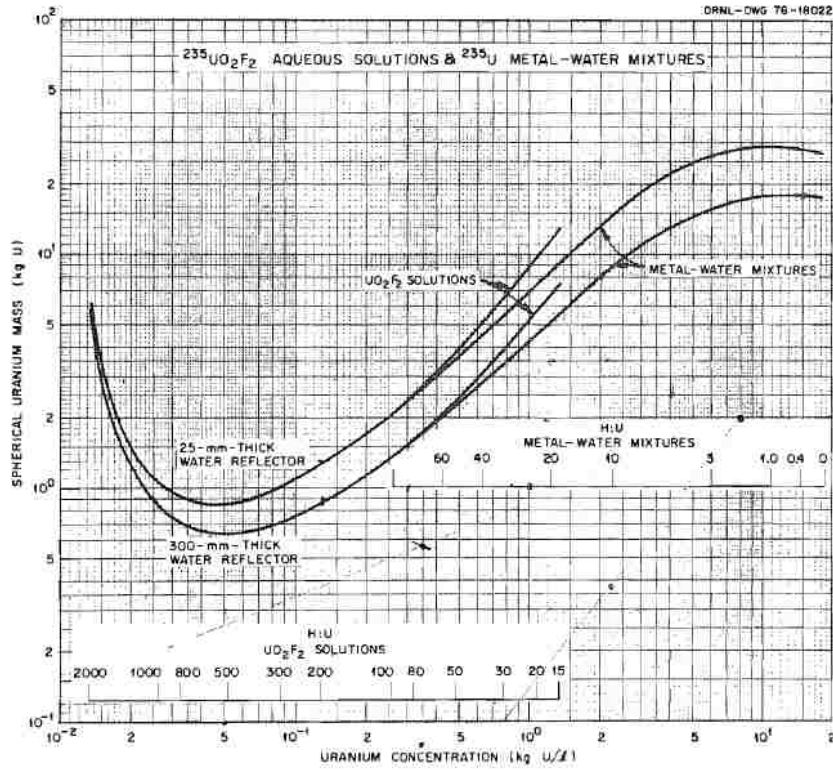


Figure 5 - Single-Parameter Limit Curve for ²³⁵U Metal-Water Mixtures².

MCNPX Input Decks

MCNPX is an inherently steady state computational analysis tool. After building the geometric models, several model inclusions are necessary to promote realistic physics that are found in the spherical shockwave reactor. This was accomplished in several ways, including specifying specific thermal data libraries, source distribution, and particle cutoffs.

² (J. T. Thomas)

The ENDF/B data libraries are a massive conglomeration of reaction probabilities across a large portion of the energy spectrum. The ENDF/B.VII data library has five different sets of these libraries that account for changes in temperature, generally due to fission heat from the reaction, however, they can be specified for individual material inputs. In this analysis, all five of the built-in data libraries are specified. The nominal temperature uses the base library for 300K. As the temperature increases, in accordance with the temperature profile specified in Chapter 6, Fig. 14, the material input card is modified to utilize built-in 600K, 900K, 1200K, or 2500K data sets. The specific shockwave rings are delineated as shown in Table 5. It is important to note that Taylor predicts the temperature within the transient state region of the shockwave will continuously rise toward infinity as the density decreases asymptotically to a perfect vacuum. The maximum ratio axis of Fig. 14 in Chapter 6 has been arbitrarily limited in order to focus on the primary ratio of analysis, density, however, the numerical profile shows the larger range as predicted by Taylor. The centermost shells of the MCNPX model were limited by the applicability of the built-in MCNPX data libraries. Therefore, the temperature profiles in Table 5 are arbitrarily limited compared to the true profile.

Cutoffs are also a very important physical event that is necessary to account for. The entirety of the shockwave event is less than one millisecond. This means that during the shockwave event, neutrons do not necessarily have time to thermalize. Furthermore, in order to reduce the redundancy of neutron sources as a function of time, a cutoff card was selected and defined to limit neutron histories to the time step of analysis. This effectively eliminates long-term delayed fission neutrons from the shockwave analysis.

Table 5 - Temperature Library Profile for MCNPX Input Cards

<i>Shockwave Temperature</i>			
Temp Ratio	Temperature	Library	Cell #
1	300	300K	10
1.015	304.5		11
1.0302	309.06		12
1.0611	318.33		13
1.1258	337.74		14
1.5157	454.71		15
1.9363	580.89	600K	16
2.4984	749.52		17
3.2628	978.84	900K	18
4.3194	1295.82	1200K	19
5.8054	1741.62		20
7.9352	2380.56	2500K	21
11.0524	3315.72		22
15.7235	4717.05		23
22.9134	6874.02		24
22.9134	6874.02		25
22.9134	6874.02		26

The MCNPX computation was performed with 10^8 initial particles. Through the SDEF card, the source particles were limited to the shockwave front cell (Cell 10) at an average point within the cell thickness. MCNPX defaults to starting neutron sources at 14MeV, however, this is done to capture all possible reactions during the course of thermalization. Neutrons are rarely born at this energy, therefore, a random variation on initial energy was specified for this analysis, based on the Watt spectrum as defined in [3-4], as the initial energy of all source neutrons in the system. The decision to use starting neutron energies based on the Watt spectrum is based on concept that neutron thermalization in the spherical shockwave reactor will be limited as described in Chapters 4 and 5.

CHAPTER 6 – RESULTS

Compressible Flow Results

The compressible flow results were primarily calculated using Mathcad computational software. The initial parameters are defined in Tables 6 through 8, including the calculated parameters based on equations [3-11] to [3-19].

Table 6 - Atomic Weights of Atoms, Isotopes, Molecules, and Mixture

<i>Atomic Weights [g/mole] – 80% Enrichment and 20% UF₆ Concentration</i>						
Helium	Fluorine	²³⁵ U	²³⁸ U	Uranium	UF ₆	Mixture
4.002	18.994	235.044	238.051	235.6	349.5	73.1

Table 7 - Specific Heats of the Reactor Medium Components

<i>Specific Heats</i>		
Helium	UF ₆	Mixture
1.667	1.065	1.541

Table 8 - Additional Constants and Initial Derived Parameters

<i>Miscellaneous Constants</i>			
R_{mix} [J/kgK] (Mixture Gas Constant)	T₀ [°C] (Nominal Temperature)	P₀ [kPa] (Nominal Pressure)	a₀ [m/s] (Speed of Sound)
113.718	25	1000	228.577
E₀ [J] (Initiation Energy)	E₀ [g-TNT] (Initiation Energy)	ρ₀ [g/cm³] (Nominal Density)	A [m^{2.5}/s] (Kinetic Energy Constant)
50,000	11.945	0.0295	40.235

Several of the compressible flow parameters are variable as the shockwave expands from the center initiation point. Figs. 6 through 9 detail the travel and parameter changes neglecting the effects of subsonic wave speed. As the wave speed passes through Mach 1, the wave transforms from supersonic flow to subsonic flow. The analysis of flow

type is beyond the scope of the work presented herein; therefore, all calculations are performed and analyzed for supersonic flows only. Technically, Mach number should be asymptotic to Mach 1, however, due to the derivation of A as shown in Table 8 and [3-17], the wave speed is proportional to the radius to the $-3/2$ power.

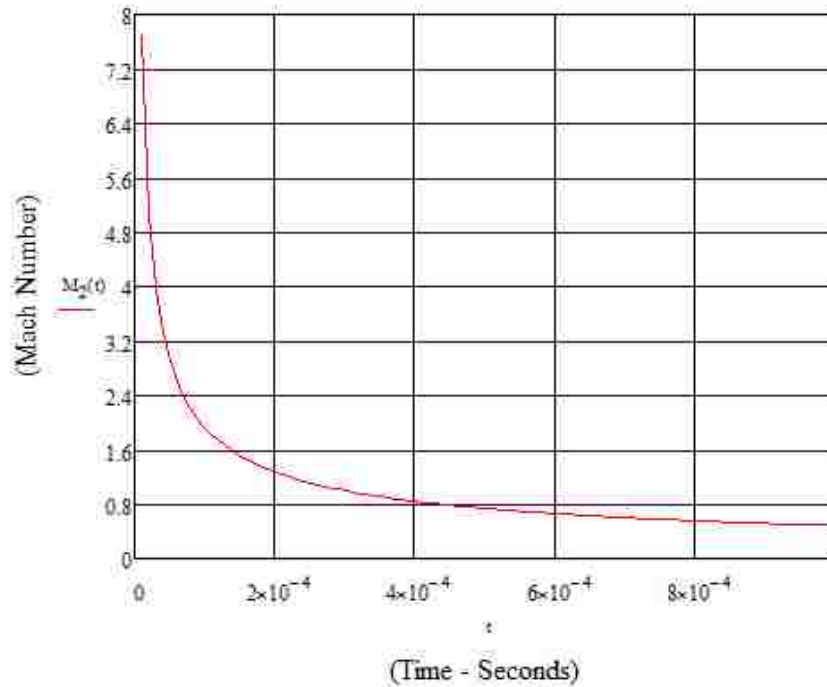


Figure 6 - Shockwave Mach Number in an Infinite Reactor Medium

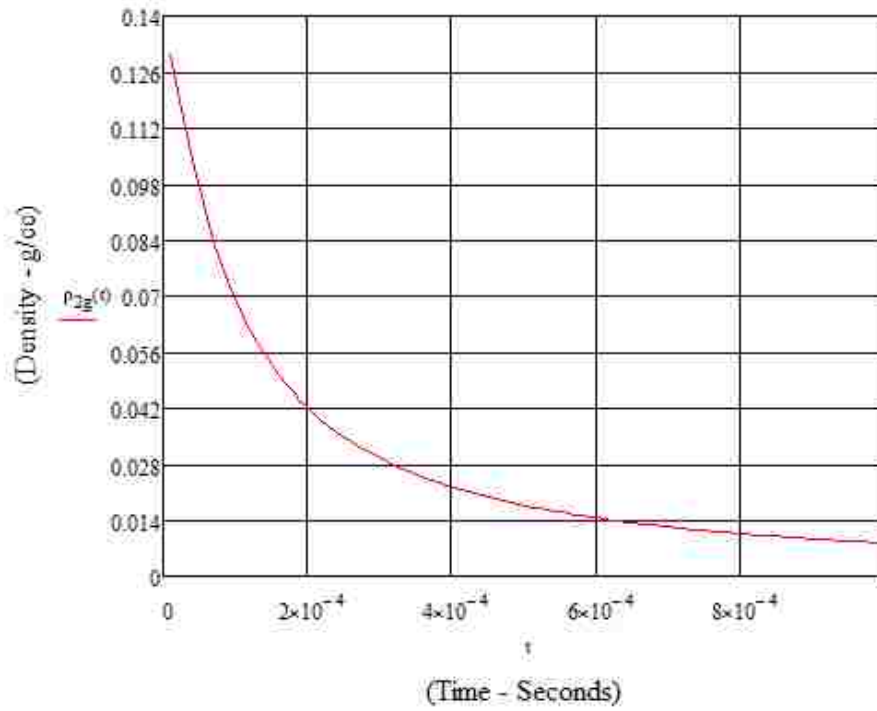


Figure 7 - Maximum Shockwave Density in an Infinite Reactor Medium

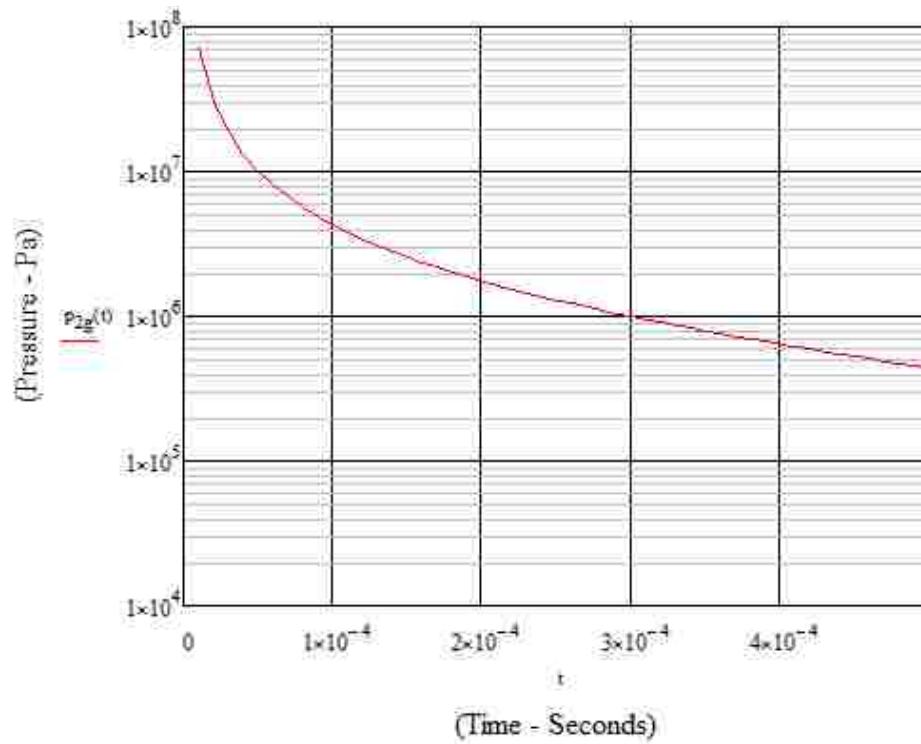


Figure 8 - Maximum Shockwave Pressure in an Infinite Reactor Medium

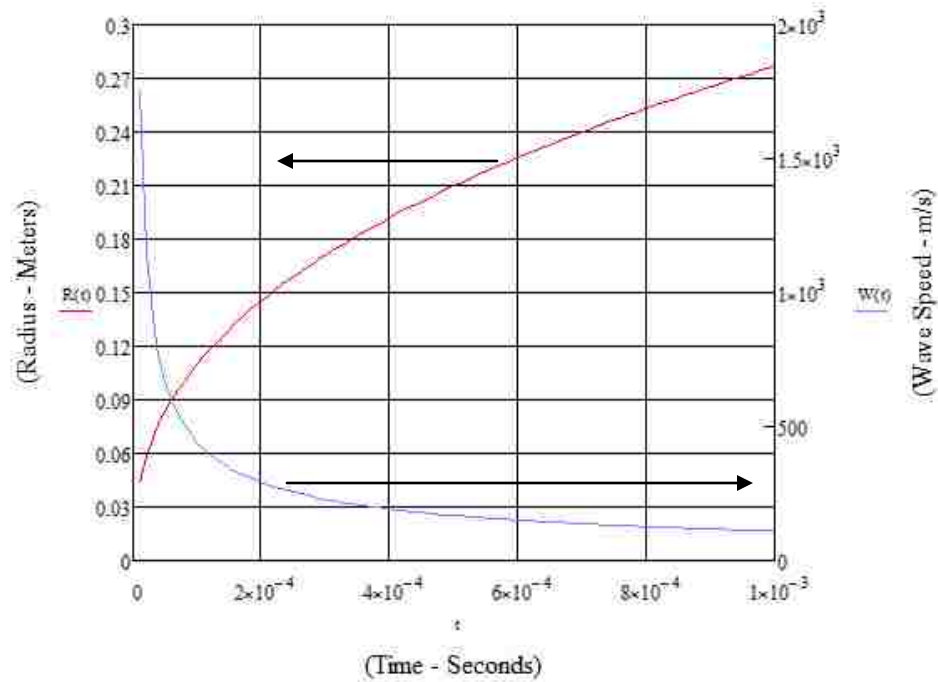


Figure 9 - Shockwave Radius and Shockwave Speeds in an Infinite Reactor Medium

The above results shown in Figs. 6 through 9 satisfy the equations of continuity, [3-23] and [3-24], as shown in the Mathcad Appendix. The conservation of energy analysis was not performed here and the internal energy analysis of the reactor is outside the scope of this study.

With continuity satisfied, limits were determined for the extent of the compressible flow analysis based on the Mach number results shown in Figs. 10 through 13.

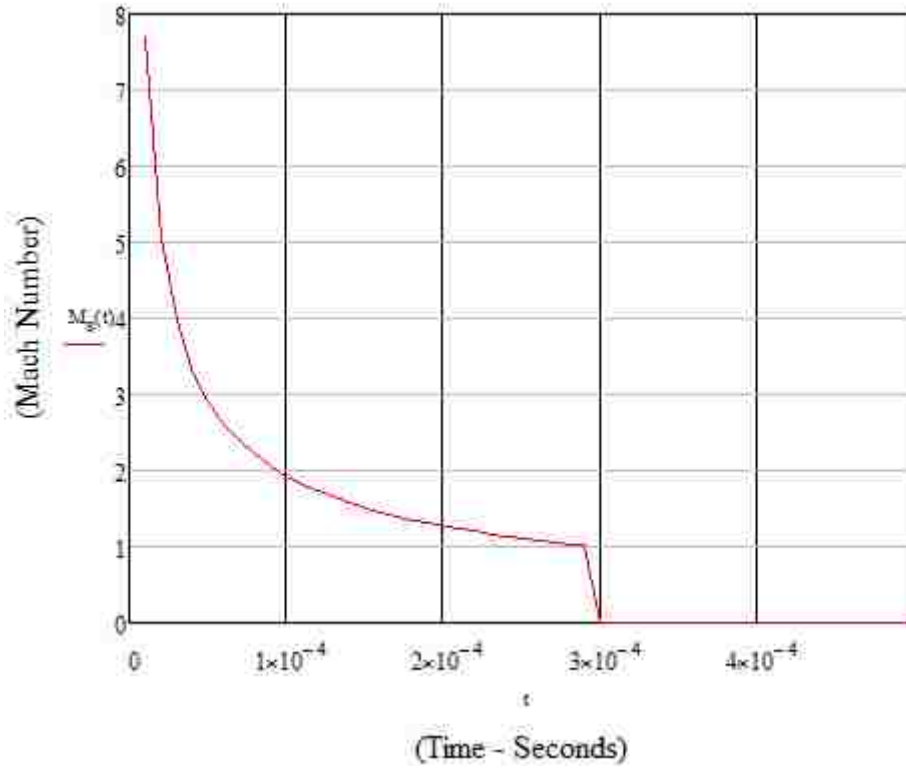


Figure 10 - Actual Shockwave Mach Number in the Reactor Medium

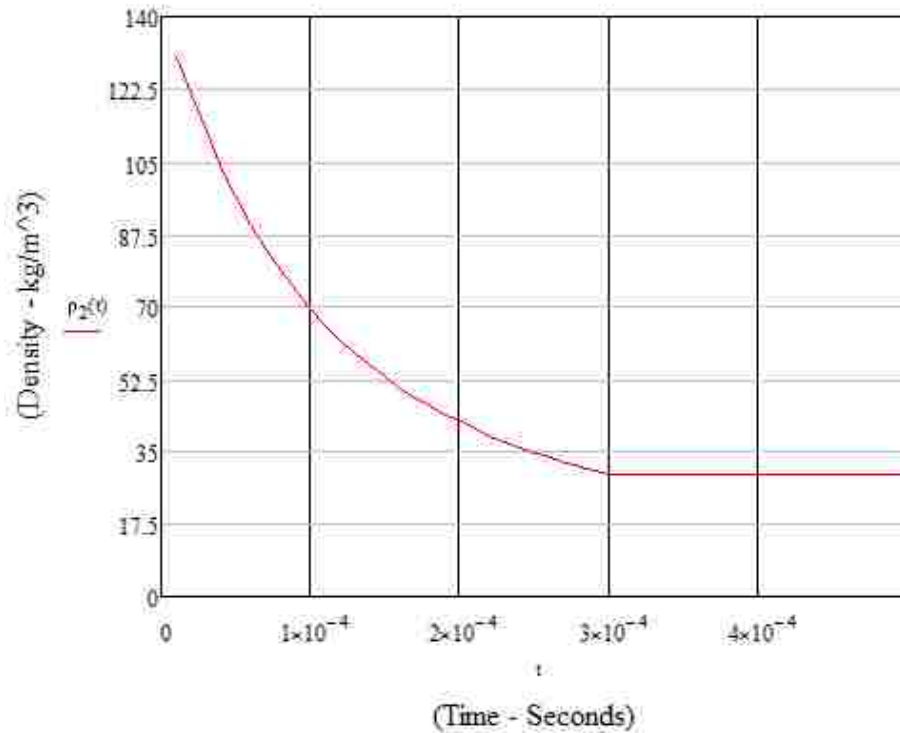


Figure 11 - Maximum Shockwave Density in the Reactor Medium as Bounded by Mach Number

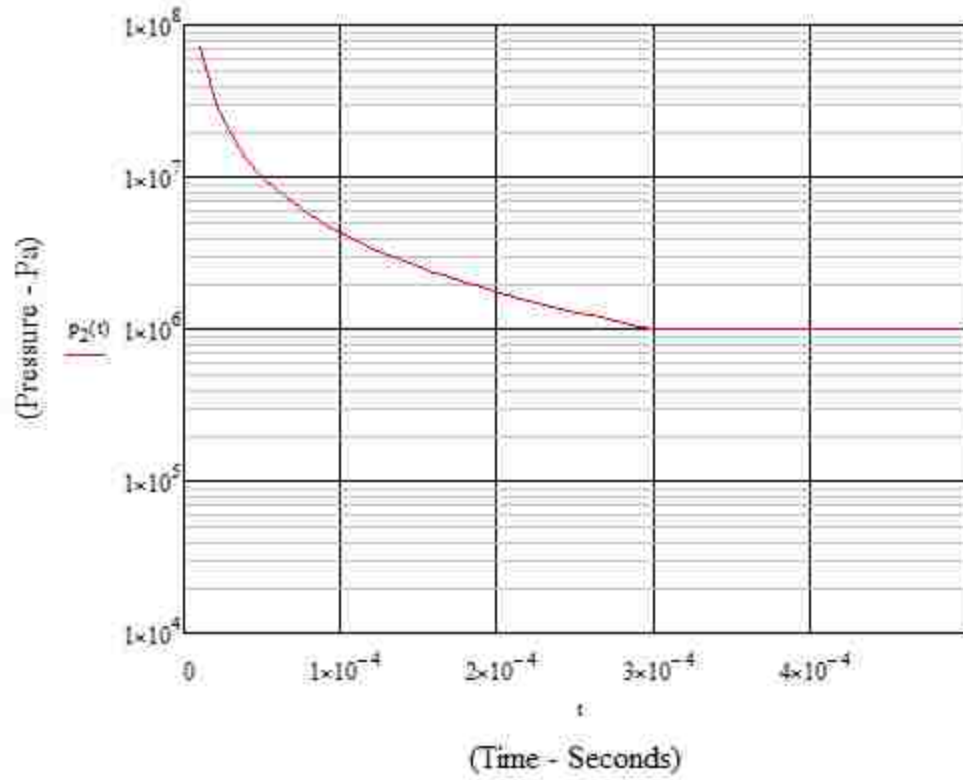


Figure 12 - Maximum Shockwave Pressure in the Reactor Medium as Bounded by Mach Number

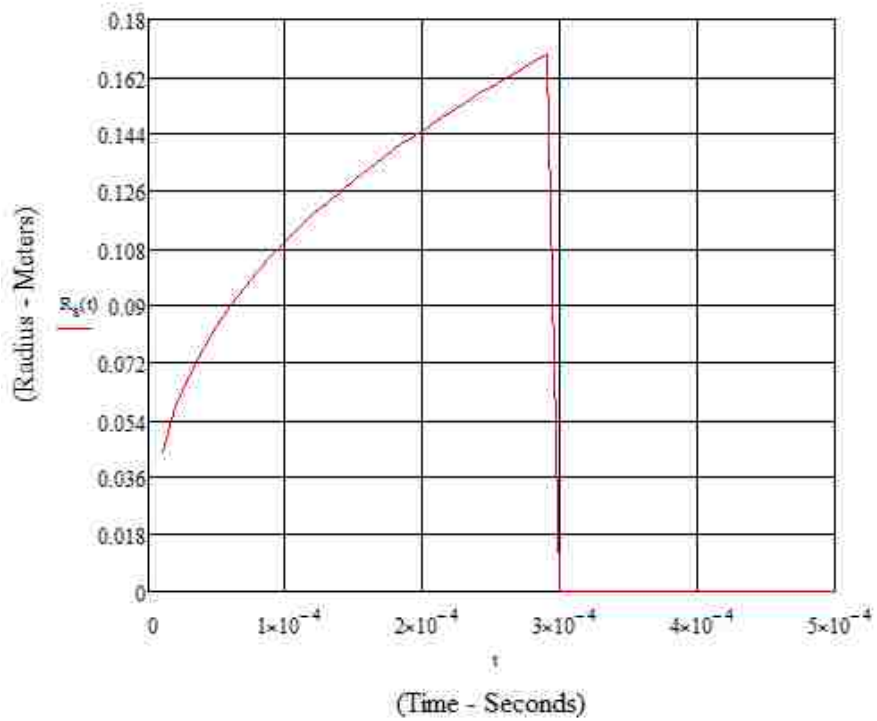


Figure 13 - Actual Radius of Shockwave Expansion in the Reactor Medium as Bounded by Mach Number

The compressible flow results in Figs. 10 through 13 present the setup for and bounding extent of the analysis for neutronic computations presented in subsequent subchapters here.

Shockwave and Explosive Events Results

Using MATLAB, a code was developed in order to solve for the solutions presented by Taylor in equations [3-27] thru [3-41]. The specific algorithm syntax is shown in the MATLAB Appendix. Using the MATLAB output for $\gamma=1.4$, the values of f , ϕ , and ψ are very close to the hand calculations performed by Taylor. The error rate for this value of γ is less than 0.2%. The computational algorithm was then compared to the values of Taylor for the case of $\gamma = 1.3$ with the difference between the computational algorithm and Taylor being approximately 4% and giving a high degree of confidence in the computational method.

Based on the shockwave algorithm, curves were generated for ψ, f , and ϕ as functions of η for values of η between 1 and 0 and shown in Fig. 14. These curves use the derived input values tabulated in Tables 7 and 8.

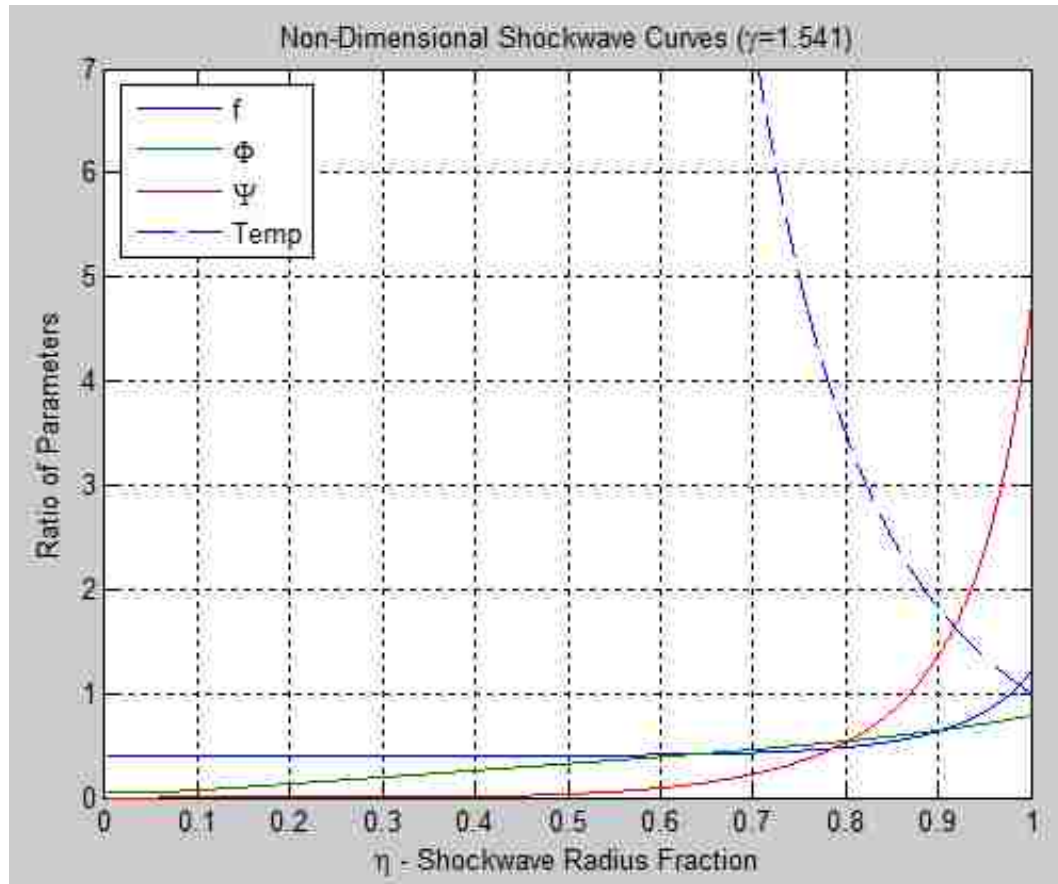


Figure 14 - Non-Dimensional Shockwave Curves as Determined for an Arbitrary Shockwave Radius (R)

The ψ curve is the ratio for density. This curve, when compared to compressible flow theory for initial density, is in very close agreement. Compressible flow theory calculates a maximum density ratio of 4.4, while shockwave theory predicts a maximum density ratio of 4.7. This results in a difference of approximately 7%.

As noted in Chapter 3, the pressure of the shockwave can be estimated using equation [3-41]. Additionally, Taylor notes that there is significant error associated with his estimation of the pressure and pressure ratio (Taylor, The Formation of a Blast Wave by a Very Intense Explosion I. Theoretical Discussion). Nonetheless, the pressure was calculated using his equation to determine if the approaches assumed in compressible

flow are applicable. The derived pressure results as calculated by shockwave theory are shown in Fig. 15.

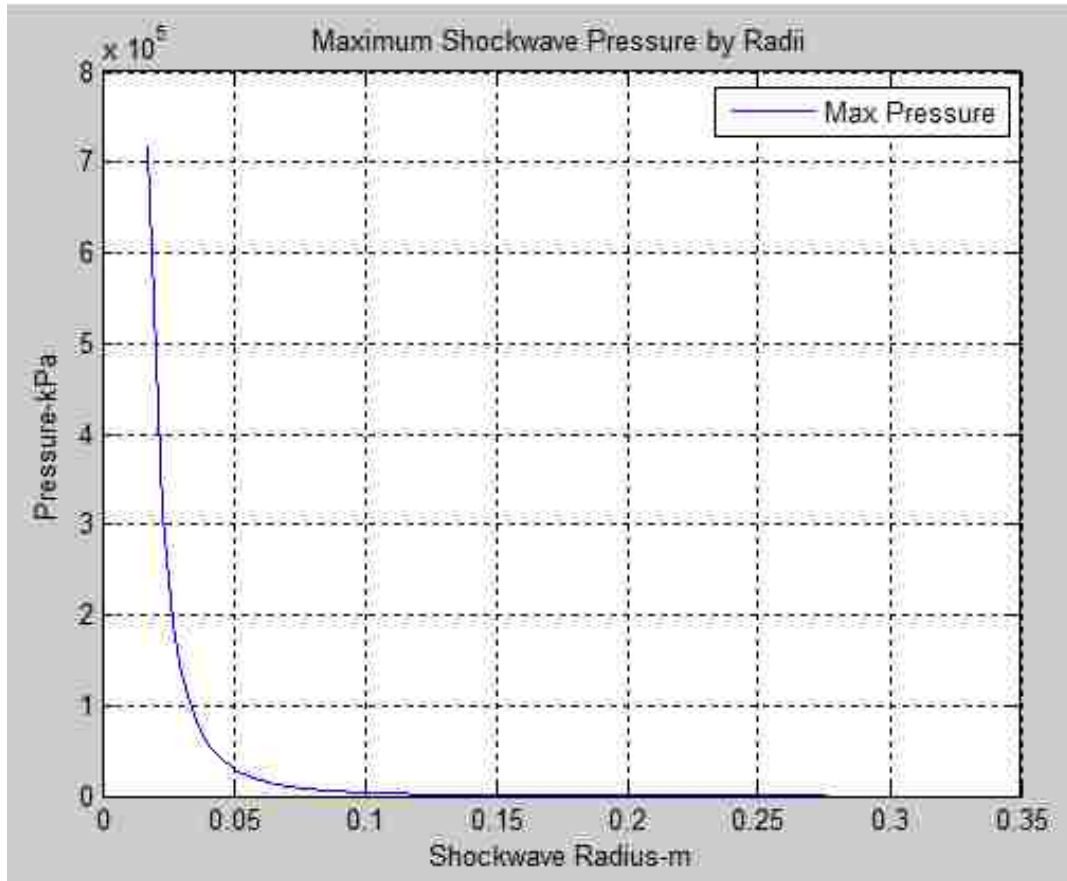


Figure 15 - Maximum Shockwave Pressure as Determined by Taylor Similarity Methods

As it can be seen, the pressure, as calculated by Taylor, follows a similar pattern. At the near instant of the event initiation, the maximum pressure is different from compressible flow theory by approximately 37%. There is plausible explanation for this difference, however, that may lie in the applicability of both theories to the spherical shockwave reactor problem. Compressible flow theory was developed and studied primarily for shock tube analysis. This means the lack of boundaries and particle velocity may be over-estimating the actual pressure of the shockwave. Furthermore, shockwave

theory, as presented by Taylor, was primarily analyzed for a hemi-spherical shockwave in atmospheric air, using only non-computational, analog methods.

Analytical Neutron Transport Results

Using the calculated density and spherical volume, coupled with conversions for molar fractions, the initial quantities of each element can be calculated as shown in Tables 9 and 10. This information can be used to compute the number densities of each element and isotope when applied to [3-5]. All results are calculated assuming 80% Uranium (235) enrichment and 20% Uranium Concentration in the reactor medium.

Table 9 - Composition Parameters for Nuclear Variable Determinations

<i>Composition Parameters</i>			
Reactor Volume [cm ³]	Mass of Mixture [kg]	Mass UF ₆ [kg]	Wt.% UF ₆
65,450	1.93	1.846	0.956
Mass Helium [kg]	Mass ²³⁵ U [kg]	Mass ²³⁸ U [kg]	Mass Fluorine [kg]
0.085	0.993	0.251	0.602
Wt.% Helium	Wt.% ²³⁵ U	Wt.% ²³⁸ U	Wt.% Fluorine
0.04380	0.51426	0.13021	0.31174

Table 10 - Atomic Number Densities Corresponding to Composition Parameters

<i>Composition Number Densities [at./barn-cm]</i>			
Helium	²³⁵ U	²³⁸ U	Fluorine
1.943E-04	3.887E-05	9.717E-06	2.915E-04
UF ₆		Mixture	
4.859E-05		2.429E-04	

From the detailed composition, it is possible to calculate the macroscopic cross-sections, as required for the criticality and transport equations and shown in [3-6] thru [3-10] and [4-2] thru [4-18], given the composition number densities in Table 10 and the microscopic cross-sections shown in Table 11. For One-group theory, the average microscopic cross-sections are shown as:

Table 11 - Microscopic Cross-Section Data from ENDF/B Nuclear Data Library³

<i>Microscopic Cross-Sections [barn]</i>				
	Helium	²³⁵ U	²³⁸ U	Fluorine
Absorption (σ_a)	0	681	2.717	0.1
Scattering (σ_s)	0.759	15	10	3.8
Fission (σ_f)	0	584	12E-06	0

Table 12 - Calculated Macroscopic Cross-Sections for UF₆

<i>Macroscopic Cross-Section [1/m]</i>		
Absorption (Σ_a)	Fission (Σ_f)	Transport (Σ_{tr})
2.328	2.27	6.51E-03

Using the macroscopic cross-sections as shown in Table 12, the diffusion coefficient, diffusion length, material buckling, and migration length can be determined for the undisturbed region of the reactor.

Table 13 - Material Constants in Undisturbed Region of the Reactor Medium

<i>Material Constants in Undisturbed Reactor Medium</i>			
D ₁ [m]	L ₁ [m]	B _m ² [1/m ²]	M ² [m ²]
51.201	4.690	0.056	33.113

³ (Korea Atomic Energy Research Institute (KAERI))

Using the given average value of ν and the assumed values for ε and ρ as shown in Table 14, k_{inf} is calculated for the gaseous reactor medium as shown in equations [3-6] thru [3-10].

Table 14 - Calculation of k_{inf} for the Reactor Medium in an Undisturbed State

<i>Calculation of k_{inf}</i>					
ν	η	f	ε	ρ	k_{inf}
2.43	2.08	0.99	1.05	1.00	2.16

Using the material constants specified in Table 13 and k_{inf} in the undisturbed reactor medium, the steady state k_{eff} in the undisturbed reactor, is estimated to be:

$$k_{eff} = 0.785$$

The steady state multiplication factor is calculated in accordance with [4-18]. Considerations of the Beryllium reflector surrounding the reactor medium are not factored into this calculation. While the diffusion methodology used for calculating k_{eff} does have inherent limitations, it provides a relatively reliable estimation of reactor criticality for steady state design experiments.

As the shockwave is applied, the parameters at the shockwave front change sharply. Using One-group theory, analysis of k_{eff} is only possible as a step-type function. It is helpful, however to analyze the effects of the shockwave on the diffusion constants that are specified for steady state in Table 13. These results include the cutoff effects of the shockwave dissipation at Mach 1, which occurs at 2.9×10^{-4} seconds.

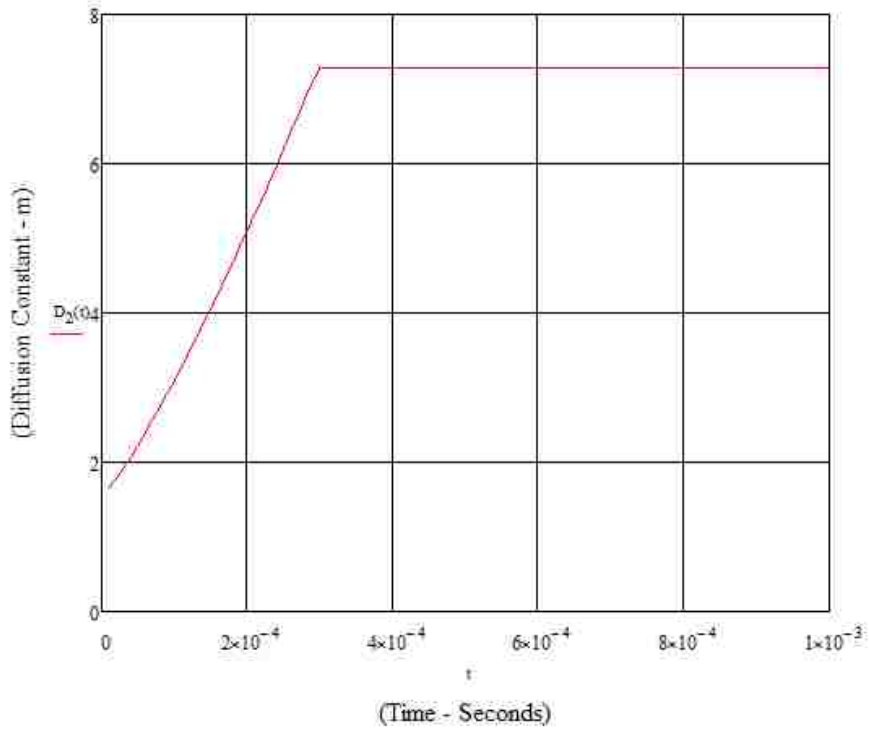


Figure 16 - Diffusion Constant (D) within the Transient Reactor Region

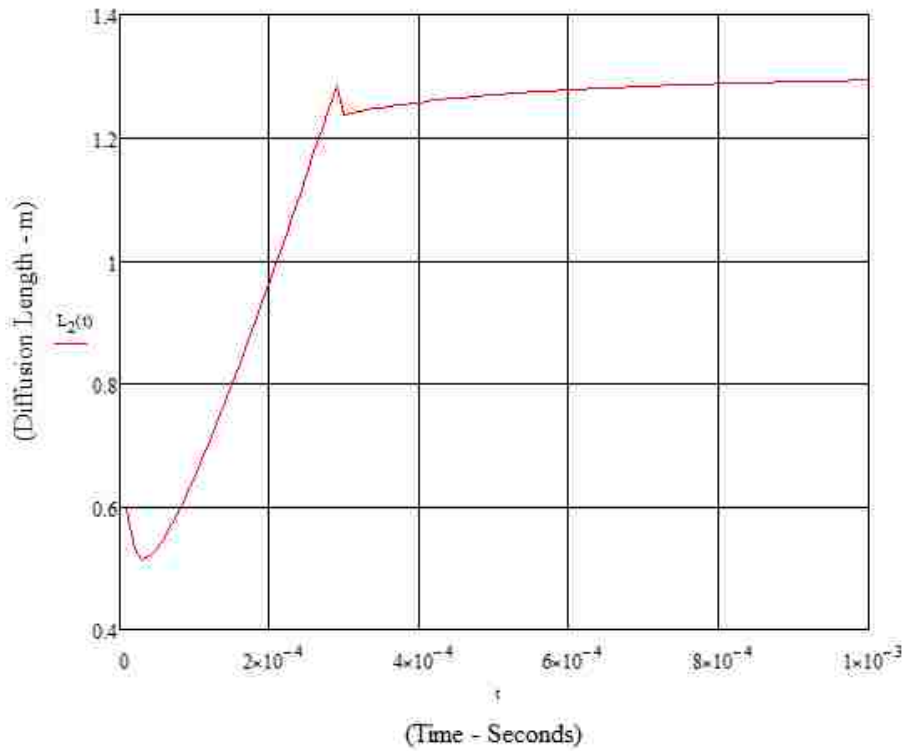


Figure 17 - Diffusion Length (L) within the Transient Reactor Region

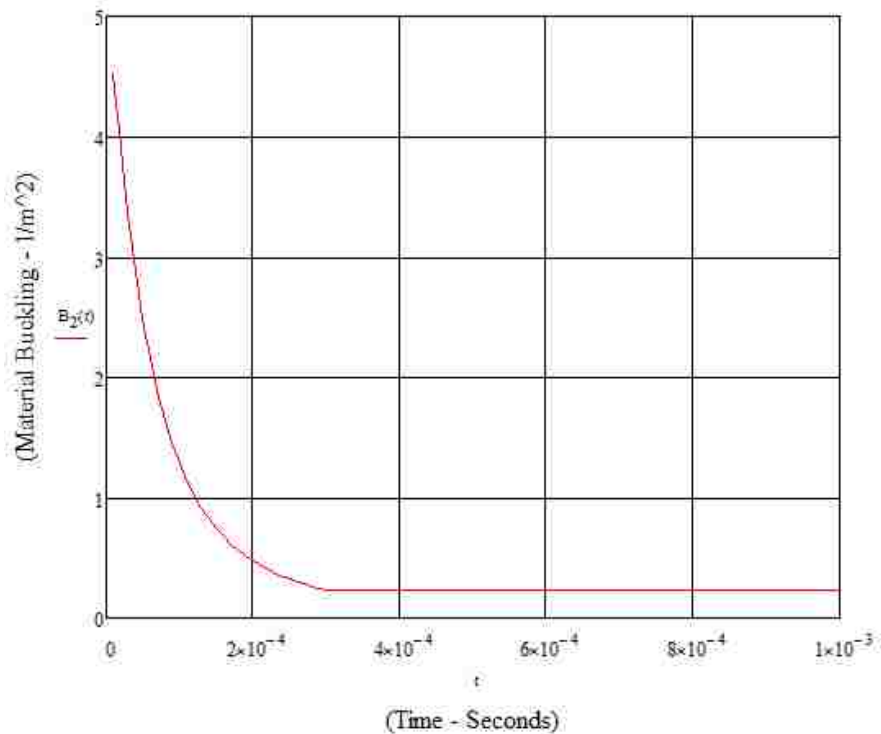


Figure 18 - Material Buckling (B_m^2) within the Transient Reactor Region

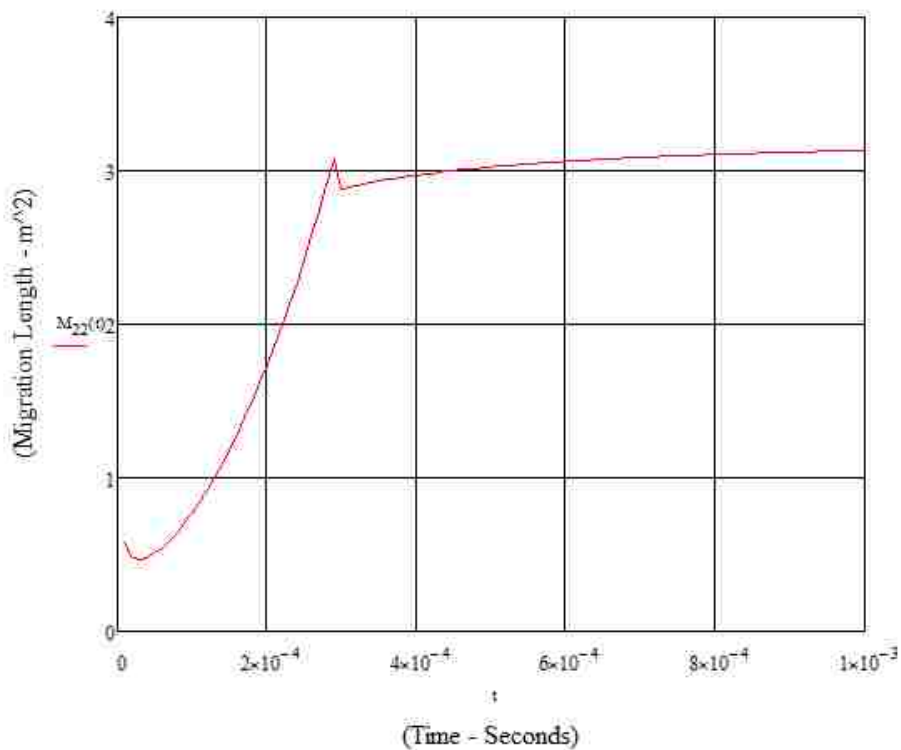


Figure 19 - Migration Length (M^2) within the Transient Reactor Region

Therefore, the k_{eff} step across the shockwave, as a function of time is shown to reach a maximum at the limit where the shockwave transforms from supersonic to subsonic.

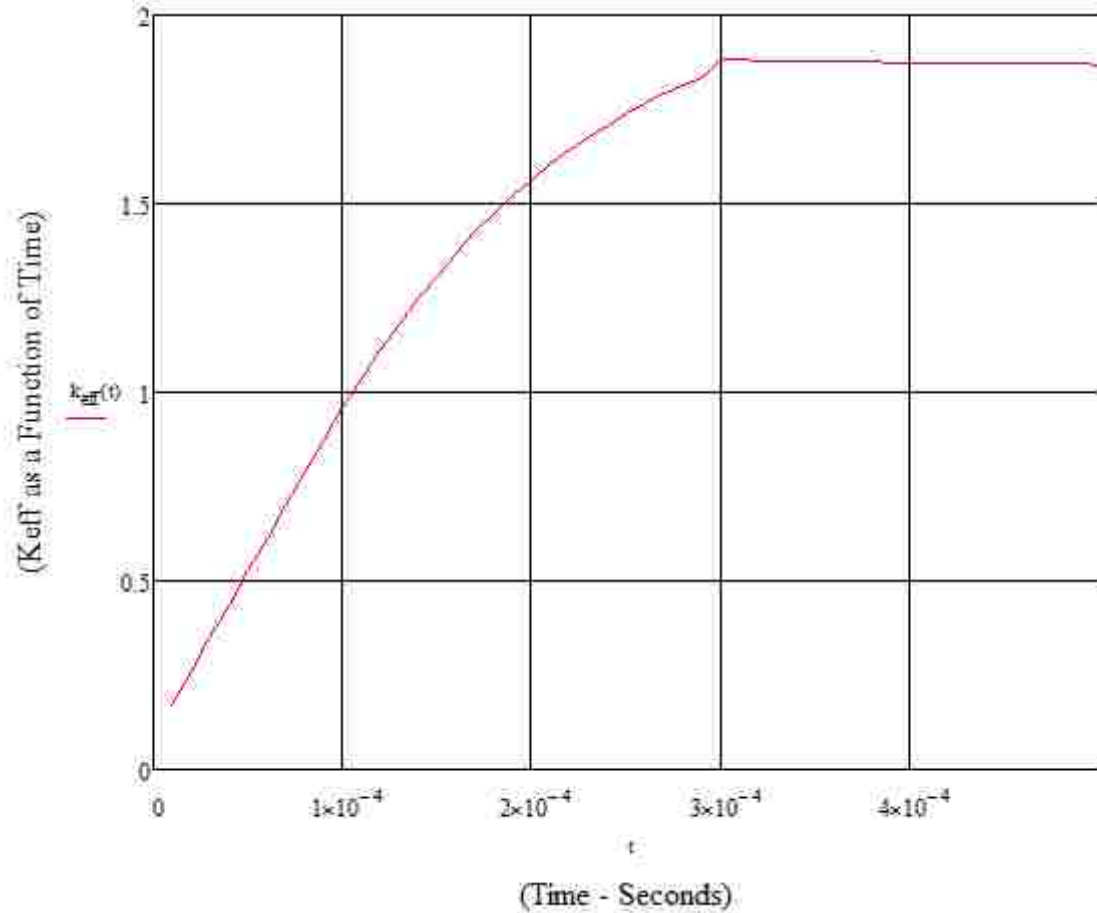


Figure 20 - Analytical Solution to Transient Region k_{eff}

Additionally, the solution to the transport equation can provide a unique perspective into the flux of the reactor and the neutron rates as a function of time. This is the graphical representations of [5-8a] and [5-8b]. An arbitrary initial flux of 10^8 neutrons per cubic centimeter was used as the initial point source value of the solution.

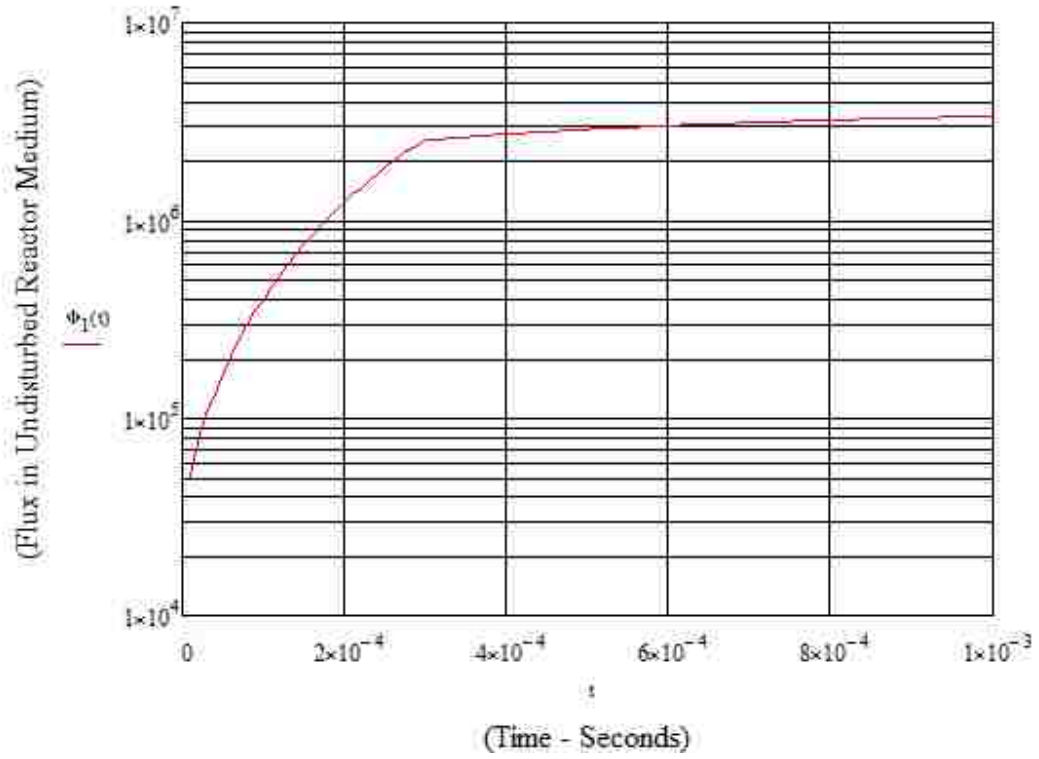


Figure 21 - Neutron Flux in the Undisturbed Region of the Reactor Medium

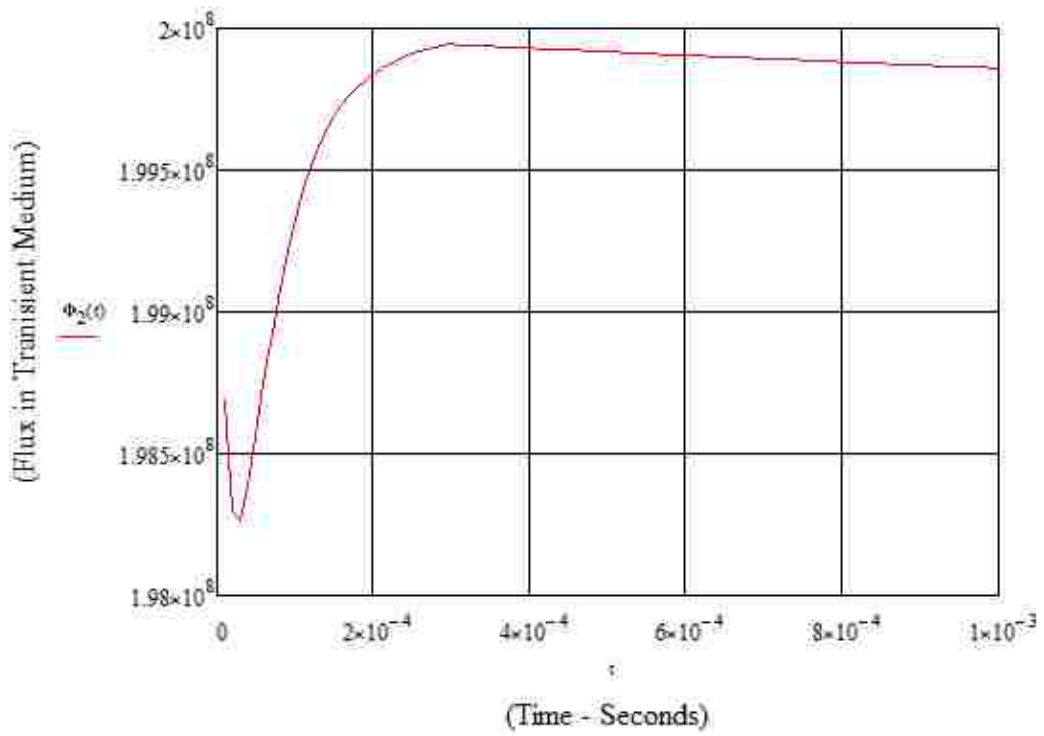


Figure 22 - Neutron Flux in the Transient Region of the Reactor Medium

Figs. 21 and 22 imply the flux in the undisturbed medium increases by several orders of magnitude based on outward-direction fissions and neutron scattering at energies greater than the speed of the shockwave.

MCNPX Results

Computation analysis of the reactor is accomplished using MCNPX as described in Chapter 4. MCNPX is the preferred computational analysis tool used in the United States for reactor analyses. MCNPX is used to accurately determine criticality and reactor kinetics, generally by validating the system against known results and computational models. The spherical shockwave reactor analysis, however, is not validated for here because several additional parameters related to released fission energy and fission product modeling, which is beyond the scope of this study; affect the validity the results presented herein. Using the parameter inputs determined in Table 9, Fig.13, and the Numerical Results Appendix; MCNPX computations were ran in an attempt to determine a one-for-one comparison between the computational analysis and the analytical results. Initially, a kcode input deck was run for understanding of the effect of the shockwave on the criticality of the system as a whole. The results of the kcode analysis are detailed in Table 15. As the table shows, MCNPX predicts that changes in k_{eff} are minimal, regardless of the position of the shockwave. This is most likely due to the way source particles are handled with kcode computations as discussed in Chapter 4. Since the majority of neutrons thermalize in the undisturbed reactor region, MCNPX interprets the undisturbed region to be the appropriate source medium and shifts the focus of the

analysis to this region, rather than the shockwave, which is also discussed further in Chapter 4.

Table 15 - Criticality Value with Standard Deviation as Determined in MCNPX

<i>Kcode Calculations for Full MCNPX Model</i>		
Shock Radius	k_{eff}	Std Deviation
No Shock	0.84141	0.00114
1cm	0.84338	0.00108
2cm	0.84171	0.00113
5cm	0.84107	0.00116
11cm	0.84683	0.00117

The consistency of the k_{eff} calculations validates the need for a new or different method for calculating multiplication factors based on the descriptions described in Chapter 5. It is important to compare the MCNPX model results to the analytical solution. Using \hat{M} values, calculated as shown in [5-10] through [5-14], the multiplication value is determined for the shockwave only MCNPX models. The result is presented in graphical format in Fig. 23 with specific data points listed in Table 16. This data can be compared to the analytical k_{eff} solution shown in Fig. 20.

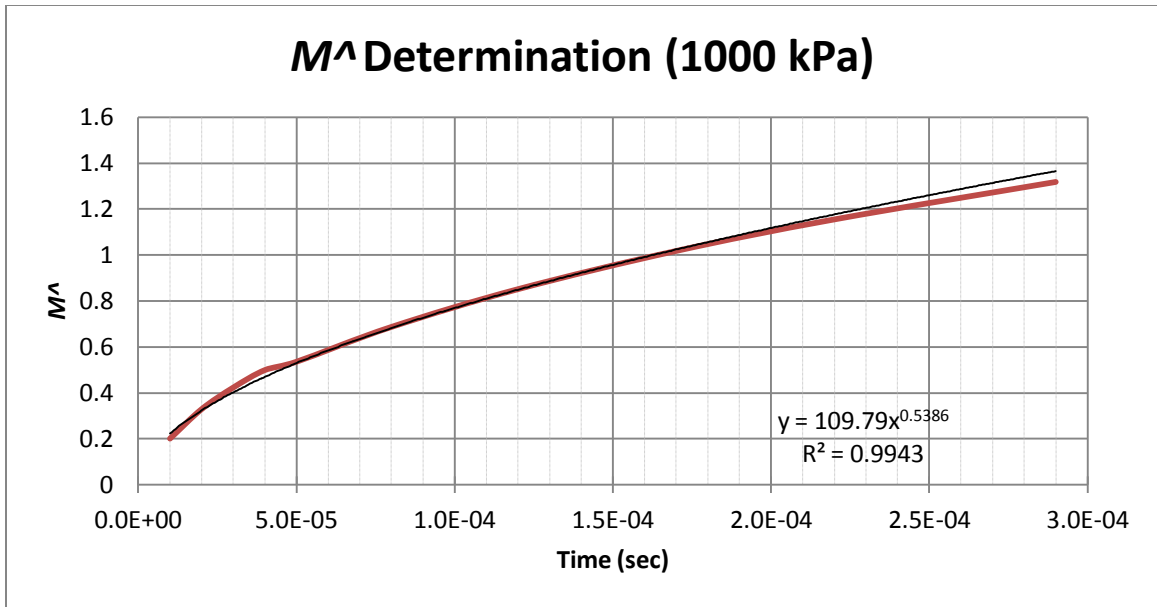


Figure 23 - Computational Solution to Transient Region M^{\wedge}

Table 16 - Select Values to the Computational Solution to Transient Region M^{\wedge}

<i>M^{\wedge} by Radius and Time</i>					
M^{\wedge}	2.02E-01	3.30E-01	4.24E-01	5.00E-01	5.36E-01
radius	4.38	5.78	6.8	7.6	8.3
time	1.00E-05	2.00E-05	3.00E-05	4.00E-05	5.00E-05
M^{\wedge}	6.87E-01	8.51E-01	1.02E+00	1.15E+00	1.32E+00
radius	10	11.8	13.6	15.1	16.8
time	8.00E-05	1.20E-04	1.70E-04	2.20E-04	2.90E-04

The results of the computed \hat{M} values are in good agreement with the much more conservative analytical results. Going a step further, the MCNPX outputs were used to calculate M^* as a function of the discontinuity as described by [5-15] and [5-16]. This is shown in Fig. 24. As expected M^* results closely resemble the analytical results of the Mach number calculations, proving that neutron multiplication becomes subcritical at the end of the shockwave event.

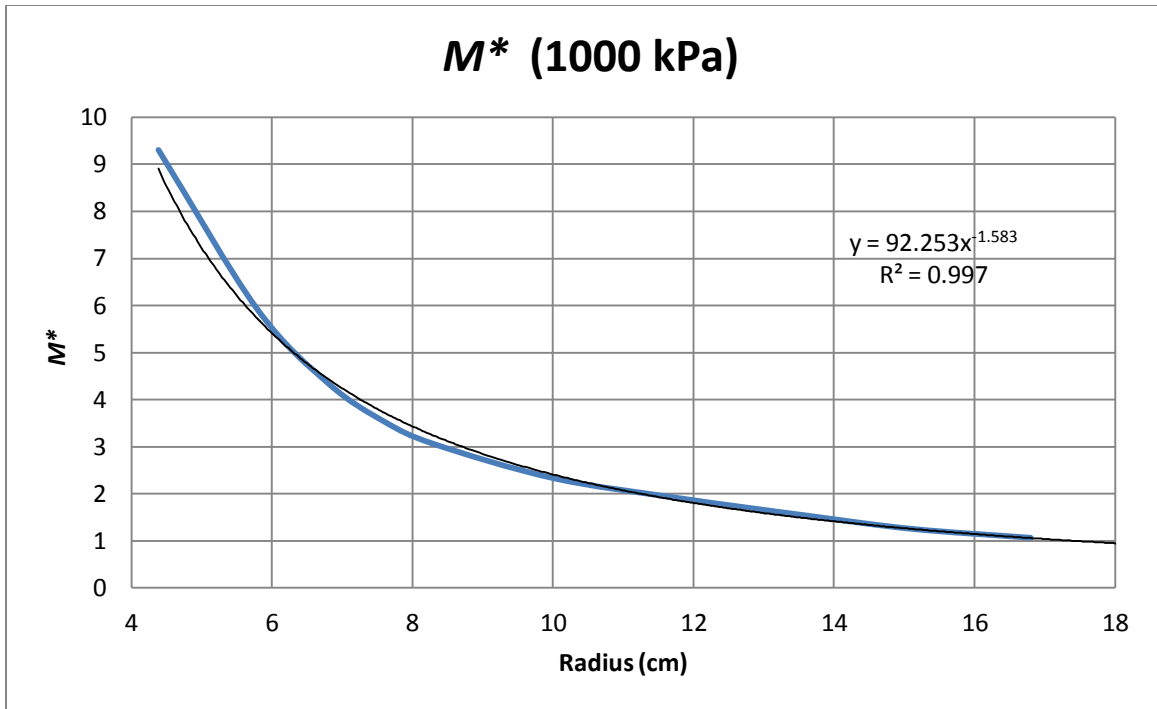


Figure 24 - Local Shockwave M^* as a Function of Radius

A quick regression of M^* shows a power curve fit to resemble the most accurate regression.

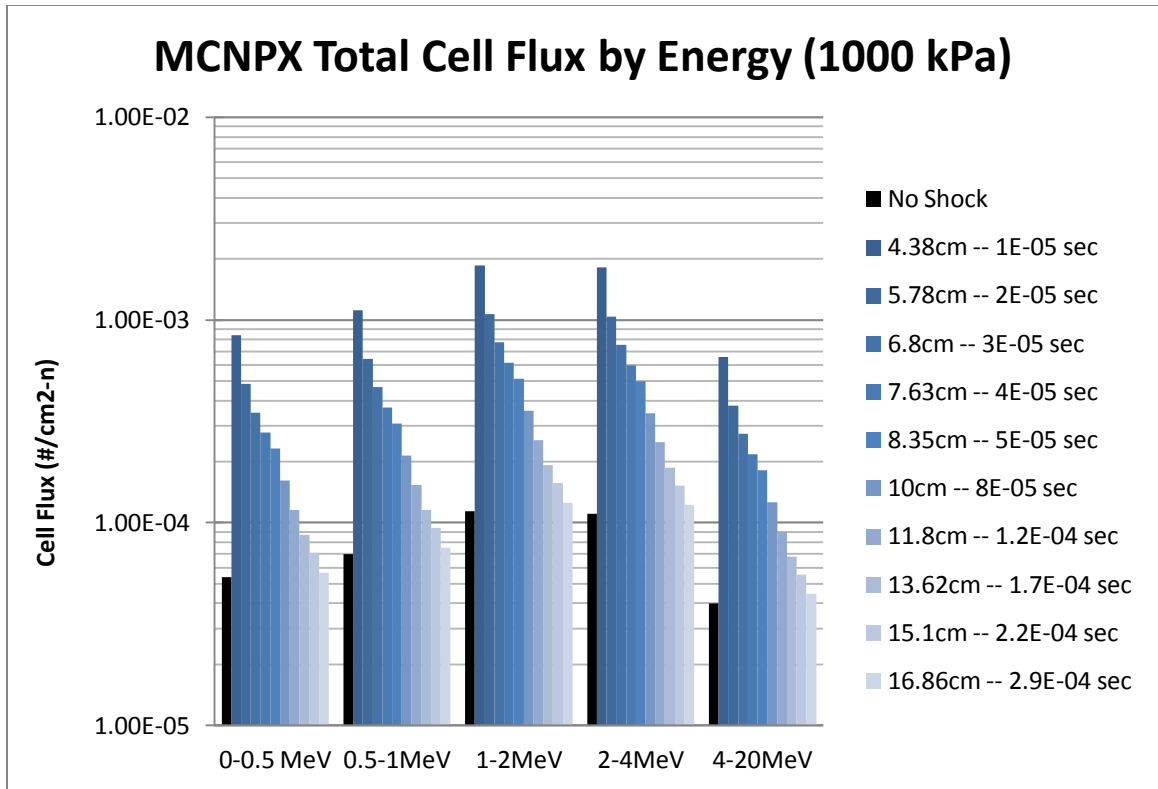


Figure 25 - Cellular Flux by Track Length as Determined by MCNPX for Radial-Time Steps by Energy Bin

Analyzing the shockwave fluxes as a function of radius, by energy, as shown in Fig. 25, shows a trend similar to M^* . It is clear from Fig. 25 that the neutrons are generally in the much faster region of the energy spectrum. The results shown in Fig. 25 are normalized per source particle and not adjusted for the differential volume of the transient region. Figs. 24 and 25 confirm that once the Mach number of the shockwave reaches subsonic values, the system returns to a subcritical state and the neutron population will decrease appropriately until nominal a subcritical state is reached.

Variation of Parameters

Complete analysis of the system is accomplished by looking at the trends of the system. To do this, single parameters were varied in a controlled manner and MCNPX input files were run.

Understanding the initial relationship between the fraction of helium and percent enrichment is one of the more complicated starting points in determining the setup for proper analysis. Based on [3-3], and [3-5] through [3-9], assuming ε and ρ are equal to one, the results for k_{eff} were graphed and contoured. The numeric value of k_{eff} is shown on the right hand side of Fig. 26.

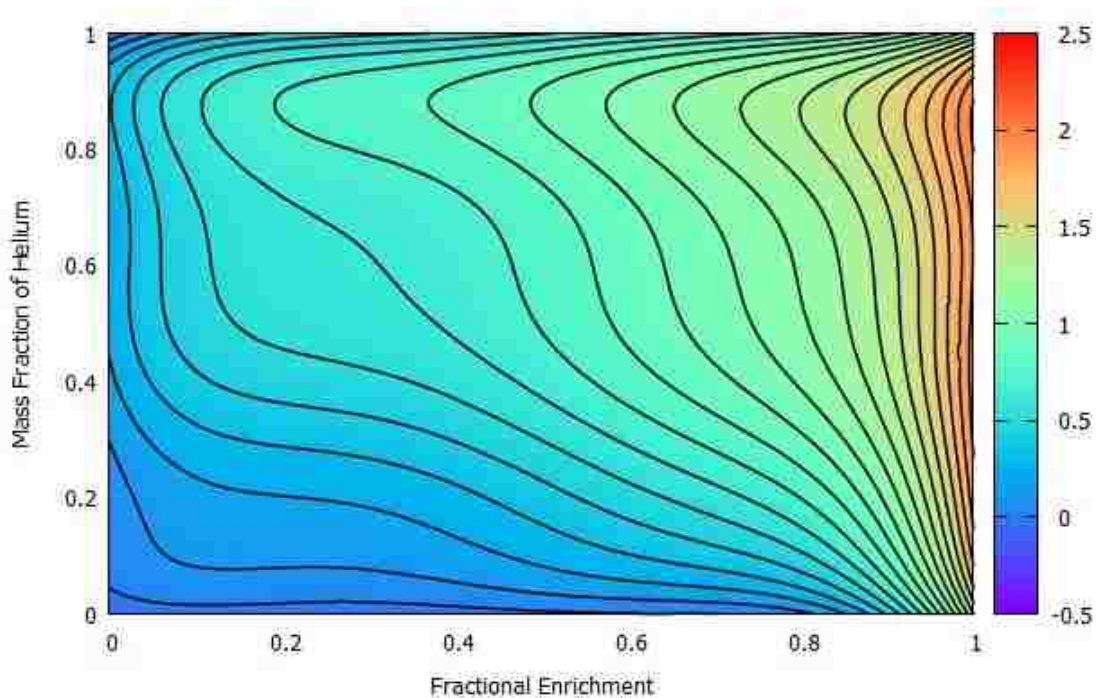


Figure 26 - Contoured Results for k_{eff} for the Undisturbed Reactor Configuration Analyzing Enrichment and Concentration

Using MCNPX, a kcode input for atmospheric pressure and no shockwave was run to determine the effects of nominal pressure. MCNPX has no input deck for pressure,

however, since density and pressure are intricately linked by the ideal gas equation, changes in pressure will change the density of the gaseous reactor medium. The same approach was taken for varying the concentration of the gaseous medium. Variation of the concentration of the medium changes the weight percent and the density to a minimal respect. The MCNPX results of these variations are shown in Figs. 27 and 28.

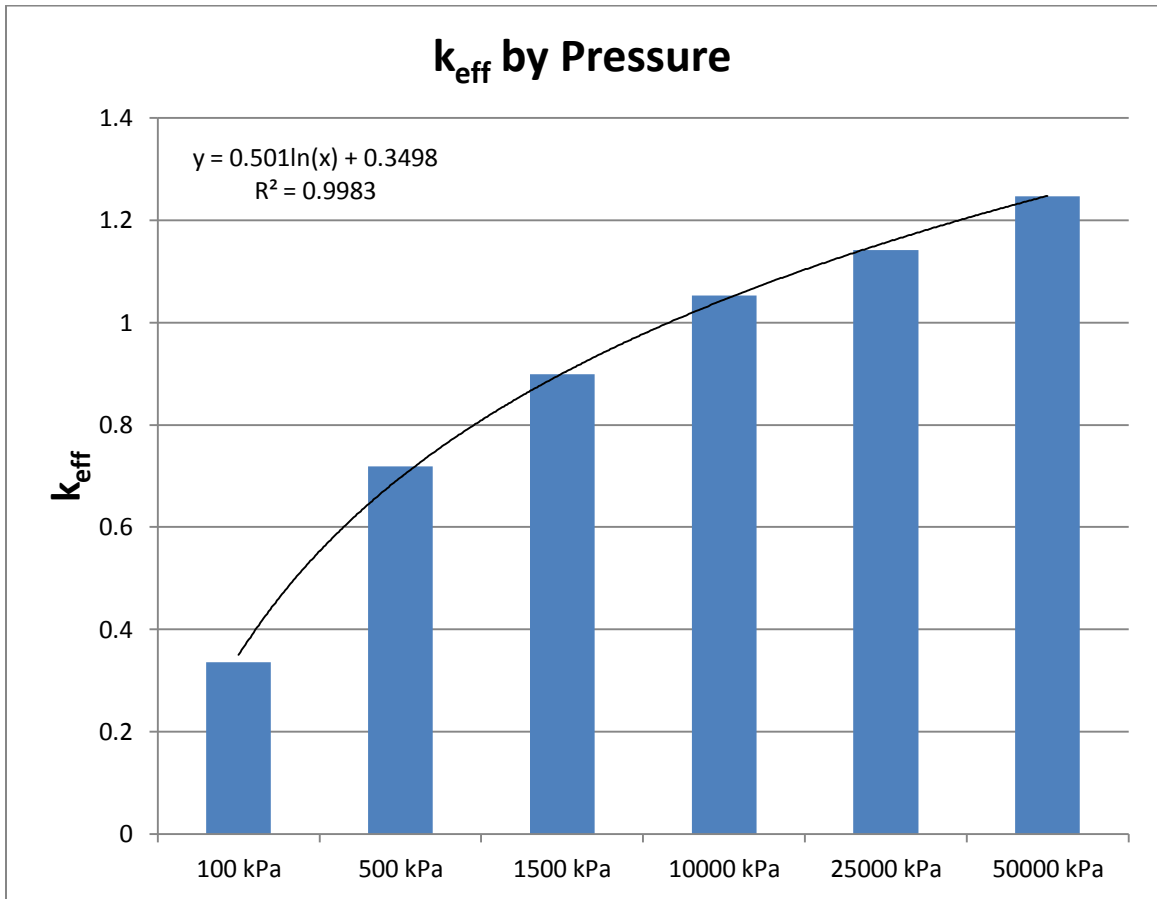


Figure 27 - Variation of Nominal k_{eff} Based on Changes in Pressure

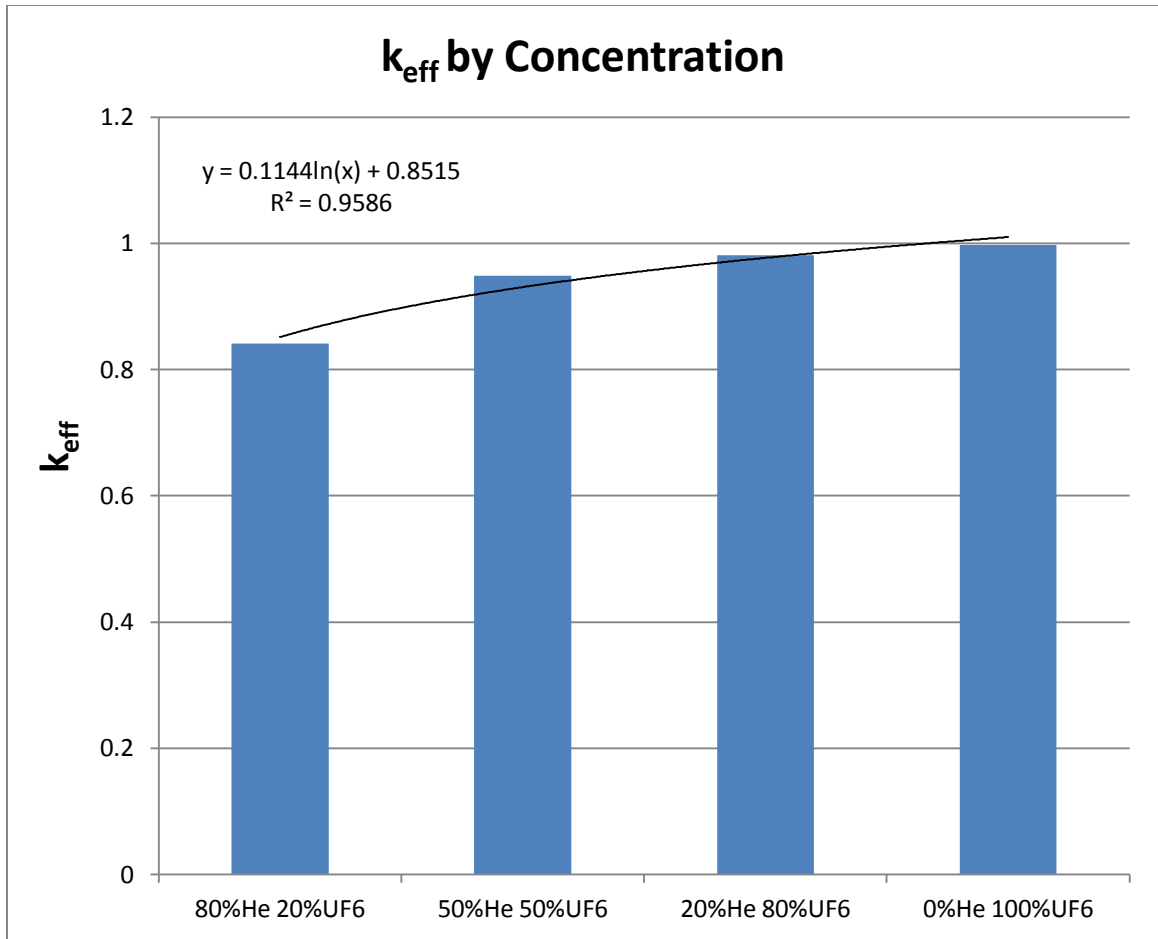


Figure 28 - Variation of Nominal k_{eff} Based on Changes in Concentration

Since variations in pressure seems to be the dominating factor, a second shockwave analysis was performed for \hat{M} and M^* at atmospheric pressure. For a one-to-one comparison to the \hat{M} and M^* results shown in Figs. 23 and 24, the initiating energy was not manipulated. Several other factors would be present in this variation of the analysis that are not considered here, such as effects of shockwave reflection on the transient medium. Because the initiating energy was not adjusted for the decrease in the reactor medium density, the intensity of the shockwave is much more acute. The effect of the increase in intensity is shown as an increase in M^* in Fig. 30. Using a simple kcode

MCNPX computation, k_{eff} of the nominal system at atmospheric pressure is determined to be 0.3363 ± 0.00068 . Extrapolation of the results along the regression curve estimates the shockwave to be approximately 36 cm in radius over the course of 640-microseconds.

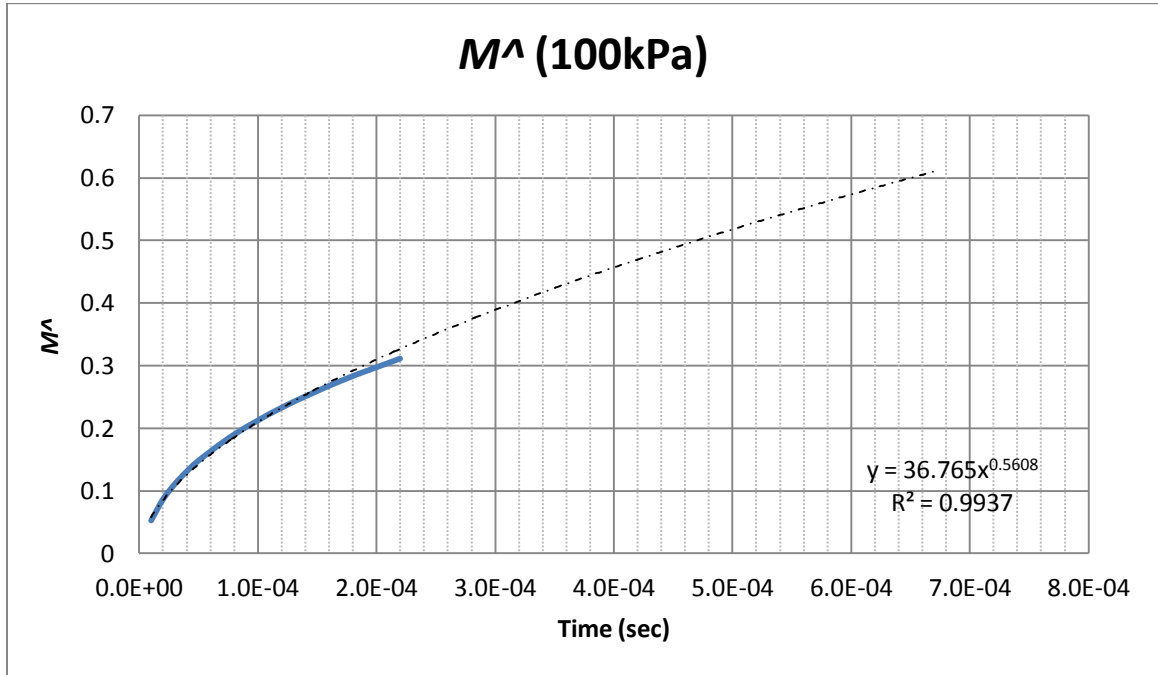


Figure 29 - Computational Solution to Transient Region $M^$ for Nominal Atmospheric Reactor Pressure

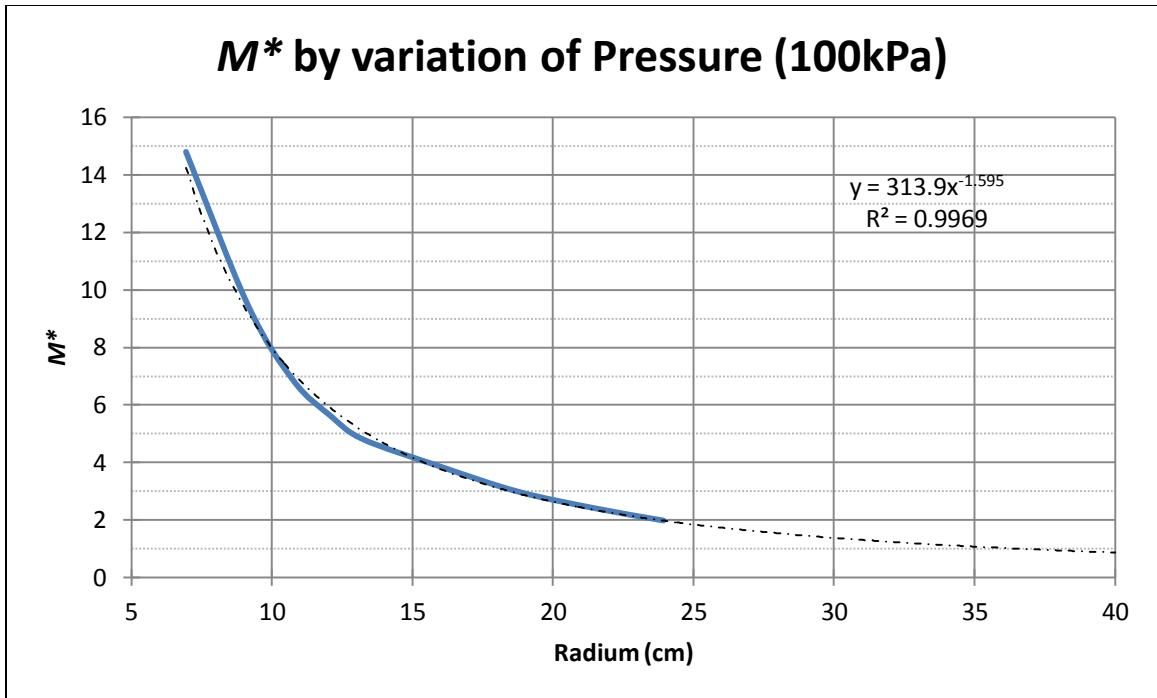


Figure 30 - Shockwave M^* as a Function of Radius for Nominal Atmospheric Reactor Pressure

Finally, the cellular flux of the shockwave by energy bin was also determined for complete analysis of the effect of the change in pressure. The results are shown in Fig. 31 along with an analysis of the kcode computation and labeled “keff run.” The kcode computation was included in this figure as an example of the weighting placed on thermal neutrons by MCNPX.

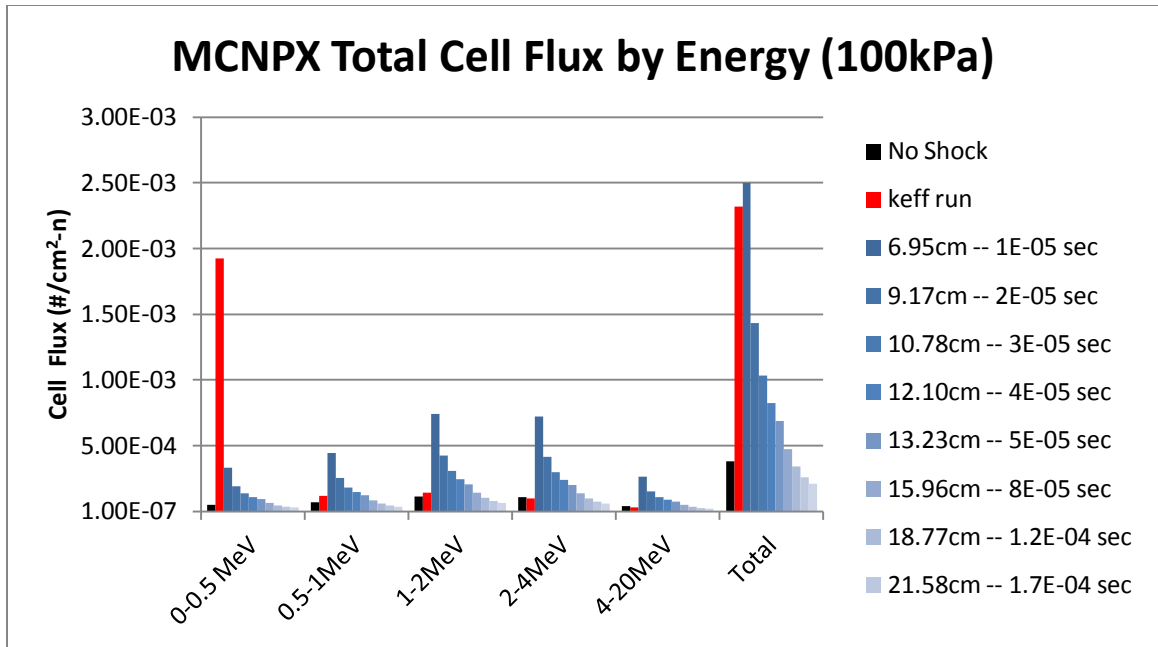


Figure 31 - Cellular Flux by Track Length as Determined by MCNPX for Radial-Time Steps by Energy Bin for Nominal Atmospheric Reactor Pressure

Design Cost

The spherical shockwave reactor requires a significant number of variables to operate in concert and harmony to function properly and safely. Several of these variables, such as enrichment, and the mechanical parameters of pressure and temperature design, can be defined from the outset.

Utilizing the results of Fig. 32 and [5-17a] & [5-17b], the cost of UF_6 can be optimally determined for incorporation into the reactor. For an enrichment of 80%, the cost per SWU is expected to be approximately \$850 for a tails depletion of approximately 0.18%. Based on the proposed design of the reactor, 1.846 kg of UF_6 is required. Using the equations, the kilograms SWU required is about 214. Therefore, the cost of UF_6 is

about \$182,000. The cost of Helium is assumed nominal for concentration purposes of this study.

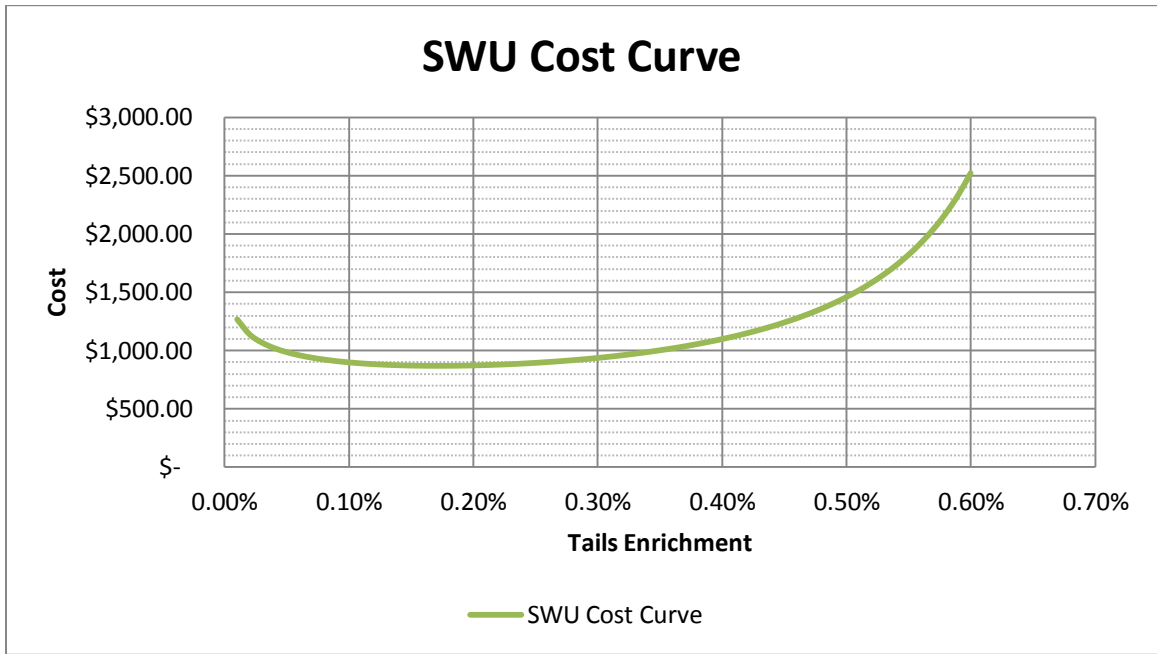


Figure 32 - SWU Cost Curve Results for Enrichment of UF₆

The outer pressure vessel is composed of AISI 302 steel. The yield strength for AISI 302 Steel is about 150MPa. Using a Factor of Safety of three and [3-46], the allowable stress is determined to be:

$$\sigma_{allow} = 50MPa$$

Back-calculating [3-47] for the thickness of the pressure vessel, the walls are determined to be a minimum of 12.5 cm in thickness. Using this steel thickness and [3-47] and [3-48], the maximum strains are determined to be approximately:

$$\delta \cong 10^{-8}$$

$$\delta_T \cong 10^{-6}$$

Therefore, the thermal strain from pressure will cause a greater risk of fatigue failure. However, the amount of deformation is insignificant for this design. The volume of steel required is then approximately 1.45 m^3 . Assuming a nominal cost \$1000/ton and a density of 8000 kg /m^3 , the total quantity of steel required is 12000kg with a cost of \$12,000.

Fig. 12 shows the pressure discontinuity will have dissipated by the time the shockwave reaches the interior reactor reflector; therefore, no additional analysis is required.

The Beryllium reflector is a softer metal as discussed in Chapter 3, therefore, its physical properties are not considered in this study. MCNPX results imply a reflector thickness of 65 cm is sufficient to contain the majority of the neutron radiation within the reactor medium. For this thickness, assuming the density of Beryllium is material to be 1850 kg/m^3 , the volume of Beryllium being approximately 3 m^3 , and a price for the material of approximately \$750/kg, the quantity of Beryllium required is about 6000 kg for a cost of \$4.5 million.

The final material cost of the reactor would be expected to be approximately \$4.6 million, not including the manufacturing costs associated with production.

CHAPTER 7 – CONCLUSIONS

The spherical gaseous shockwave reactor has been analyzed. A new generation of nuclear reactor is proposed and the feasibility of this reactor is studied. The spherical shockwave reactor is not limited to the constraints the Carnot heat cycle. This reactor design proposes using particle kinetic energy to create a voltage potential that can be converted directly into electricity. The large number of atomic particles and ions necessary for direct energy conversion is dependent upon the neutron population generated from the intensity of the shockwave. The focus of this study has determined the parameter changes and resulting nuclear criticality of the gaseous medium across the shockwave. Parameters such as pressure, density, and temperature all contribute to the criticality of the system. The local effects of the shockwave induce a change in the neutron generation rate and neutron population as the shockwave expands through the fissionable medium. The neutron generation rate is used to calculate the criticality of the system as induced from the shockwave and the instantaneous neutron population is used to determine intensity of the shockwave neutronics throughout the course of the shockwave.

Final Reactor Design as Proposed

The transient-state pulsed spherical uranium-hexafluoride reactor design is proposed. The reactor medium is a fissile gaseous mixture composed of UF₆ and Helium. The UF₆ is enriched to 80% ²³⁵U in order to provide a large probability of high-yield fission neutrons. Trace amounts of ²³⁴U are not analyzed in this study. The concentration of the fissile gaseous mixture is 20% UF₆, with the remaining 80% comprised of pure

Helium gas. This enrichment and concentration of UF_6 correspond to masses of each isotope and atom as specified in Table 9. The mass of ^{235}U is in accordance with the single-parameter mass limit curve shown in Fig. 5. The reactor size available for operations is spherical with a radius of 25cm, which equates to a reactor volume of $65,450 \text{ cm}^3$. At the center of the reactor is an energy initiation device that imparts 50,000 Joules of energy, the equivalent of 11.945 grams of TNT. The resulting shockwave discontinuity expands from the initiation point at the center of the reactor for approximately 16.86cm over the course of 0.29 milliseconds. Surrounding the reactor is a reflecting shield of pure Beryllium. This shell is 65cm thick and provides a source of radiation shielding as well as a mechanical boundary to assist the pressure vessel in containing excess pressure and heat. Finally, the outermost shell of the reactor comprises the pressure vessel. The pressure vessel material is AISI 302 stainless steel and 12.5cm thick. The pressure vessel is designed to withstand up to 50MPa with a safety factor of 3.

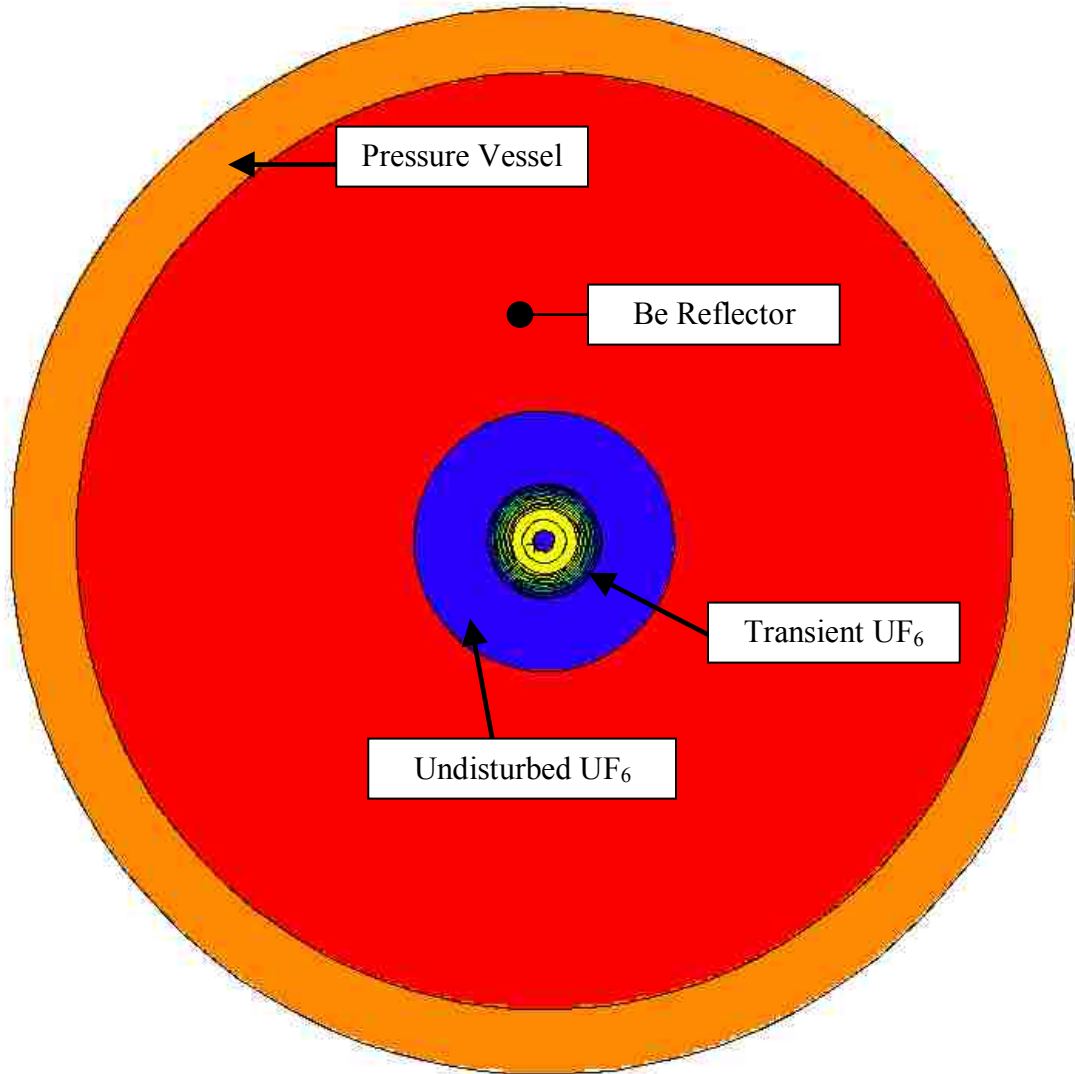


Figure 33 - Final Design of the Transient-State Pulsed Spherical Uranium-Hexafluoride Reactor

Summary of Results

The novelty of the reactor design proposed here is the utilization of a pressure shockwave in order to increase system density and provide a short physical window for an increase in localized system reactivity. As the shockwave travels through the fluid medium, the localized characteristics parameters, such as pressure, temperature, and

density, change across the shockwave boundary. Changes in these parameters affect the neutronic characteristics of the fissile medium. The system is initially in a subcritical state, therefore, increases in pressure and density increase the reactivity of the system. Increases in temperature, on the other hand, reduce the reactivity of the system. While the effects of temperature on the system are important for determining the reaction probabilities of the system, they are overshadowed by the general trend of increasing criticality that is induced by changes in pressure and density. The system will create a brief physical window of supercritical reactions as the parameters change across the shockwave front, then return to a subcritical state after the shockwave passes and parameters return to nominal state.

The physics of the shockwave are well described. Compressible flow theory analyzes the magnitude of the discontinuity as a function of time and radial distance from the initiating event. The UF_6 fissionable medium is assumed calorically perfect and properly described by the ideal gas law Equation of State. Using the given initial parameter values as presented in Chapter 6, the Mach number analysis shows the initiating energy event produces a shockwave discontinuity at a speed of nearly Mach 8, which decreases exponentially for the first 290-microseconds, before retreating through Mach 1 and ending the discontinuity event. The variable Mach number can be used to calculate the discontinuity pressure and density changes as a function of radius and time in accordance with the continuity and conservation equations derived from the Navier-Stokes equation. For the given Mach number, the radial expansion of the shockwave during the given time of the event is slightly under 17 cm. In the 17 cm of radial expansion, the pressure ratio decreases from its maximum of approximately 71 times

nominal to initial pressure and the density ratio decreases from its maximum of approximately 4.4 times nominal to initial density.

Behind the shockwave front is a very turbulent and transient medium. In order to maintain continuity and conservation principles, the increases in mass, momentum, and energy at the discontinuity result in decreases in these states behind the shockwave front to a point where they are lower than the initial given values. Studies in support of large-scale explosion events have defined the ratio changes of the parameters throughout the locality behind the discontinuity. The differential equation used to describe the changes in these parameters is solved using Euler's method and assuming initial conditions that approach infinite at the moment of initiation. The primary ratio of interest from the solution is the density ratio. The solution predicts the maximum density ratio to be approximately 4.7, which is a difference of less than 7%. The maximum pressure ratio as defined by the shockwave solution is approximately 45 times nominal pressure. This result differs from compressible flow theory by about 37%.

With the radius, pressure ratio and density ratio defined for points before, across, after, and along the shockwave discontinuity, a proper neutronic analysis of the reactor can be verified. First, using the analytical One-group theory solution to the neutron transport equation, the general solution is set up as a spherical fissile medium with a spherical fissile blanket material. The infinite reactor multiplication factor is calculated to be 2.16, resulting in an effective multiplication factor of 0.785, which means the reactor is nominally subcritical by design. The analytical solution does not account for the Beryllium reflector. As the shockwave is initiated and applied, variations to the parameters implement changes to the material buckling value, migration length, diffusion

length, and number densities of the neutron transport solution behind the shockwave front. The resulting radial dependent analytical solution for k_{eff} in the shocked region increases to a maximum of 1.9, which is well into the supercritical regime. The neutron flux throughout the different fissile regions is also analyzed from the transport equation solution. The results show the neutron flux in the region behind the shockwave is nearly constant at a ratio close to that of k_{eff} . The neutron flux in the undisturbed medium ahead of the shockwave increases by nearly a factor of 100. This is most likely due to neutron leakage from the shockwave fission events in an outward direction. The energy imparted to neutrons from a fission event is described by the Watt Energy Spectrum curve. The physical speed associated with these energies is a minimum of 1.25 times faster than the maximum speed of the shockwave.

The accuracy of the analytical solution is considered through comparison to the computational analysis derived from MCNPX output results. MCNPX utilizes Monte Carlo methods to perform a statistical analysis of the reactor geometry. MCNPX uses millions of neutron histories repeated over and over with perturbations implemented through the use of random numbers. Two different types of computational analyses were performed; one using kcode inputs to analyze the initial criticality of the system before the shockwave is applied, and a second using SDEF inputs and cutoffs for time to analyze the neutron generation rate and instantaneous neutron populations of the shockwave discontinuity by itself. The kcode computations reveal a k_{eff} value of 0.84141 ± 0.00114 , which shows the analytical solution to criticality is different by approximately 7%. Kcode calculations did not effectively analyze the implementation of the shockwave discontinuity in the computation; therefore, using the SDEF code, a multiplication factor,

\widehat{M} , is derived and calculated based on the tallied neutron flux and source rates. \widehat{M} , for the system as a whole, is shown to rise in a manner similar to the analytical method to a value of 1.32. This implies the reactor will reach a supercritical state during the course of the shockwave event. A definition for the instantaneous multiplication ratio of the shockwave was derived and calculated based on the instantaneous neutron population. This multiplication ratio, M^* , is a measure of criticality analysis that is performed for quasi-static shockwave time-steps. M^* shows the instantaneous multiplication ratio of the shockwave as it emanates from the initiation point. The maximum ratio value of 9.3 leads to the conclusion that the initiation event is followed by an intense release in neutronic activity. M^* decreases as the shockwave intensity decreases until the local criticality of the discontinuity becomes subcritical at the point where the shockwave event dissipates to normal Mach 1 parameters and the discontinuity no longer exists.

Further analysis of the calculation trends are confirmed by analyzing the shockwave in atmospheric pressure conditions of the UF_6 medium. The nominal k_{eff} , as calculated from MCNPX using kcode inputs is determined to be 0.3363 ± 0.00068 . Application of the shockwave shows criticality can be extrapolated to show a rise in \widehat{M} to a value of just less than 0.6 throughout the 36 cm, 640-microsecond course of the discontinuity provided there is no boundary limit to the shockwave. The local M^* is higher for this configuration, approaching a maximum value of 14, however, that is most likely due to keeping the initiating energy event constant, which creates a sharper, more intense discontinuity through the reactor.

In summary, this study shows the proposed transient-state pulsed spherical gaseous uranium-hexafluoride reactor is a viable research project worth pursuing.

Application of a shockwave to a gaseous fissile medium can induce criticality. Adjustment of the initial conditions can allow conditions for controlled study of the reactor without inducing supercritical states in the fissile medium. While the initial cost of building this reactor is great, the additional value of scientific knowledge and understanding of nuclear physics would be priceless in terms of setting this industry and world on a path of long-term and future energy needs.

Recommendations for Future Work

Many questions regarding the proposed reactor design remain unanswered. Chief among these questions are regarding the feasibility of electrical production. Future research will require substantial analysis on the validity of converting atomic kinetic energy to electricity. Additionally, designing a system for accomplishing this goal will have to be done in a manner that does not greatly disturb the shockwave discontinuity. One possible solution to this challenge is repurposing this reactor for use as a kinetic energy device for travel in non-atmospheric environments, such as space.

One significant challenge related to the Nuclear Engineering of the spherical shockwave reactor is the analysis and study of the effects of neutron leakage from the shockwave into the undisturbed medium. Neutrons that are fissioned or scattered forward, ahead of the shockwave into the undisturbed medium, will cause significant impact on the analysis of the later time steps since they may have time to thermalize before being enveloped back into the expanding radius of the shockwave. Furthermore, when considering these scattered neutrons as new sources particles to the undisturbed medium, the criticality value of the undisturbed medium will rise, necessitating an in-

depth study of the mean free path length and its relationship to the criticality of this portion of the medium and the shockwave.

Another pertinent challenge in the field of Nuclear Engineering is to understand the thermal effects of the transient medium and fission source contributions to thermal energy. All heat and temperature analysis performed in this study was minimal and assumed to be understood in the context of compressible flow theory and shockwave analysis. Future studies of this reactor will be required to confirm the intensity of fission heat generation, shockwave heat generation, temperature buildup, and reactor cooling times. Without these studies, it may be difficult to understand the effects of cycle times, cycle duration, and system return times for future criticality and neutron flux analyses.

Finally, future studies should further investigate the effects of initial parameter variations such as lower enrichments, different moderation isotopes, variations in concentration, and intensity of the initiating event. A unique study of the relationship between enrichment, moderation, and concentration could yield a critical mass curve that would assist in determining the optimum ratios of these three parameters. Changes in the initiating energy event would also assist in studying the local criticality effects of the discontinuity. \hat{M} and M^* are determined for this analysis to assist in this study, however, it would need to be validated for incorporation into the study other transient systems.

APPENDIX

MATLAB Results

Spherical Shockwave Properties

Euler Method

```
clear; clc; close all; format compact;

gamma=1.541;
n=1;
y=1;

f=(2*gamma)/(gamma+1);
Phi=2/(gamma+1);
Psi=[(gamma+1)/(gamma-1)];

dn=0.0001;

for s=2:12
    while n>0
        df=(f.*(-3*n+Phi.*(3+gamma/2)-(2*gamma*Phi.^2)./n))./((n-Phi).^2-(f/Psi));
        dPhi=((1/gamma).*(df./Psi)-3/2.*Phi)/(n-Phi);
        dPsi=(Psi.*(dPhi+(2.*Phi)/n))./(n-Phi);

        if df<0
            df=0;
            f=f-df.*dn;
        else
            f=f-df.*dn;
        end
        if dPhi<0
            dPhi=0;
            Phi=Phi-dPhi.*dn;
        else
            Phi=Phi-dPhi.*dn;
        end
        if dPsi<0
            dPsi=0;
            Psi=Psi-dPsi.*dn;
        else
            Psi=Psi-dPsi.*dn;
        end
        F(y)=f;
        H(y)=Phi;
        I(y)=Psi;
        N(y)=n;
        F1(y)=df;
        H1(y)=dPhi;
        I1(y)=dPsi;
        y=y+1;
        n=n-dn;
    end

    for i=1:(length(N)/2)
        T(i)=(I(1)/F(1))*(F(i)/I(i));
    end
end
plot(N,F,N,H,N,I)
hold on
plot(N(1:5000),T,'--')
grid on; legend('f','\Phi','\Psi','Temp','Location','nw');
axis([0 1 0 7]); xlabel('\eta - Shockwave Radius Fraction')
ylabel('Ratio of Parameters')
title('Non-Dimensional Shockwave Curves (\gamma=1.541)')
```

```

t=25; Dens(1)=I(1,1); Count(1)=N(1,1); Temp(1,1)=T(1,1);
for i=2:5
    Dens(i)=I(t+1);
    Count(i)=N(t+1);
    Temp(i)=T(t+1);
    t=t*2;
    m=t*.75;
end
for i=6:15
    m=t+m;
    Dens(i)=I(m+1);
    Count(i)=N(m+1);
    Temp(i)=T(m+1);
end
Dens
Count
Temp

p0=1000/101.325;
rho=0.0295;
time=0:10^-6:10^-3;
A=40.235;
R=A^0.4*((time).^0.4);
a2=gamma*p0/rho;

psh0=F(1).*R.^-3.*(A^2/a2); % Max Pressure @ Shockwave (y1 in Taylor)
WallPressY=psh0(end-225);
ShockPressY=psh0(270);
WallRad=R(end-225);
ShockRad=R(270);
ShockTime=time(270);
Table1=[WallPressY ShockPressY WallRad ShockRad ShockTime];
fprintf('Pressure and Radius \n')
fprintf('WallPress ShockPress WallRad ShockRad Shocktime \n' );
fprintf('%8.5f %8.5f %8.3f %8.5f %8.5f \n', Table1');

pp0=F(1).*R.^-3; % Shockwave Pressure Ratio
Y=2:10:length(time);
tstep=time(Y)';
Radius=R(Y)';
% PressRatio=pp0(Y)';
MaxPress=psh0(Y)';

SpeedSound=228.577;
WaveSpeed=A^(.4)*2/5.*time.^(-0.6);
Mach=WaveSpeed./SpeedSound;
M=2:10:length(time);
MachNum=Mach(M)';

Table2=[tstep Radius MaxPress MachNum];
fprintf('Time, ShockRadius, Pressure, Mach# \n')
fprintf(' Time Radius MaxPress(y1) Mach# \n' );
fprintf('%8.5f %8.5f %8.1f %8.3f \n', Table2');

figure
plot(R,Mach,R,1,'--')
grid on; ylabel('Mach');xlabel('Shockwave Radius-m')

figure
plot(R,psh0)
grid on;legend('Max Pressure');title('Maximum Shockwave Pressure by Radii')
ylabel('Pressure-kPa');xlabel('Shockwave Radius-m')
Dens =
    Columns 1 through 7
    4.6898  4.5174  4.3532  4.0477  3.5164  1.8853  1.2301
    Columns 8 through 14
    0.8364  0.5836  0.4129  0.2935  0.2081  0.1463  0.1014
    Column 15

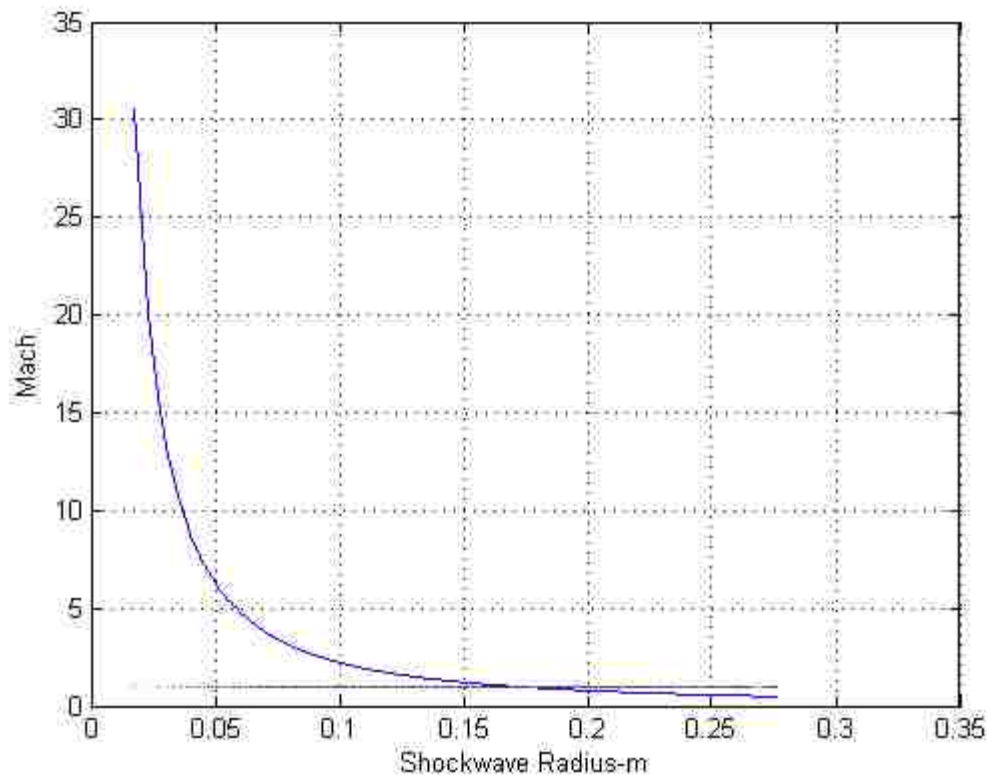
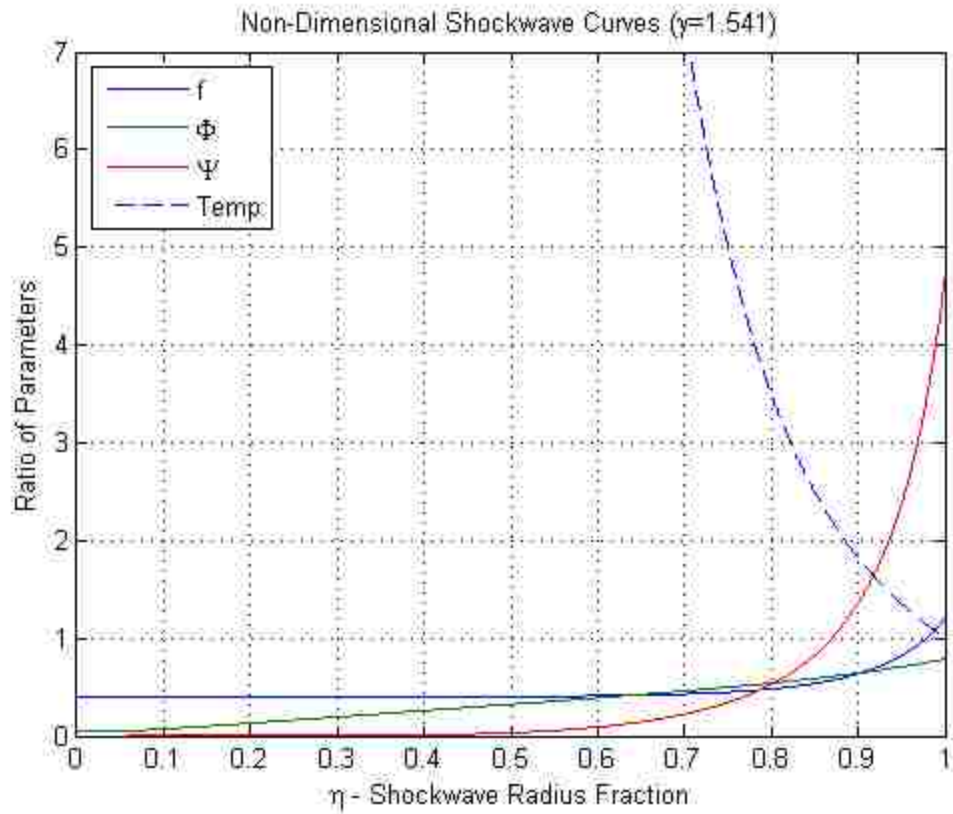
```

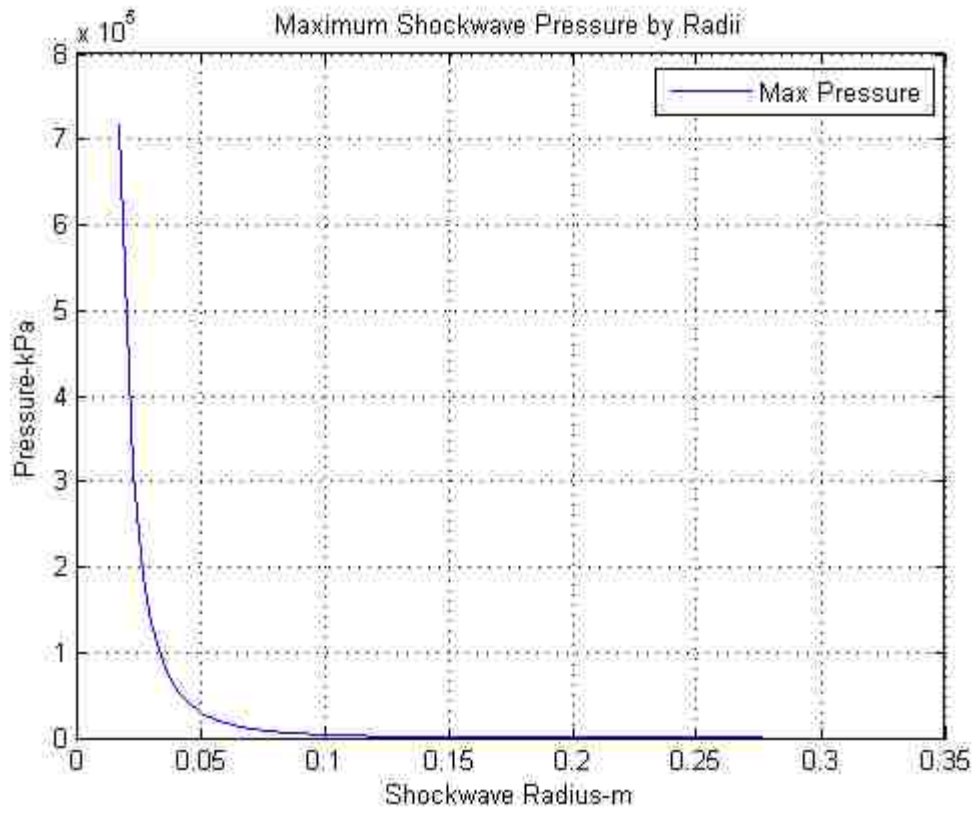
```

0.0690
Count =
  Columns 1 through 7
    1.0000    0.9975    0.9950    0.9900    0.9800    0.9300    0.8900
  Columns 8 through 14
    0.8500    0.8100    0.7700    0.7300    0.6900    0.6500    0.6100
  Column 15
    0.5700
Temp =
  Columns 1 through 7
    1.0000    1.0150    1.0302    1.0611    1.1258    1.5157    1.9363
  Columns 8 through 14
    2.4984    3.2628    4.3194    5.8054    7.9352    11.0524    15.7235
  Column 15
    22.9134
Pressure and Radius
WallPress ShockPress WallRad ShockRad Shocktime
244.16808 869.25699    0.250 0.16358 0.00027
Time, ShockRadius, Pressure, Mach#
  Time      Radius  MaxPress(y1) Mach#
0.00000    0.01745 715897.6    30.540
0.00001    0.04554 40288.4     7.245
0.00002    0.05898 18543.3     4.915
0.00003    0.06893 11620.3     3.891
0.00004    0.07708 8308.3      3.290
0.00005    0.08411 6393.9      2.886
0.00006    0.09036 5157.7      2.592
0.00007    0.09602 4298.7      2.367
0.00008    0.10121 3670.0      2.187
0.00009    0.10604 3191.5      2.039
0.00010    0.11055 2816.2      1.915
0.00011    0.11481 2514.6      1.810
0.00012    0.11884 2267.3      1.719
0.00013    0.12267 2061.2      1.639
0.00014    0.12634 1887.1      1.568
0.00015    0.12985 1738.1      1.505
0.00016    0.13322 1609.4      1.448
0.00017    0.13647 1497.1      1.397
0.00018    0.13961 1398.4      1.350
0.00019    0.14264 1311.0      1.307
0.00020    0.14559 1233.1      1.268
0.00021    0.14844 1163.4      1.231
0.00022    0.15122 1100.5      1.197
0.00023    0.15392 1043.6      1.166
0.00024    0.15655 991.8       1.137
0.00025    0.15911 944.6       1.109
0.00026    0.16162 901.3       1.084
0.00027    0.16407 861.6       1.059
0.00028    0.16647 824.9       1.037
0.00029    0.16881 791.0       1.015
0.00030    0.17111 759.6       0.995
0.00031    0.17336 730.4       0.975
0.00032    0.17557 703.1       0.957
0.00033    0.17773 677.7       0.940
0.00034    0.17986 654.0       0.923
0.00035    0.18196 631.7       0.907
0.00036    0.18401 610.7       0.892
0.00037    0.18603 591.0       0.877
0.00038    0.18802 572.5       0.864
0.00039    0.18998 554.9       0.850
0.00040    0.19191 538.4       0.837
0.00041    0.19381 522.7       0.825
0.00042    0.19568 507.8       0.813
0.00043    0.19753 493.7       0.802
0.00044    0.19935 480.3       0.791
0.00045    0.20115 467.6       0.780
0.00046    0.20292 455.4       0.770
0.00047    0.20467 443.8       0.760
0.00048    0.20640 432.8       0.751
0.00049    0.20810 422.2       0.742
0.00050    0.20979 412.1       0.733

```

0.00051	0.21145	402.5	0.724
0.00052	0.21310	393.2	0.716
0.00053	0.21472	384.4	0.708
0.00054	0.21633	375.8	0.700
0.00055	0.21792	367.7	0.692
0.00056	0.21950	359.8	0.685
0.00057	0.22105	352.3	0.677
0.00058	0.22259	345.0	0.670
0.00059	0.22412	338.0	0.664
0.00060	0.22563	331.3	0.657
0.00061	0.22712	324.8	0.650
0.00062	0.22860	318.5	0.644
0.00063	0.23007	312.5	0.638
0.00064	0.23152	306.6	0.632
0.00065	0.23296	301.0	0.626
0.00066	0.23438	295.5	0.621
0.00067	0.23579	290.3	0.615
0.00068	0.23719	285.2	0.610
0.00069	0.23858	280.2	0.604
0.00070	0.23995	275.4	0.599
0.00071	0.24132	270.8	0.594
0.00072	0.24267	266.3	0.589
0.00073	0.24401	261.9	0.584
0.00074	0.24534	257.7	0.579
0.00075	0.24666	253.6	0.575
0.00076	0.24797	249.6	0.570
0.00077	0.24927	245.7	0.566
0.00078	0.25055	241.9	0.561
0.00079	0.25183	238.3	0.557
0.00080	0.25310	234.7	0.553
0.00081	0.25436	231.2	0.549
0.00082	0.25561	227.8	0.545
0.00083	0.25685	224.6	0.541
0.00084	0.25808	221.4	0.537
0.00085	0.25931	218.2	0.533
0.00086	0.26052	215.2	0.530
0.00087	0.26173	212.2	0.526
0.00088	0.26293	209.4	0.522
0.00089	0.26411	206.5	0.519
0.00090	0.26530	203.8	0.515
0.00091	0.26647	201.1	0.512
0.00092	0.26764	198.5	0.509
0.00093	0.26880	195.9	0.505
0.00094	0.26995	193.4	0.502
0.00095	0.27109	191.0	0.499
0.00096	0.27223	188.6	0.496
0.00097	0.27336	186.3	0.493
0.00098	0.27448	184.0	0.490
0.00099	0.27559	181.8	0.487





Mathcad Results

$$\text{atoms} := 1 \quad m_u := 10^{-3} \text{ kg} \quad A_v := 6.022121415 \cdot 10^{23} \frac{\text{atoms}}{\text{mole}} \quad R_{\text{universal}} := 8.3144621 \frac{\text{J}}{\text{mole} \cdot \text{K}}$$

Ratio of Specific Heats $\gamma_{\text{UF}_6} := 1.065$

$$\gamma_{\text{He}} := 1.66$$

$$T_{\text{melt_UF}_6} := 65.05 \text{ } ^\circ\text{C}$$

Atomic Weights $A_{\text{He}} := 4.002602 \frac{\text{g}}{\text{mole}}$

$$A_{\text{F}} := 18.994 \frac{\text{g}}{\text{mole}}$$

$$A_{\text{U}238} := 238 \frac{\text{g}}{\text{mole}}$$

$$\text{enrich} := .80$$

$$A_{\text{U}235} := 235 \frac{\text{g}}{\text{mole}}$$

$$A_{\text{U}} := (1 - \text{enrich}) \cdot A_{\text{U}238} + (\text{enrich}) \cdot A_{\text{U}235}$$

$$A_{\text{UF}_6} := 352.02 \frac{\text{g}}{\text{mole}}$$

$$A_{\text{U}} = 235.6 \frac{\text{g}}{\text{mole}}$$

$$A_{\text{UF}_6\text{s}} := A_{\text{U}} + 6A_{\text{F}} = 349.564 \frac{\text{g}}{\text{mole}}$$

+

Original Temperatures and Pressures

$$T_{\text{inf}} := 25 \text{ } ^\circ\text{C}$$

$$F_{\text{He}} := 0.80$$

Mole Fraction of Helium

$$P_{\text{inf}} := 1000 \text{ kPa}$$

Gas Constants $A_{\text{mix}} := F_{\text{He}} \cdot A_{\text{He}} + (1 - F_{\text{He}}) \cdot A_{\text{UF}_6\text{s}} = 73.115 \frac{\text{g}}{\text{mole}}$

$$R_{\text{mix}} := \frac{R_{\text{universal}}}{A_{\text{mix}}} = 113.718 \frac{\text{J}}{\text{kg} \cdot \text{K}}$$

Density of Gas Mixture

$$\rho_{\text{inf}} := \frac{P_{\text{inf}}}{R_{\text{mix}} \cdot T_{\text{inf}}} = 0.02949 \frac{\text{g}}{\text{cm}^3}$$

$$\rho_{\text{inf}} = 29.494 \frac{\text{kg}}{\text{m}^3}$$

Ratio of Specific Heats for the Mixture

$$\gamma := (1 - F_{\text{He}}) \gamma_{\text{UF}_6} + F_{\text{He}} \gamma_{\text{He}} = 1.541$$

Speed of Sound in Undisturbed Mixture

$$a_{\text{inf}} := \sqrt{\gamma R_{\text{mix}} T_{\text{inf}}} = 228.577 \frac{\text{m}}{\text{s}}$$

Reactor Dimensions

$$R_o := .25\text{m} \quad \text{Outer Radius}$$

Mass of UF6 and He used in the reactor

$$\text{Volume}_{\text{reactor}} := \frac{4}{3} \pi R_o^3 = 6.545 \times 10^{-4} \text{m}^3$$

$$m_{\text{mix}} := \rho_{\text{inf}} \text{Volume}_{\text{reactor}} = 1.93 \text{kg}$$

$$\text{moles}_{\text{mix}} := \frac{m_{\text{mix}}}{A_{\text{mix}}} = 26.402 \text{mol}$$

$$m_{\text{UF}_6} := A_{\text{UF}_6} (1 - F_{\text{He}}) \text{moles}_{\text{mix}} = 1.846 \text{kg}$$

$$m_{\text{He}} := A_{\text{He}} (F_{\text{He}}) \text{moles}_{\text{mix}} = 0.085 \text{kg}$$

$$m_{\text{F}_6} := m_{\text{UF}_6} \frac{6A_{\text{F}}}{A_{\text{UF}_6}} = 0.602 \text{kg}$$

$$m_{\text{U}235} := m_{\text{UF}_6} \text{enrich} \frac{A_{\text{U}235}}{A_{\text{UF}_6}} = 0.993 \text{kg}$$

$$m_{\text{U}238} := m_{\text{UF}_6} (1 - \text{enrich}) \frac{A_{\text{U}238}}{A_{\text{UF}_6}} = 0.251 \text{kg}$$

$$w_{\text{UF}_6} := \frac{m_{\text{UF}_6}}{m_{\text{mix}}} = 0.9562$$

$$w_{\text{U}235} := w_{\text{UF}_6} \frac{m_{\text{U}235}}{m_{\text{UF}_6}} = 0.51426$$

$$w_{\text{He}} := \frac{m_{\text{He}}}{m_{\text{mix}}} = 0.0438$$

$$w_{\text{F}_6} := w_{\text{UF}_6} \frac{m_{\text{F}_6}}{m_{\text{UF}_6}} = 0.31174$$

$$w_{\text{U}238} := w_{\text{UF}_6} \frac{m_{\text{U}238}}{m_{\text{UF}_6}} = 0.13021$$

$$w_{\text{P}_{\text{mix}}} := w_{\text{UF}_6} + w_{\text{He}} = 1$$

$$w_{\text{P}_{\text{tot}}} := w_{\text{He}} + w_{\text{F}_6} + w_{\text{U}235} + w_{\text{U}238} = 1$$

Compute Kinfinity as a function of gas pressure

Microscopic Cross sections

$$\begin{aligned} \sigma_{a_He} &:= 0 \text{ barn} & \sigma_{s_He} &:= 0.759 \text{ barn} \\ \sigma_{a_F} &:= 0.1 \text{ barn} & \sigma_{s_F} &:= 3.8 \text{ barn} \\ \sigma_{a_U235} &:= 681 \text{ barn} & \sigma_{s_U235} &:= 15 \text{ barn} & \sigma_{f_U235} &:= 584 \text{ barn} \\ \sigma_{a_U238} &:= 2.717 \text{ barn} & \sigma_{s_U238} &:= 10 \text{ barn} & \sigma_{f_U238} &:= 12 \times 10^{-6} \text{ barn} \end{aligned}$$

Four Factor Formula Components

$$P_{DNF} := 1 \quad f_{inf} := 1 \quad \epsilon_{inf} := 1.05 \quad \nu := 2.43 \quad \text{Number of fissions per neutron}$$

$$\eta_{inf} := \frac{\nu \cdot (1 - F_{He}) \cdot \text{enrich} \cdot \sigma_{f_U235} + (1 - \text{enrich}) \cdot \sigma_{f_U238} \cdot (1 - F_{He})}{(1 - F_{He}) \cdot \text{enrich} \cdot \sigma_{a_U235} + 6 \cdot (1 - F_{He}) \cdot \sigma_{a_F} + F_{He} \cdot \sigma_{a_He} + (1 - \text{enrich}) \cdot \sigma_{a_U238} \cdot (1 - F_{He})} = 2.08$$

$$k_{inf} \text{ in the blanket material (undisturbed fluid)} \quad k_{inf} := \eta_{inf} \cdot \epsilon_{inf} \cdot f_{inf} \cdot P_{DNF} = 2.183$$

Computing the cross-sections needed to find the thermal diffusion length, L(b).

Number densities

$$N_{He} := \frac{w_{He} \cdot A_v \cdot \rho_{inf}}{A_{He}} = 1.943 \times 10^{-4} \frac{\text{atoms}}{\text{barn-cm}}$$

$$N_{UF6} := \frac{w_{UF6} \cdot A_v \cdot \rho_{inf}}{A_{UF6a}} = 4.859 \times 10^{-5} \frac{\text{atoms}}{\text{barn-cm}}$$

$$N_{U235} := \text{enrich} \cdot N_{UF6} = 3.887 \times 10^{-5} \frac{\text{atoms}}{\text{barn-cm}}$$

$$N_F := 6 \cdot N_{UF6} = 2.915 \times 10^{-4} \frac{\text{atoms}}{\text{barn-cm}}$$

$$N_{U238} := (1 - \text{enrich}) \cdot N_{UF6} = 9.717 \times 10^{-6} \frac{\text{atoms}}{\text{barn-cm}}$$

$$N_{tot1} := N_{He} + N_{U235} + N_F = 5.247 \times 10^{-4} \frac{\text{atoms}}{\text{barn-cm}}$$

$$N_{tot2} := N_{He} + N_{UF6} = 2.429 \times 10^{-4} \frac{\text{atoms}}{\text{barn-cm}}$$

Macroscopic Cross-sections

$$\Sigma_a := (N_{\text{He}} \cdot \sigma_a_{\text{He}} + N_{\text{U235}} \cdot \sigma_a_{\text{U235}} + N_{\text{F}} \cdot \sigma_a_{\text{F}}) \frac{\sqrt{\pi}}{2} \sqrt{\frac{293\text{K}}{T_{\text{inf}}}} = 2.328 \frac{1}{\text{m}}$$

$$\Sigma_{\text{tr}} := N_{\text{He}} \left[\frac{2 \left(\frac{1}{\text{mole}} \right)}{3 \cdot A_{\text{He}}} \right] \cdot \sigma_s_{\text{He}} + N_{\text{U235}} \left[\frac{2 \left(\frac{1}{\text{mole}} \right)}{3 \cdot A_{\text{U235}}} \right] \cdot \sigma_s_{\text{U235}} + N_{\text{F}} \left[\frac{2 \left(\frac{1}{\text{mole}} \right)}{3 \cdot A_{\text{F}}} \right] \cdot \sigma_s_{\text{F}} = 6.51 \times 10^{-3} \frac{1}{\text{m}}$$

$$\Sigma_{\text{fU235}} := N_{\text{U235}} \cdot \sigma_{\text{fU235}} = 2.27 \frac{1}{\text{m}} \quad \Sigma_a = 2.328 \frac{1}{\text{m}} \quad \Sigma_{\text{tr}} = 6.5104 \times 10^{-3} \frac{1}{\text{m}}$$

Diffusion Coefficient

$$D_1 := \frac{1}{(3 \cdot \Sigma_{\text{tr}})} = 51.201 \text{m} \quad L_1 := \sqrt{\frac{1}{3 \cdot \Sigma_{\text{tr}} \cdot \Sigma_a}} = 4.69 \text{m}$$

$$M_{12} := L_1^2 + \frac{D_1}{\Sigma_a + \Sigma_{\text{tr}} + N_{\text{U235}} \cdot \sigma_{\text{fU235}}} = 33.113 \text{m}^2$$

$L_1 = 4.68968487 \text{m}$ Distance neutrons travel before undergoing scatter or absorption

Buckling within the blanket material

$$B_{11} := \frac{k_{\text{inf}} - 1}{L_1^2} = 0.054 \frac{1}{\text{m}^2} \quad B_1 := \sqrt{B_{11}} = 0.232 \frac{1}{\text{m}}$$

$$B_{12} := \frac{N_{\text{U235}} \cdot \sigma_{\text{fU235}} - N_{\text{U235}} \cdot \sigma_a_{\text{U235}}}{D_1} = 0.056 \frac{1}{\text{m}^2} \quad \text{Classical Definition of Buckling}$$

Calculation of keff

$$k_{\text{eff}} := \frac{k_{\text{inf}}}{1 + B_1^2 \left(L_1^2 + \frac{D_1}{\Sigma_a + \Sigma_{\text{tr}} + N_{\text{U235}} \cdot \sigma_{\text{fU235}}} \right)} \quad k_{\text{eff}} = 0.785$$

Shockwave Calculations

$$t := 0.00001\text{-sec}, 0.00002\text{-sec}, \dots, 0.001\text{-sec}$$

Energy to generate shock

$$TNT := 4.186 \cdot 10^9 \text{ J}$$

$$uTNT := 10^{-6} \cdot TNT$$

(TNT is tonnes of TNT)

$$E_0 := 50000 \text{ J}$$

$$E_0 = 11.945 \cdot uTNT$$

(uTNT is grams of TNT)

$$K := \sqrt{\frac{3}{\pi} \frac{E_0}{\rho_{inf}}} = 40.235 \frac{\text{m}}{\text{s}} \quad \text{Kappa} = A$$

$$R_s(t) := K \cdot \frac{2}{5} \cdot \frac{2}{5} \cdot t^{\frac{2}{5}} \quad \text{Radial distance with time}$$

$$W_s(t) := K \cdot \frac{2}{5} \cdot \frac{2}{5} \cdot t^{\frac{-3}{5}} \quad \text{Speed of Wave}$$

$$s_1 := \sqrt{\gamma \cdot E_{mix} \cdot T_{inf}} = 228.577 \frac{\text{m}}{\text{s}}$$

$$M_2(t) := \frac{W(t)}{s_1}$$

$$M_1 := 0 \quad M_s(t) := \begin{cases} M_2(t) & \text{if } \frac{W(t)}{s_1} \geq 1 \\ M_1 & \text{otherwise} \end{cases}$$

Properties on the back of the shock:

Considering Mach Number

No Mach Number Consideration

$$p_2(t) := \begin{cases} \left[2\gamma M_s(t)^2 - (\gamma - 1) \right] \left(\frac{p_{inf}}{\gamma + 1} \right) & \text{if } M_s(t) > 0 \\ p_{inf} & \text{otherwise} \end{cases}$$

$$p_{2g}(t) := \left[2\gamma M_2(t)^2 - (\gamma - 1) \right] \frac{p_{inf}}{\gamma + 1}$$

$$p_m(t) := 1 + \frac{2\gamma}{\gamma + 1} \left(M_2(t)^2 - 1 \right)$$

Pressure Ratio

Shockwave Pressure

$\frac{p_2(t)}{p_{inf}}$	$p_2(t)$ - kPa
71.165	$7.117 \cdot 10^4$
30.856	$3.086 \cdot 10^4$
18.886	$1.889 \cdot 10^4$
...	...

Pressure Ratio

Shockwave Pressure

$p_m(t)$	$p_{2g}(t)$ - kPa
71.165	$7.117 \cdot 10^4$
30.856	$3.086 \cdot 10^4$
18.886	$1.889 \cdot 10^4$
...	...

$$T_2(t) := \begin{cases} \frac{p_2(t)}{p_{inf}} \left[\frac{\gamma + 1 + \frac{p_2(t)}{p_{inf}}}{\gamma - 1 + \frac{p_2(t)}{p_{inf}}} \right] T_{inf} & \text{if } M_s(t) > 0 \\ \left[\frac{1}{T_{inf}} - \frac{\gamma - 1}{2 T_{inf}} \left(\frac{W(t)}{s_1} \right)^2 \right]^{-1} & \text{otherwise} \end{cases}$$

Temperature Across Shock by Radius

$T_2(t)$ - K
$4.801 \cdot 10^3$
$2.241 \cdot 10^3$
$1.48 \cdot 10^3$
...

Density across Shockwave

$$\rho_2(t) := \left[\frac{1 + \left(\frac{\gamma + 1}{\gamma - 1} \right) \frac{p_2(t)}{p_{inf}}}{\left(\frac{\gamma + 1}{\gamma - 1} \right) + \frac{p_2(t)}{p_{inf}}} \right] \rho_{inf}$$

$$\rho_{2g}(t) := \left[\frac{1 + \left(\frac{\gamma + 1}{\gamma - 1} \right) \frac{p_{2g}(t)}{p_{inf}}}{\left(\frac{\gamma + 1}{\gamma - 1} \right) + \frac{p_{2g}(t)}{p_{inf}}} \right] \rho_{inf}$$

$\rho_2(t) =$	$\frac{\rho_2(t)}{\rho_{inf}} =$	$\rho_{2g}(t) =$	$\frac{\rho_{2g}(t)}{\rho_{inf}} =$
130.342 $\frac{kg}{m^3}$	4.419	0.1303	4.419
121.059 $\frac{kg}{m^3}$	4.104	0.1211	4.104
...

Particle Velocity across Shockwave

$$u_p(t) := \begin{cases} \frac{p_{inf}}{\gamma} \left(\frac{p_2(t)}{p_{inf}} - 1 \right) \sqrt{\frac{2\gamma}{\gamma + 1} \frac{p_2(t)}{p_{inf} - \left(\frac{\gamma - 1}{\gamma + 1} \right)}} & \text{if } M_1(t) > 0 \\ 0 & \text{otherwise} \end{cases}$$

$u_p(t) =$	$\frac{m}{s}$
1.357 · 10 ³	
875.012	
668.588	
...	

Changes to Speed of Sound Variable

$$a_2(t) := \sqrt{\gamma \cdot p_{min} \cdot T_2(t)}$$

$a_2(t) =$	$\frac{m}{s}$
917.26	
626.721	
509.328	
...	

Calculating keff(t) No fertile material

- Fast Fission Factor $\epsilon := 1.05$
- Resonance escape probability $p := 1$

$$\eta_f := \frac{\nu \cdot (1 - F_{He}) \cdot N_{U235} \cdot \sigma_{f,U235}}{(1 - F_{He}) \cdot N_{U235} \cdot \sigma_{a,U235} + 6 \cdot (1 - F_{He}) \cdot N_F \cdot \sigma_{a,F} + F_{He} \cdot N_{He} \cdot \sigma_{a,He}} = 2.0702$$

$$\eta_{inf} = 2.0795$$

Temperature and Density variation affects cancel in both the equation for η and for fission and absorption cross-sections.

Infinite neutron multiplication factor $k_{inf} := \epsilon \cdot p \cdot \eta_f = 2.174$

Cross sections needed for thermal diffusion length, L

Number densities:

$$N_{\text{He}}(t) := \frac{F_{\text{He}} \rho_2(t) \cdot A_v}{A_{\text{He}}} \quad N_{\text{UF}_6}(t) := \frac{(1 - F_{\text{He}}) \rho_2(t) \cdot A_v}{A_{\text{UF}_6}} \quad N_{\text{U235}}(t) := N_{\text{UF}_6}(t) \quad N_{\text{F}}(t) := 6 N_{\text{UF}_6}(t)$$

$N_{\text{He}}(t) =$

0.016	atoms
0.015	barn-cm
...	

$N_{\text{UF}_6}(t) =$

$4.46 \cdot 10^{-5}$	atoms
$4.142 \cdot 10^{-5}$	barn-cm
...	

$N_{\text{U235}}(t) =$

$4.46 \cdot 10^{-5}$	atoms
$4.142 \cdot 10^{-5}$	barn-cm
...	

$N_{\text{F}}(t) =$

$2.676 \cdot 10^{-4}$	atoms
$2.485 \cdot 10^{-4}$	barn-cm
...	

$$N_{\text{tot}}(t) := N_{\text{He}}(t) + N_{\text{U235}}(t) + N_{\text{F}}(t)$$

$N_{\text{tot}}(t) =$

0.016	atoms
0.015	barn-cm
...	

Macroscopic Cross Sections on Backside of Shockwave

$$\Sigma_a(t) := (N_{\text{He}}(t) \cdot \sigma_a_{\text{He}} + N_{\text{U235}}(t) \cdot \sigma_a_{\text{U235}} + N_{\text{F}}(t) \cdot \sigma_a_{\text{U235}}) \frac{\sqrt{\pi}}{2} \sqrt{\frac{293\text{K}}{T_2(t)}}$$

$$\Sigma_{tr}(t) := N_{\text{He}}(t) \left[\frac{2 \cdot \left(\frac{1}{\text{mole}} \right)}{3 \cdot A_{\text{He}}} \right] \sigma_a_{\text{He}} + N_{\text{U235}}(t) \left[\frac{2 \cdot \left(\frac{1}{\text{mole}} \right)}{3 \cdot A_{\text{U235}}} \right] \sigma_a_{\text{U235}} + N_{\text{F}}(t) \left[\frac{2 \cdot \left(\frac{1}{\text{mole}} \right)}{3 \cdot A_{\text{F}}} \right] \sigma_a_{\text{F}}$$

$\Sigma_a(t) =$

4.654	$\frac{1}{\text{m}}$
6.327	
...	

$\Sigma_{tr}(t) =$

0.202	$\frac{1}{\text{m}}$
0.188	
...	

Diffusion Coefficient and Thermal Diffusion Length

$$D_2(t) := \frac{1}{(3 \cdot \Sigma_{tr}(t))}$$

$$L_2(t) := \sqrt{\frac{1}{3 \cdot \Sigma_{tr}(t) \cdot \Sigma_a(t)}}$$

$$B_2(t) := \left[\left(\frac{\rho_2(t)}{\rho_{trF}} \right)^2 \cdot B_1 \right]$$

$$M_{22}(t) := L_2(t)^2 = \frac{D_2(t)}{(\Sigma_a(t) + N_{\text{U235}}(t) \cdot \sigma_{tr_{\text{U235}}} + \Sigma_{tr}(t))}$$

$D_2(t) -$	$B_2(t) -$	$L_2(t) -$	$\left(\frac{\rho_2(t)}{\rho_{inf}}\right)^2 -$	$M_s(t) -$
1.649 m	4.53 $\frac{1}{m}$	0.595 m	19.53	7.671
...	5.061
				3.968
				...

Radius of Shockwave

keff as a function of time

$$R_s(t) = \begin{cases} R(t) & \text{if } M_s(t) > 0 \\ 0 & \text{otherwise} \end{cases}$$

$$k_{eff}(t) = \frac{k_{inf}}{1 - B_2(t)^2 \left[L_2(t)^2 + \frac{D_2(t)}{(\Sigma_s(t) - N_{U235}(t) \cdot \sigma_{fU235} - \Sigma_H(t))} \right]}$$

Calculation of Analytical Fluxes

$$\phi_0 := 10^8$$

$$r_1 = \frac{B_1 R_0 - \tan(B_1 R_0)}{1 - R_0 B_1 \tan(B_1 R_0)}$$

$$r_2(t) = \frac{\sin(B_2(t) R(t))}{\sin(B_1 R(t)) + r_1 \cos(B_1 R(t))}$$

$$C_1(t) = \frac{\left[\phi_0 D_2(t) R(t) \cos(B_2(t) R(t)) \left[1 + \left(\tan(B_2(t) R(t)) \right)^2 \right] \right]}{D_1 \cos(B_1 R(t)) \left[\left[B_1 R(t) - \tan(B_1 R(t)) + r_1 B_1 R(t) \tan(B_1 R(t)) \right] + r_1 \right] + D_2(t) r_2(t) \cos(B_2(t) R(t)) \left[B_2(t) R(t) \tan(B_2(t) R(t)) + 1 \right]}$$

$$\phi_1(t) = \frac{C_1(t)}{R(t)} \left(\sin(B_1 R(t)) - r_1 \cos(B_1 R(t)) \right)$$

$$\phi_2(t) = \frac{\phi_0}{R(t) B_2(t)} \left(\sin(B_2(t) R(t)) - \tan(B_2(t) R(t)) \cos(B_2(t) R(t)) \right) - C_1(t) r_1 \frac{\cos(B_2(t) R(t))}{R(t)}$$

$\phi_1(t) -$

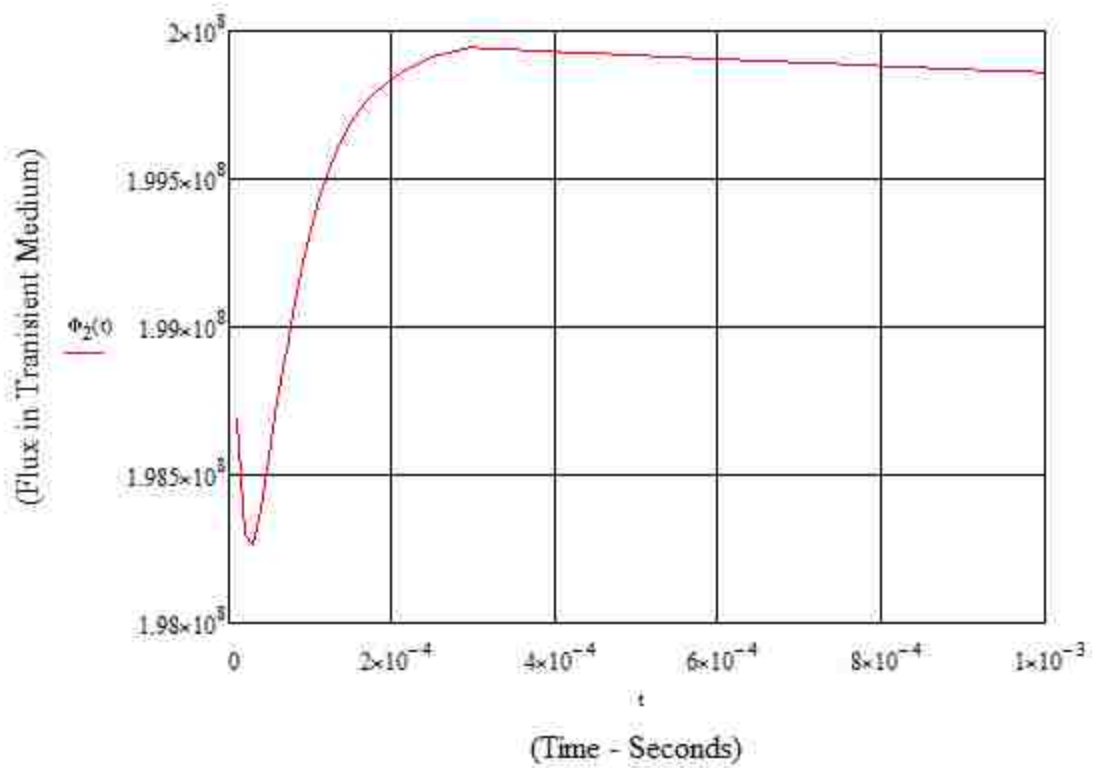
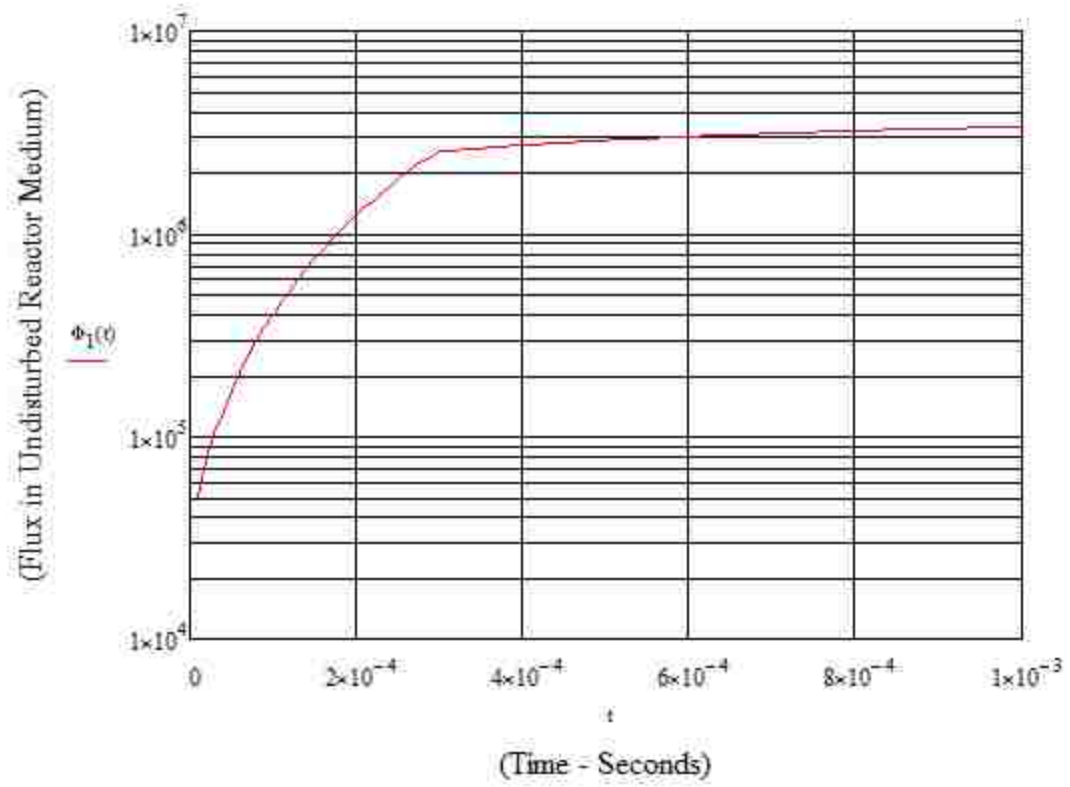
5.019·10 ⁴
7.62·10 ⁴
1.033·10 ⁵
1.333·10 ⁵
1.669·10 ⁵
2.045·10 ⁵
...

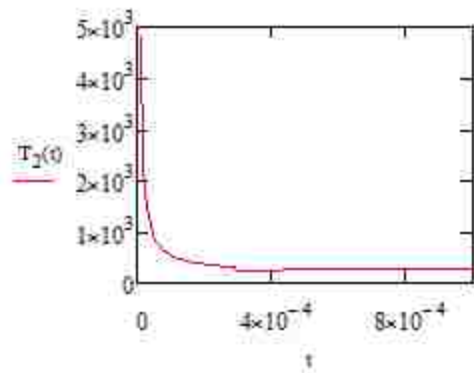
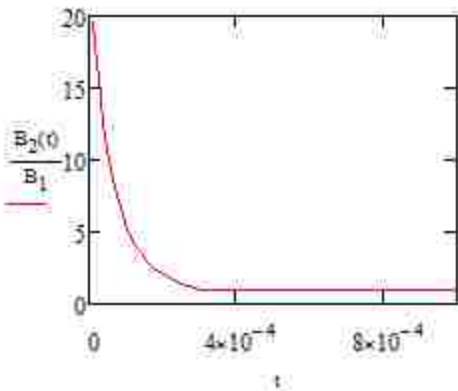
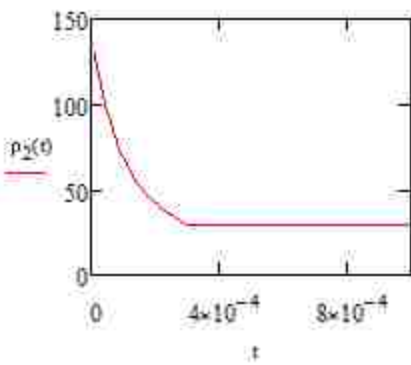
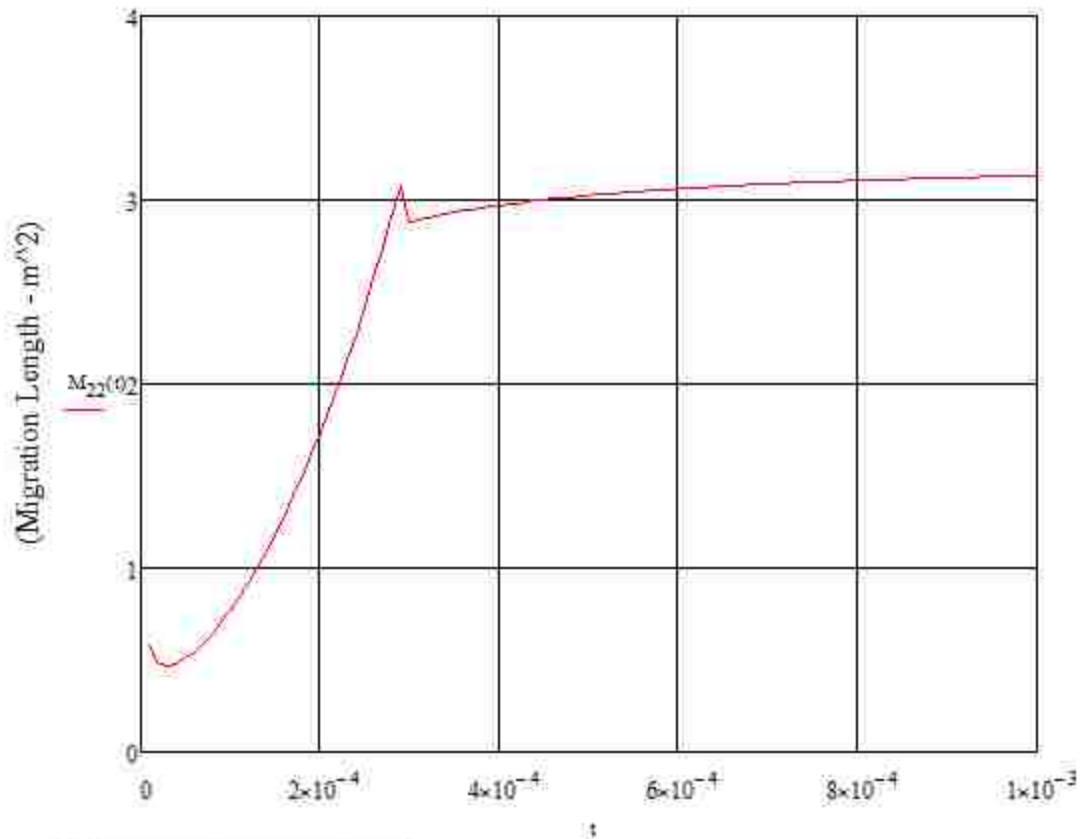
$\phi_2(t) -$

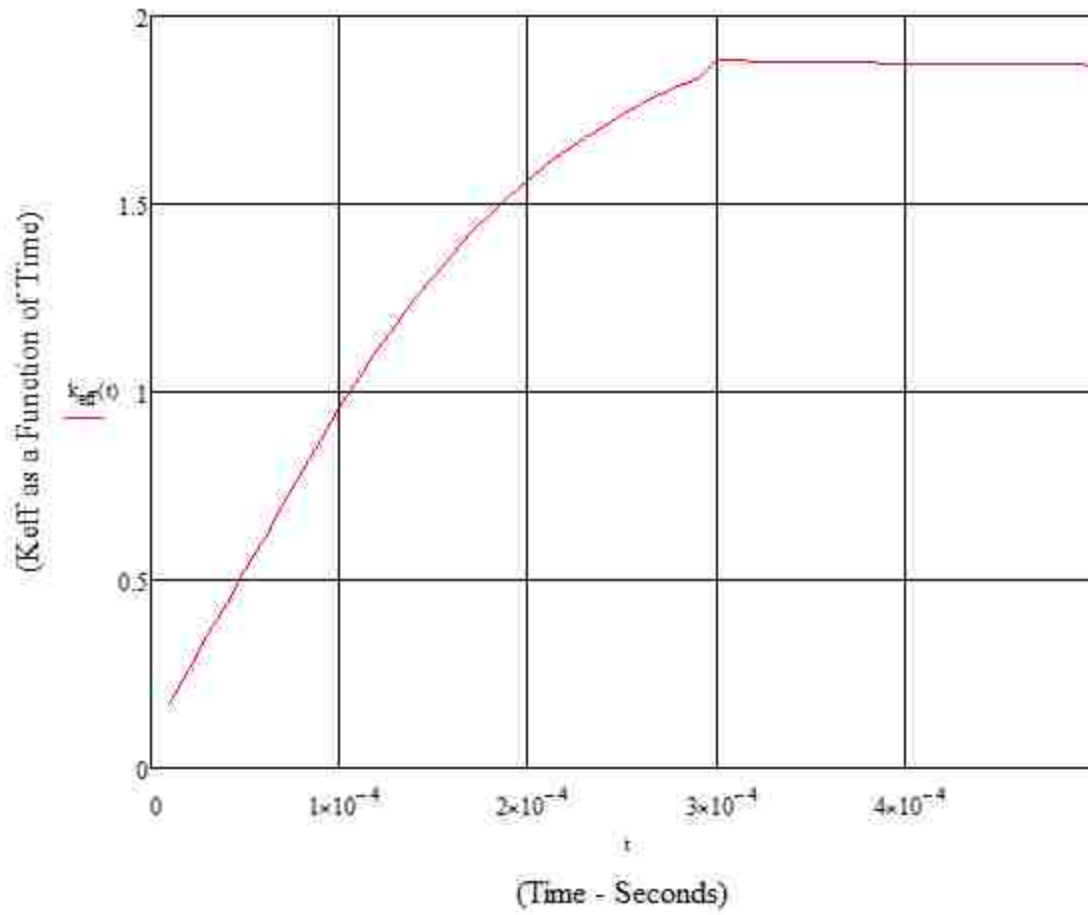
1.987·10 ⁸
1.983·10 ⁸
1.983·10 ⁸
1.984·10 ⁸
1.986·10 ⁸
1.987·10 ⁸
...

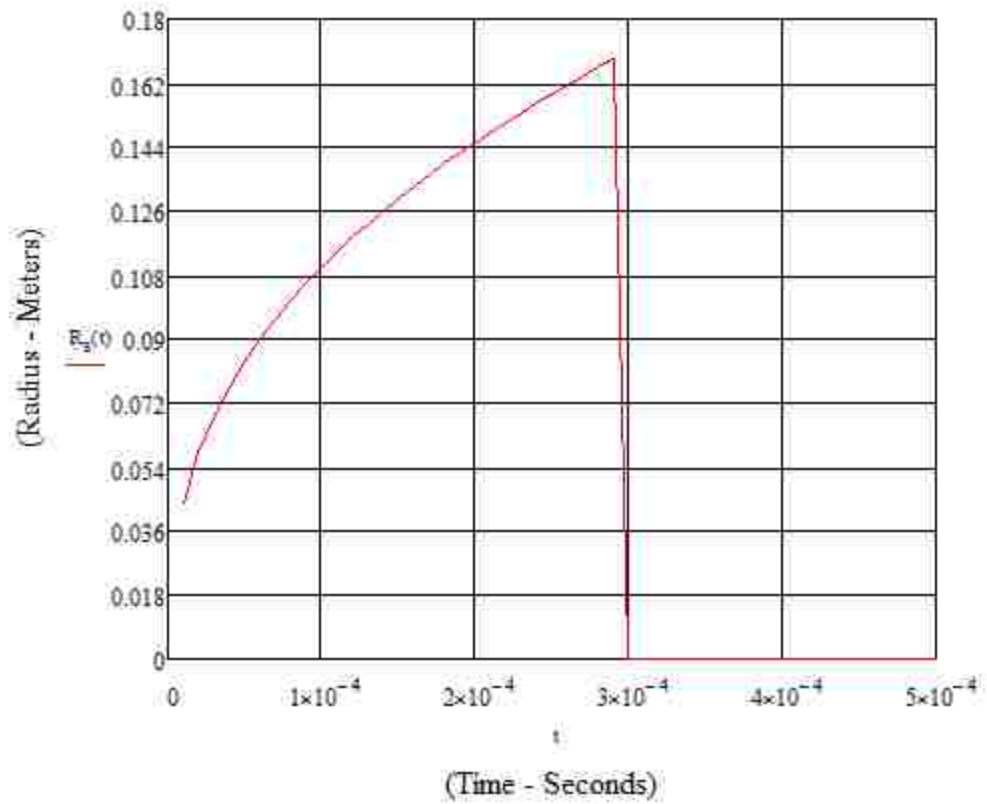
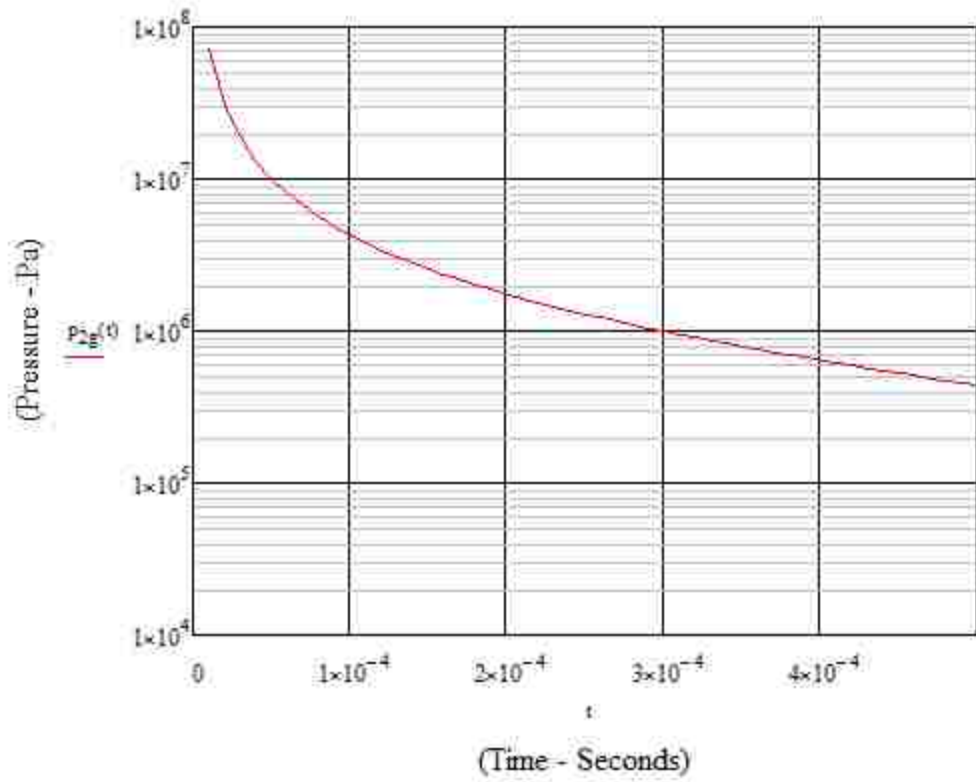
$k_{eff}(t) -$

0.17
0.261
0.349
0.437
0.525
0.614
...









Numerical Results

MICROSOFT EXCEL CALCULATIONS

Mach #	Time	Pressure	Radius	Density
7.671	1.00E-05	7.12E+04	0.04384	0.1303
5.061	2.00E-05	3.09E+04	0.05784	0.1211
3.968	3.00E-05	1.89E+04	0.06803	0.1122
3.339	4.00E-05	1.33E+04	0.07632	0.104
2.921	5.00E-05	1.01E+04	0.08345	0.0966
2.618	6.00E-05	8.10E+03	0.08976	0.09
2.387	7.00E-05	6.70E+03	0.09547	0.084
2.203	8.00E-05	5.67E+03	0.1	0.0786
2.053	9.00E-05	4.90E+03	0.10557	0.0738
1.927	1.00E-04	4.29E+03	0.11011	0.0694
1.82	1.10E-04	3.80E+03	0.11439	0.0655
1.727	1.20E-04	3.41E+03	0.11844	0.0619
1.646	1.30E-04	3.07E+03	0.1223	0.0586
1.575	1.40E-04	2.80E+03	0.12598	0.0556
1.511	1.50E-04	2.56E+03	0.1295	0.0529
1.453	1.60E-04	2.35E+03	0.13289	0.0504
1.402	1.70E-04	2.17E+03	0.13615	0.0481
1.354	1.80E-04	2.01E+03	0.1393	0.0459
1.311	1.90E-04	1.87E+03	0.14235	0.044
1.271	2.00E-04	1.75E+03	0.1453	0.0421
1.235	2.10E-04	1.64E+03	0.14816	0.0404
1.201	2.20E-04	1.54E+03	0.15094	0.0389
1.169	2.30E-04	1.45E+03	0.15365	0.0374
1.14	2.40E-04	1.36E+03	0.15629	0.036
1.112	2.50E-04	1.29E+03	0.15886	0.0347
1.086	2.60E-04	1.22E+03	0.16137	0.0335
1.062	2.70E-04	1.16E+03	0.16383	0.0324
1.039	2.80E-04	1.10E+03	0.16623	0.0313
1.017	2.90E-04	1.04E+03	0.16858	0.0303
0	3.00E-04	1.00E+03	0.17088	0.0293

Time	1.00E-05	2.00E-05	3.00E-05	4.00E-05	5.00E-05	8.00E-05	1.20E-04	1.70E-04	2.20E-04	2.90E-04	
Radius	0.04384	0.05784	0.06803	0.07632	0.08345	0.1	0.11844	0.13615	0.15094	0.16858	
1	4.38	5.78	6.80	7.63	8.35	10.00	11.84	13.62	15.09	16.86	10
0.9975	4.37	5.77	6.79	7.61	8.32	9.98	11.81	13.58	15.06	16.82	11
0.995	4.36	5.76	6.77	7.59	8.30	9.95	11.78	13.55	15.02	16.77	12
0.99	4.34	5.73	6.73	7.56	8.26	9.90	11.73	13.48	14.94	16.69	13
0.98	4.30	5.67	6.67	7.48	8.18	9.80	11.61	13.34	14.79	16.52	14
0.93	4.08	5.38	6.33	7.10	7.76	9.30	11.01	12.66	14.04	15.68	15
0.89	3.90	5.15	6.05	6.79	7.43	8.90	10.54	12.12	13.43	15.00	16
0.85	3.73	4.92	5.78	6.49	7.09	8.50	10.07	11.57	12.83	14.33	17
0.81	3.55	4.69	5.51	6.18	6.76	8.10	9.59	11.03	12.23	13.65	18
0.77	3.38	4.45	5.24	5.88	6.43	7.70	9.12	10.48	11.62	12.98	19
0.73	3.20	4.22	4.97	5.57	6.09	7.30	8.65	9.94	11.02	12.31	20
0.69	3.02	3.99	4.69	5.27	5.76	6.90	8.17	9.39	10.41	11.63	21
0.65	2.85	3.76	4.42	4.96	5.42	6.50	7.70	8.85	9.81	10.96	22
0.61	2.67	3.53	4.15	4.66	5.09	6.10	7.22	8.31	9.21	10.28	23
0.57	2.50	3.30	3.88	4.35	4.76	5.70	6.75	7.76	8.60	9.61	24
half	1.67	2.20	2.59	2.90	3.17	3.80	4.50	5.17	5.74	6.41	25
full	0.83	1.10	1.29	1.45	1.59	1.90	2.25	2.59	2.87	3.20	26

Density	0.1303	0.1211	0.1122	0.104	0.0966	0.0786	0.0619	0.0481	0.0389	0.0324	
0.0295	4.416949	4.105085	3.80339	3.525424	3.274576	2.664407	2.098305	1.630508	1.318644	1.098305	
4.6898	0.1303	0.1211	0.1122	0.1040	0.0966	0.0786	0.0619	0.0481	0.0389	0.0324	10
4.5174	0.1255	0.1166	0.1081	0.1002	0.0930	0.0757	0.0596	0.0463	0.0375	0.0312	11
4.3532	0.1209	0.1124	0.1041	0.0965	0.0897	0.0730	0.0575	0.0446	0.0361	0.0301	12
4.0477	0.1125	0.1045	0.0968	0.0898	0.0834	0.0678	0.0534	0.0415	0.0336	0.0280	13
3.5164	0.0977	0.0908	0.0841	0.0780	0.0724	0.0589	0.0464	0.0361	0.0292	0.0243	14
1.8853	0.0524	0.0487	0.0451	0.0418	0.0388	0.0316	0.0249	0.0193	0.0156	0.0130	15
1.2301	0.0342	0.0318	0.0294	0.0273	0.0253	0.0206	0.0162	0.0126	0.0102	0.0085	16
0.8364	0.0232	0.0216	0.0200	0.0185	0.0172	0.0140	0.0110	0.0086	0.0069	0.0058	17
0.5836	0.0162	0.0151	0.0140	0.0129	0.0120	0.0098	0.0077	0.0060	0.0048	0.0040	18
0.4129	0.0115	0.0107	0.0099	0.0092	0.0085	0.0069	0.0054	0.0042	0.0034	0.0029	19
0.2935	0.0082	0.0076	0.0070	0.0065	0.0060	0.0049	0.0039	0.0030	0.0024	0.0020	20
0.2081	0.0058	0.0054	0.0050	0.0046	0.0043	0.0035	0.0027	0.0021	0.0017	0.0014	21
0.1463	0.0041	0.0038	0.0035	0.0032	0.0030	0.0025	0.0019	0.0015	0.0012	0.0010	22
0.1014	0.0028	0.0026	0.0024	0.0022	0.0021	0.0017	0.0013	0.0010	0.0008	0.0007	23
0.069	0.0019	0.0018	0.0017	0.0015	0.0014	0.0012	0.0009	0.0007	0.0006	0.0005	24
	0.0295	0.0295	0.0295	0.0295	0.0295	0.0295	0.0295	0.0295	0.0295	0.0295	25
	0.0295	0.0295	0.0295	0.0295	0.0295	0.0295	0.0295	0.0295	0.0295	0.0295	26

	keff	std dev	Total Cell Flux (F14) (#/cm2)	F14 Energy Bin 0-0.5MeV	F14 Energy Bin 0.5-1MeV	F14 Energy Bin 1-2MeV	F14 Energy Bin 2-4MeV	F14 Energy Bin 4-20MeV
0cm*	0.84141	0.00114						
1cm	0.84338	0.00108	1.459E-03	1.020E-03	1.220E-04	1.611E-04	1.079E-04	4.830E-05
2cm	0.84171	0.00113	1.48E-03	1.04E-03	1.30E-04	1.55E-04	1.14E-04	3.99622E-05
5cm	0.84107	0.00116	1.49E-03	1.05E-03	1.27E-04	1.57E-04	1.17E-04	3.94651E-05
11cm	0.84683	0.00117	1.48E-03	1.05E-03	1.25E-04	1.53E-04	1.13E-04	3.84151E-05

Concentration			Pressure		
	keff	std dev		keff	std dev
80%He 20%UF6	0.84141	0.00114	100 kPa	0.33630	0.00068
50%He 50%UF6	0.94930	0.00124	500 kPa	0.71925	0.00106
20%He 80%UF6	0.98097	0.00120	1500 kPa	0.89919	0.00119
0%He 100%UF6	0.99768	0.00144	10000 kPa	1.05222	0.00118
			25000 kPa	1.14209	0.00110
			50000 kPa	1.24625	0.00107
			25000 kPa	1.14209	0.00110
			50000 kPa	1.24625	0.00107

Selected MCNPX Outputs Data formatted for EXCEL Calculations

4.38cm -- 1E-05 sec

	<u>Surface Flux</u>		<u>Surface Flux by Cell (#/cm2) (F2)</u>															
<u>Energy</u>	<u>Total (F12)</u>	10	11	12	13	14	15	16	17	18	19	20	21	22	23	24	25	26
0-0.5 MeV	1.22E-03	2.27E-03	1.94E-03	1.72E-03	1.52E-03	1.30E-03	9.89E-04	8.91E-04	8.22E-04	7.76E-04	7.38E-04	7.10E-04	6.85E-04	6.66E-04	6.48E-04	6.34E-04	5.88E-04	5.66E-04
0.5-1MeV	1.63E-03	3.03E-03	2.59E-03	2.29E-03	2.02E-03	1.73E-03	1.32E-03	1.19E-03	1.09E-03	1.03E-03	9.83E-04	9.43E-04	9.11E-04	8.85E-04	8.62E-04	8.44E-04	7.82E-04	7.53E-04
1-2MeV	2.72E-03	5.06E-03	4.32E-03	3.83E-03	3.38E-03	2.89E-03	2.20E-03	1.97E-03	1.82E-03	1.72E-03	1.64E-03	1.57E-03	1.52E-03	1.48E-03	1.44E-03	1.41E-03	1.30E-03	1.25E-03
2-4MeV	2.65E-03	4.93E-03	4.21E-03	3.73E-03	3.30E-03	2.81E-03	2.14E-03	1.92E-03	1.77E-03	1.67E-03	1.59E-03	1.53E-03	1.48E-03	1.44E-03	1.40E-03	1.36E-03	1.26E-03	1.22E-03
4-20MeV	9.63E-04	1.79E-03	1.53E-03	1.36E-03	1.20E-03	1.02E-03	7.77E-04	6.99E-04	6.45E-04	6.09E-04	5.79E-04	5.57E-04	5.37E-04	5.22E-04	5.08E-04	4.97E-04	4.59E-04	4.39E-04
Total	9.18E-03	1.71E-02	1.46E-02	1.29E-02	1.14E-02	9.76E-03	7.42E-03	6.67E-03	6.16E-03	5.81E-03	5.53E-03	5.31E-03	5.13E-03	4.98E-03	4.85E-03	4.75E-03	4.39E-03	4.23E-03
	<u>Cell Flux</u>		<u>Cell Flux by Cell (#/cm2) (F4)</u>															
<u>Energy</u>	<u>Total (F14)</u>	10	11	12	13	14	15	16	17	18	19	20	21	22	23	24	25	26
0-0.5 MeV	8.39E-04	2.34E-03	1.89E-03	1.64E-03	1.41E-03	1.12E-03	9.38E-04	8.56E-04	7.99E-04	7.57E-04	7.24E-04	6.98E-04	6.75E-04	6.57E-04	6.41E-04	6.11E-04	5.77E-04	5.64E-04
0.5-1MeV	1.12E-03	3.12E-03	2.52E-03	2.18E-03	1.87E-03	1.48E-03	1.25E-03	1.14E-03	1.06E-03	1.01E-03	9.63E-04	9.26E-04	8.99E-04	8.73E-04	8.52E-04	8.12E-04	7.69E-04	7.50E-04
1-2MeV	1.86E-03	5.21E-03	4.20E-03	3.64E-03	3.12E-03	2.47E-03	2.08E-03	1.90E-03	1.77E-03	1.68E-03	1.60E-03	1.54E-03	1.50E-03	1.46E-03	1.42E-03	1.35E-03	1.28E-03	1.24E-03
2-4MeV	1.81E-03	5.07E-03	4.10E-03	3.54E-03	3.04E-03	2.41E-03	2.02E-03	1.85E-03	1.72E-03	1.63E-03	1.56E-03	1.50E-03	1.46E-03	1.42E-03	1.38E-03	1.32E-03	1.24E-03	1.21E-03
4-20MeV	6.59E-04	1.85E-03	1.49E-03	1.29E-03	1.11E-03	8.77E-04	7.36E-04	6.71E-04	6.26E-04	5.94E-04	5.67E-04	5.47E-04	5.30E-04	5.15E-04	5.02E-04	4.78E-04	4.52E-04	4.41E-04
Total	6.29E-03	1.76E-02	1.42E-02	1.23E-02	1.05E-02	8.36E-03	7.02E-03	6.40E-03	5.98E-03	5.67E-03	5.42E-03	5.22E-03	5.06E-03	4.92E-03	4.80E-03	4.57E-03	4.32E-03	4.20E-03
Mean Free Path (cm)		113.69	118.03	122.52	131.66	151.6	282.64	433.02	638.28	914.06	1287.6	1805.8	2552.8	3611.2	5287.7	7792.3	501.94	501.77
<u>Number</u>		<u>Number</u>		E_i	dE_i	M_n	$Flux/n$	$Flux$										
(n,xn)	406	Escape	100029379	0.25	0.5	939.5	1.82E-02	1.82E+06										
Prompt Fission	46907	Time Cut	334	0.75	0.5		1.40E-02	1.40E+06										
Delayed Fission	334	Capture	0	1.5	1	dt_i	3.29E-02	3.29E+06										

		Loss (n,xn)	203
		loss (fission)	17731
Total Neut.	100047647		
Difference	47647	29176	

3	2	1.00E-05	4.53E-02	4.53E+06	<i>r_i</i>	<i>dr_i</i>	
12	16		6.59E-02	6.59E+06	0.0438	0.0219	
		<i>n-s/m3</i>		1.76E+07	<i># Neut-s</i>	9.31E+03	<i>keff*</i>
		<i>Src/min</i>	<i>Src/sec</i>		<i>#neuts</i>	9.31E+08	9.31E+00
		2.76E+06	4.60E+04		<i>keff</i>	2.02E-01	

Example Input File

```
UF6 Shockwave Reactor No Shockwave
c
c
c CELL CARDS
c
1 13 -0.02511 -1 imp:n=1
30 4 -1.85 -30 1 imp:n=1
3 2 -7.92 -3 30 imp:n=1
6 0 3 imp:n=0

c SURFACE CARDS
c
1 so 25 $ Gaseous Mixture-UF6
3 so 102.5 $ S. Steel Containment
30 so 90 $ Beryllium Reflector

c MATERIAL CARDS
c
c UF6 e=80% (He Mod. 80%)
c (density = 29.5 kg/m3)
m13 92235.70c -0.51426
92238.70c -0.13021
9019.70c -0.31174
2004.70c -0.04380
c
c Stainless Steel AISI 302
c (density = 7920 kg/m3)
m2 6000.70c -0.0015
24052.70c -0.19
26056.70c -0.77775
25055.70c -0.02
28058.70c -0.1
15031.70c -0.00045
14028.70c -0.01
16032.70c -0.0003
c
c Water
c (density = 1000 kg/m3)
c m3 1001.70c 2
c 8016.70c 1
c
c Beryllium Reflector
c (density = 1850 kg/m3)
m4 4009.70c 1
c
c Heavy Water
c (density = 1100 kg/m3)
c m5 1002.70c 2
c 8016.70c 1
c
c
kcode 700 1.00 100 1010
ksrc 0 0 0
c
c F4:N 10 11 12 13 14 15 16 17 18 19 20 21 22 23 24 25 26
c FM4 -1 -6
c E4 .5 1 2 4 20 T
c
F4:N 1
```

```

FM4 -1 -6
E4 .5 1 2 4 20 T
c
c F2:N 10 11 12 13 14 15 16 17 18 19 20 21 22 23 24 25 26
c FM2 -1 -6
c E2 .5 1 2 4 20 T
c
F2:N 1
FM2 -1 -6
E2 .5 1 2 4 20 T
c
print

```

UF6 Shockwave Reactor No Shockwave

```

c
c
c CELL CARDS
c
1 13 -0.0295 -1 imp:n=1
99 0 1 imp:n=0

```

c SURFACE CARDS

```

c
1 so 25 $ Gaseous Mixture-UF6

```

c MATERIAL CARDS

```

c
c UF6 e=80% (He Mod. 80%)
c (density = 29.5 kg/m3)
m13 92235.70c -0.51426
92238.70c -0.13021
9019.70c -0.31174
2004.70c -0.04380

```

```

c
sdef cel=1 erg=D1
SP1 -3
nps 100000000
c cut:n 24000 4J
c
F4:N 1
E4 .5 1 2 4 20 T
c
c
print

```

UF6 Shockwave Reactor 7.63cm wave

```
c
c
c CELL CARDS
c
1      0      10      imp:n=0
c
c Shockwave Cells
10 13 -0.1040 -10 11 imp:n=1 $ Shockwave Front
11 13 -0.1002 -11 12 imp:n=1
12 13 -0.0965 -12 13 imp:n=1
13 13 -0.0898 -13 14 imp:n=1
14 13 -0.0780 -14 15 imp:n=1
15 13 -0.0418 -15 16 imp:n=1
16 16 -0.0273 -16 17 imp:n=1
17 16 -0.0185 -17 18 imp:n=1
18 19 -0.0129 -18 19 imp:n=1
19 112 -0.0092 -19 20 imp:n=1
20 112 -0.0065 -20 21 imp:n=1
21 125 -0.0046 -21 22 imp:n=1
22 125 -0.0032 -22 23 imp:n=1
23 125 -0.0022 -23 24 imp:n=1
24 125 -0.0015 -24 25 imp:n=1
25 125 -0.0295 -25 26 imp:n=1 $ Property Return 50%
26 125 -0.0295 -26 imp:n=1 $ Property Return 100%
```

c SURFACE CARDS

```
c
c Shockwave Surfaces
10 so 7.63 $ Shockwave Front
11 so 7.61
12 so 7.59
13 so 7.55
14 so 7.48
15 so 7.10
16 so 6.79
17 so 6.49 $ 85%
18 so 6.18
19 so 5.88
20 so 5.57
21 so 5.26
22 so 4.96 $ 65%
23 so 4.65
24 so 4.35
25 so 2.90 $ Property Return 50%
26 so 1.45 $ Property Return 100%
```

c MATERIAL CARDS

```
c
c UF6 e=80% (He Mod. 80%)
c (density = 29.5 kg/m3)
m13 92235.70c -0.51426
    92238.70c -0.13021
    9019.70c -0.31174
    2004.70c -0.04380
c
c UF6 e=80% (He Mod. 80%)
c (density = 29.5 kg/m3)
m16 92235.71c -0.51426
    92238.71c -0.13021
    9019.71c -0.31174
    2004.71c -0.04380
```

```

c
c UF6 e=80% (He Mod. 80%)
c (density = 29.5 kg/m3)
m19 92235.72c -0.51426
    92238.72c -0.13021
    9019.72c -0.31174
    2004.72c -0.04380

c
c UF6 e=80% (He Mod. 80%)
c (density = 29.5 kg/m3)
m112 92235.73c -0.51426
    92238.73c -0.13021
    9019.73c -0.31174
    2004.73c -0.04380

c
c UF6 e=80% (He Mod. 80%)
c (density = 29.5 kg/m3)
m125 92235.74c -0.51426
    92238.74c -0.13021
    9019.74c -0.31174
    2004.74c -0.04380

c
sdef cel=10 pos=0 0 0 rad=7.62 erg=D1
SP1 -3
nps 100000000
cut:n 1000 4J

c
F4:N 10 11 12 13 14 15 16 17 18 19 20 21 22 23 24 25 26
FM4 -1 -6
E4 .5 1 2 4 20 T

c
F14:N (10 11 12 13 14 15 16 17 18 19 20 21 22 23 24 25 26)
FM14 -1 -6
E14 .5 1 2 4 20 T

c
F2:N 10 11 12 13 14 15 16 17 18 19 20 21 22 23 24 25 26
FM2 -1 -6
E2 .5 1 2 4 20 T

c
F12:N (10 11 12 13 14 15 16 17 18 19 20 21 22 23 24 25 26)
FM12 -1 -6
E12 .5 1 2 4 20 T

c
print

```

Example Output File

lmcnp version 2.7.0 ld=Mon Apr 18 08:00:00 MST 2011 10/05/13 02:36:03

i=C:/MCNP/Thesis/sho5.txt o=C:/MCNP/Thesis/ShockOnly/sho5.o probid = 10/05/13 02:36:03

```
*****
*
*          *
*      MCNPX          *
*          *
* Copyright 2007. Los Alamos National Security, LLC. *
* All rights reserved.          *
*          *
* This material was produced under U.S. Government contract *
* DE-AC52-06NA25396 for Los Alamos National Laboratory, *
* which is operated by Los Alamos National Security, LLC *
* for the U.S. Department of Energy. The Government is *
* granted for itself and others acting on its behalf a *
* paid-up, nonexclusive, irrevocable worldwide license in *
* this material to reproduce, prepare derivative works, and *
* works, and perform publicly and display publicly. *
* Beginning five (5) years after June 1, 2006, subject to *
* additional five-year worldwide renewals, the Government *
* is granted for itself and others acting on its behalf *
* a paid-up, nonexclusive, irrevocable worldwide license *
* in this material to reproduce, prepare derivative works, *
* distribute copies to the public, perform publicly and *
* display publicly, and to permit others to do so. *
*          *
* NEITHER THE UNITED STATES NOR THE UNITED STATES *
* DEPARTMENT OF ENERGY, NOR LOS ALAMOS NATIONAL SECURITY, *
* LLC, NOR ANY OF THEIR EMPLOYEES, MAKES ANY WARRANTY, *
* EXPRESS OR IMPLIED, OR ASSUMES ANY LEGAL LIABILITY OR *
* RESPONSIBILITY FOR THE ACCURACY, COMPLETENESS, OR *
* USEFULNESS OF ANY INFORMATION, APPARATUS, PRODUCT, OR *
* PROCESS DISCLOSED, OR REPRESENTS THAT ITS USE WOULD NOT *
* INFRINGE PRIVATELY OWNED RIGHTS. *
*          *
*****
1- UF6 Shockwave Reactor 10cm wave
2- c
3- c
4- c CELL CARDS
5- c
6- 1 0 10 imp:n=0
7- c
8- c Shockwave Cells
9- 10 13 -0.0560 -10 11 imp:n=1 $ Shockwave Front
10- 11 13 -0.0539 -11 12 imp:n=1
11- 12 13 -0.0520 -12 13 imp:n=1
12- 13 13 -0.0483 -13 14 imp:n=1
13- 14 13 -0.0420 -14 15 imp:n=1
14- 15 13 -0.0225 -15 16 imp:n=1
15- 16 16 -0.0147 -16 17 imp:n=1
16- 17 16 -0.0100 -17 18 imp:n=1
17- 18 19 -0.0070 -18 19 imp:n=1
18- 19 112 -0.0049 -19 20 imp:n=1
19- 20 112 -0.0035 -20 21 imp:n=1
20- 21 125 -0.0025 -21 22 imp:n=1
21- 22 125 -0.0017 -22 23 imp:n=1
22- 23 125 -0.0012 -23 24 imp:n=1
23- 24 125 -0.0008 -24 25 imp:n=1
24- 25 125 -0.0295 -25 26 imp:n=1 $ Property Return 50%
25- 26 125 -0.0295 -26 imp:n=1 $ Property Return 100%
26-
27- c SURFACE CARDS
28- c
29- c Shockwave Surfaces
30- 10 so 10.00 $ Shockwave Front
31- 11 so 9.98
32- 12 so 9.95
33- 13 so 9.90
34- 14 so 9.80
35- 15 so 9.30
36- 16 so 8.90
37- 17 so 8.50 $ 85%
38- 18 so 8.10
39- 19 so 7.70
40- 20 so 7.30
41- 21 so 6.90
42- 22 so 6.50 $ 65%
43- 23 so 6.10
44- 24 so 5.70
45- 25 so 3.80 $ Property Return 50%
46- 26 so 1.90 $ Property Return 100%
47-
48- c MATERIAL CARDS
49- c
50- c UF6 e=80% (He Mod. 80%)
51- c (density = 29.5 kg/m3)
52- m13 92235.70c -0.51426
```

```

53-      92238.70c -0.13021
54-      9019.70c -0.31174
55-      2004.70c -0.04380
56-      c
57-      c UF6 e=80% (He Mod. 80%)
58-      c (density = 29.5 kg/m3)
59-      m16 92235.71c -0.51426
60-      92238.71c -0.13021
61-      9019.71c -0.31174
62-      2004.71c -0.04380
63-      c
64-      c UF6 e=80% (He Mod. 80%)
65-      c (density = 29.5 kg/m3)
66-      m19 92235.72c -0.51426
67-      92238.72c -0.13021
68-      9019.72c -0.31174
69-      2004.72c -0.04380
70-      c
71-      c UF6 e=80% (He Mod. 80%)
72-      c (density = 29.5 kg/m3)
73-      m112 92235.73c -0.51426
74-      92238.73c -0.13021
75-      9019.73c -0.31174
76-      2004.73c -0.04380
77-      c
78-      c UF6 e=80% (He Mod. 80%)
79-      c (density = 29.5 kg/m3)
80-      m125 92235.74c -0.51426
81-      92238.74c -0.13021
82-      9019.74c -0.31174
83-      2004.74c -0.04380
84-      c
85-      sdef cel=10 pos=0 0 0 rad=9.99 erg=2
warning. rad is constant. in most problems it is a variable.
86-      nps 100000000
87-      cut:n 24000 4J
88-      c
89-      F4:N 10 11 12 13 14 15 16 17 18 19 20 21 22 23 24 25 26
90-      FM4 -1 -6
91-      E4 .5 1 2 4 20 T
92-      c
93-      F14:N (10 11 12 13 14 15 16 17 18 19 20 21 22 23 24 25 26)
94-      FM14 -1 -6
95-      E14 .5 1 2 4 20 T
96-      c
97-      F2:N 10 11 12 13 14 15 16 17 18 19 20 21 22 23 24 25 26
98-      FM2 -1 -6
99-      E2 .5 1 2 4 20 T
100-      c
101-      F12:N (10 11 12 13 14 15 16 17 18 19 20 21 22 23 24 25 26)
102-      FM12 -1 -6
103-      E12 .5 1 2 4 20 T
104-      c
105-      print
106-

```

warning. total nu is now the default for fixed-source problems.
 lsource

print table 10

values of defaulted or explicitly defined source variables

```

cel 1.0000E+01
sur 0.0000E+00
erg 2.0000E+00
tme 0.0000E+00
dir isotropic
pos 0.0000E+00 0.0000E+00 0.0000E+00
x 0.0000E+00
y 0.0000E+00
z 0.0000E+00
rad 9.9900E+00
ext 0.0000E+00
axs 0.0000E+00 0.0000E+00 0.0000E+00
vec 0.0000E+00 0.0000E+00 0.0000E+00
ccc 0.0000E+00
nrm 1.0000E+00
ara 0.0000E+00
wgt 1.0000E+00
eff 1.0000E-02
par 0.0000E+00
tr 0.0000E+00
bem 0.0000E+00 0.0000E+00 0.0000E+00
bap 0.0000E+00 0.0000E+00 0.0000E+00
loc 0.0000E+00 0.0000E+00 0.0000E+00

```

order of sampling source variables.
 cel rad pos erg tme

l tally 2

tally type 2 particle flux averaged over a surface.
 particle(s): neutron

surfaces 10 11 12 13 14 15 16 17 18 19 20 21 22 23 24 25 26

print table 30

```

multiplier bins
att constant material reactions or material-rho*x pairs
1.0000E+00

attenuators
a -1.0000E+00

energy bins
0.0000E+00 to 5.0000E-01 mev
5.0000E-01 to 1.0000E+00 mev
1.0000E+00 to 2.0000E+00 mev
2.0000E+00 to 4.0000E+00 mev
4.0000E+00 to 2.0000E+01 mev
total bin
ltally 4          print table 30
tally type 4 track length estimate of particle flux.
particle(s): neutron
cells 10 11 12 13 14 15 16 17 18 19 20 21 22 23 24 25 26

```

```

multiplier bins
att constant material reactions or material-rho*x pairs
1.0000E+00

attenuators
a -1.0000E+00

energy bins
0.0000E+00 to 5.0000E-01 mev
5.0000E-01 to 1.0000E+00 mev
1.0000E+00 to 2.0000E+00 mev
2.0000E+00 to 4.0000E+00 mev
4.0000E+00 to 2.0000E+01 mev
total bin
ltally 12          print table 30
tally type 2 particle flux averaged over a surface.
particle(s): neutron
surfaces (10 11 12 13 14 15 16 17 18 19 20 21 22 23 24 25 26)

```

```

multiplier bins
att constant material reactions or material-rho*x pairs
1.0000E+00

attenuators
a -1.0000E+00

energy bins
0.0000E+00 to 5.0000E-01 mev
5.0000E-01 to 1.0000E+00 mev
1.0000E+00 to 2.0000E+00 mev
2.0000E+00 to 4.0000E+00 mev
4.0000E+00 to 2.0000E+01 mev
total bin
ltally 14          print table 30
tally type 4 track length estimate of particle flux.
particle(s): neutron
cells (10 11 12 13 14 15 16 17 18 19 20 21 22 23 24 25 26)

```

```

multiplier bins
att constant material reactions or material-rho*x pairs
1.0000E+00

attenuators
a -1.0000E+00

energy bins
0.0000E+00 to 5.0000E-01 mev
5.0000E-01 to 1.0000E+00 mev
1.0000E+00 to 2.0000E+00 mev
2.0000E+00 to 4.0000E+00 mev
4.0000E+00 to 2.0000E+01 mev
total bin

```

```

warning. 2004.70c and 2004.71c are both called for.
warning. 2004.71c and 2004.72c are both called for.
warning. 2004.72c and 2004.73c are both called for.
warning. 2004.73c and 2004.74c are both called for.
warning. 9019.70c and 9019.71c are both called for.
warning. 9019.71c and 9019.72c are both called for.
warning. 9019.72c and 9019.73c are both called for.
warning. 9019.73c and 9019.74c are both called for.
warning. 92235.70c and 92235.71c are both called for.
warning. 92235.71c and 92235.72c are both called for.
warning. 92235.72c and 92235.73c are both called for.

```

warning. 92235.73c and 92235.74c are both called for.

warning. 92238.70c and 92238.71c are both called for.

warning. 92238.71c and 92238.72c are both called for.

warning. 92238.72c and 92238.73c are both called for.

warning. 92238.73c and 92238.74c are both called for.
!material composition

print table 40

the sum of the fractions of material 13 was 1.000010E+00

not all cells containing material 13 have the same density.

the sum of the fractions of material 16 was 1.000010E+00

not all cells containing material 16 have the same density.

the sum of the fractions of material 19 was 1.000010E+00

the sum of the fractions of material 112 was 1.000010E+00

not all cells containing material 112 have the same density.

the sum of the fractions of material 125 was 1.000010E+00

not all cells containing material 125 have the same density.

material

material number	component nuclide, atom fraction					
13	92235, 7.27212679081E-02	92238, 1.81803588705E-02	9019, 5.45384971990E-01	2004, 3.63713401231E-01		
16	92235, 7.27212679081E-02	92238, 1.81803588705E-02	9019, 5.45384971990E-01	2004, 3.63713401231E-01		
19	92235, 7.27212679081E-02	92238, 1.81803588705E-02	9019, 5.45384971990E-01	2004, 3.63713401231E-01		
112	92235, 7.27212679081E-02	92238, 1.81803588705E-02	9019, 5.45384971990E-01	2004, 3.63713401231E-01		
125	92235, 7.27212679081E-02	92238, 1.81803588705E-02	9019, 5.45384971990E-01	2004, 3.63713401231E-01		

material

material number	component nuclide, mass fraction					
13	92235, 5.14254857451E-01	92238, 1.30208697913E-01	9019, 3.11736882631E-01	2004, 4.37995620044E-02		
16	92235, 5.14254857451E-01	92238, 1.30208697913E-01	9019, 3.11736882631E-01	2004, 4.37995620044E-02		
19	92235, 5.14254857451E-01	92238, 1.30208697913E-01	9019, 3.11736882631E-01	2004, 4.37995620044E-02		
112	92235, 5.14254857451E-01	92238, 1.30208697913E-01	9019, 3.11736882631E-01	2004, 4.37995620044E-02		
125	92235, 5.14254857451E-01	92238, 1.30208697913E-01	9019, 3.11736882631E-01	2004, 4.37995620044E-02		

warning. 5 materials had unnormalized fractions. print table 40.

warning. 4 of the materials appear at more than one density.

!LAHET physics options:

print table 41

```
lea ielas ipreq iexisa ichoic jcoul nexite npidk noact icem ilaq
lea 2 1 1 23 1 1 0 1 0 0
```

```
lcb flenb(i),i=1,6 ctofe flim0
lcb 3.4900E+03 3.4900E+03 2.4900E+03 2.4900E+03 8.0000E+02 8.0000E+02 -1.0000E+00 -1.0000E+00
```

```
lea ipht icc nobalc nobale ifbrk ilvden ievap nofis
lea 1 4 1 0 1 0 0 1
```

```
leb yzere bzere yzero bzzero
leb 1.5000E+00 8.0000E+00 1.5000E+00 1.0000E+01
```

warning. cross-section file bertin does not exist.

!cell volumes and masses

print table 50

cell	atom density	gram density	input volume	calculated volume	mass	reason	volume pieces	not calculated
1	1	0.00000E+00	0.00000E+00	0.00000E+00	0.00000E+00	0.00000E+00	0	infinite
2	10	1.01461E-03	5.60000E-02	0.00000E+00	2.50825E+01	1.40462E+00	1	
3	11	9.76564E-04	5.39000E-02	0.00000E+00	3.74357E+01	2.01778E+00	1	
4	12	9.42139E-04	5.20000E-02	0.00000E+00	6.18930E+01	3.21844E+00	1	
5	13	8.75102E-04	4.83000E-02	0.00000E+00	1.21923E+02	5.88889E+00	1	

6	14	7.60959E-04	4.20000E-02	0.00000E+00	5.73173E+02	2.40733E+01	1
7	15	4.07656E-04	2.25000E-02	0.00000E+00	4.16315E+02	9.36710E+00	1
8	16	2.66336E-04	1.47000E-02	0.00000E+00	3.80526E+02	5.59374E+00	1
9	17	1.81181E-04	1.00000E-02	0.00000E+00	3.46346E+02	3.46346E+00	1
10	18	1.26826E-04	7.00000E-03	0.00000E+00	3.13774E+02	2.19642E+00	1
11	19	8.87785E-05	4.90000E-03	0.00000E+00	2.82810E+02	1.38577E+00	1
12	20	6.34132E-05	3.50000E-03	0.00000E+00	2.53455E+02	8.87094E-01	1
13	21	4.52952E-05	2.50000E-03	0.00000E+00	2.25709E+02	5.64272E-01	1
14	22	3.08007E-05	1.70000E-03	0.00000E+00	1.99571E+02	3.39270E-01	1
15	23	2.17417E-05	1.20000E-03	0.00000E+00	1.75041E+02	2.10049E-01	1
16	24	1.44945E-05	8.00000E-04	0.00000E+00	5.45887E+02	4.36710E-01	1
17	25	5.34483E-04	2.95000E-02	0.00000E+00	2.01116E+02	5.93293E+00	1
18	26	5.34483E-04	2.95000E-02	0.00000E+00	2.87309E+01	8.47562E-01	1

lsurface areas print table 50

	surface	input	calculated	reason	area
	area	area	area	not	calculated
1	10	0.00000E+00	1.25664E+03		
2	11	0.00000E+00	1.25162E+03		
3	12	0.00000E+00	1.24410E+03		
4	13	0.00000E+00	1.23163E+03		
5	14	0.00000E+00	1.20687E+03		
6	15	0.00000E+00	1.08687E+03		
7	16	0.00000E+00	9.95382E+02		
8	17	0.00000E+00	9.07920E+02		
9	18	0.00000E+00	8.24480E+02		
10	19	0.00000E+00	7.45060E+02		
11	20	0.00000E+00	6.69662E+02		
12	21	0.00000E+00	5.98285E+02		
13	22	0.00000E+00	5.30929E+02		
14	23	0.00000E+00	4.67595E+02		
15	24	0.00000E+00	4.08281E+02		
16	25	0.00000E+00	1.81458E+02		
17	26	0.00000E+00	4.53646E+01		

lcells print table 60

cell	mat	atom	gram	neutron				
		density	density	volume	mass	pieces importance		
1	1	0	0.00000E+00	0.00000E+00	0.00000E+00	0.00000E+00	0	0.0000E+00
2	10	13	1.01461E-03	5.60000E-02	2.50825E+01	1.40462E+00	1	1.0000E+00
3	11	13	9.76564E-04	5.39000E-02	3.74357E+01	2.01778E+00	1	1.0000E+00
4	12	13	9.42139E-04	5.20000E-02	6.18930E+01	3.21844E+00	1	1.0000E+00
5	13	13	8.75102E-04	4.83000E-02	1.21923E+02	5.88889E+00	1	1.0000E+00
6	14	13	7.60959E-04	4.20000E-02	5.73173E+02	2.40733E+01	1	1.0000E+00
7	15	13	4.07656E-04	2.25000E-02	4.16315E+02	9.36710E+00	1	1.0000E+00
8	16	16	2.66336E-04	1.47000E-02	3.80526E+02	5.59374E+00	1	1.0000E+00
9	17	16	1.81181E-04	1.00000E-02	3.46346E+02	3.46346E+00	1	1.0000E+00
10	18	19	1.26826E-04	7.00000E-03	3.13774E+02	2.19642E+00	1	1.0000E+00
11	19	112	8.87785E-05	4.90000E-03	2.82810E+02	1.38577E+00	1	1.0000E+00
12	20	112	6.34132E-05	3.50000E-03	2.53455E+02	8.87094E-01	1	1.0000E+00
13	21	125	4.52952E-05	2.50000E-03	2.25709E+02	5.64272E-01	1	1.0000E+00
14	22	125	3.08007E-05	1.70000E-03	1.99571E+02	3.39270E-01	1	1.0000E+00
15	23	125	2.17417E-05	1.20000E-03	1.75041E+02	2.10049E-01	1	1.0000E+00
16	24	125	1.44945E-05	8.00000E-04	5.45887E+02	4.36710E-01	1	1.0000E+00
17	25	125	5.34483E-04	2.95000E-02	2.01116E+02	5.93293E+00	1	1.0000E+00
18	26	125	5.34483E-04	2.95000E-02	2.87309E+01	8.47562E-01	1	1.0000E+00

total 4.18879E+03 6.78274E+01 print table 70

surface	trans	type	surface coefficients
1	10	so	1.0000000E+01
2	11	so	9.9800000E+00
3	12	so	9.9500000E+00
4	13	so	9.9000000E+00
5	14	so	9.8000000E+00
6	15	so	9.3000000E+00
7	16	so	8.9000000E+00
8	17	so	8.5000000E+00
9	18	so	8.1000000E+00
10	19	so	7.7000000E+00
11	20	so	7.3000000E+00
12	21	so	6.9000000E+00
13	22	so	6.5000000E+00
14	23	so	6.1000000E+00
15	24	so	5.7000000E+00
16	25	so	3.8000000E+00
17	26	so	1.9000000E+00

random number control 0.830206021468160E+14 print table 72
 l cell temperatures in mev for the free-gas thermal neutron treatment.

all non-zero importance cells with materials have a temperature for thermal neutrons of 2.5300E-08 mev.

minimum source weight = 1.0000E+00 maximum source weight = 1.0000E+00

21 warning messages so far. print table 98
 lphysical constants

name	value	description
huge	1.000000000000E+37	infinity
pie	3.1415926535898E+00	pi
euler	5.7721566490153E-01	euler constant
avogad	6.0220434469282E+23	avogadro number (molecules/mole)
aneut	1.0086649670000E+00	neutron mass (amu)
avgdn	5.9703109000000E-01	avogadro number/neutron mass (1.e-24*molecules/mole/amu)
slite	2.9979250000000E+02	speed of light (cm/shake)
planck	4.1357320000000E-13	planck constant (mev shake)
fscon	1.3703930000000E+02	inverse fine structure constant h*c/(2*pi*e**2)
gpt(1)	9.3958000000000E+02	neutron mass (mev)
gpt(3)	5.1100800000000E-01	electron mass (mev)

fission q-values: nuclide q(mev) nuclide q(mev)			
90232	171.91	91233	175.57
92233	180.84	92234	179.45
92235	180.88	92236	179.50
92237	180.40	92238	181.31
92239	180.40	92240	180.40
93237	183.67	94238	186.65
94239	189.44	94240	186.36
94241	188.99	94242	185.98
94243	187.48	95241	190.83
95242	190.54	95243	190.25
96242	190.49	96244	190.49
other	180.00		

the following compilation options were used:

```

CHEAP
DEC
PLOT
MCPLT
GKSSIM
XLIB
XS64
CEM
INCL
HISTP
MESHTAL
RADIOG
SPABI
default datapath: C:\MCNP\mcnp_data
                  c:\mcnp\xs

```

1cross-section tables print table 100

table	length			
tables from file endf70a				
2004.70c	4614	2-He- 4 at 293.6K from endf/b-vii.0 njoy99.248	mat 228	08/24/07
2004.71c	4694	2-He- 4 at 600K from endf/b-vii.0 njoy99.248 temperature = 5.1704E-08 adjusted to 2.5300E-08	mat 228	08/24/07
2004.72c	4730	2-He- 4 at 900K from endf/b-vii.0 njoy99.248 temperature = 7.7556E-08 adjusted to 2.5300E-08	mat 228	08/24/07
2004.73c	4762	2-He- 4 at 1200K from endf/b-vii.0 njoy99.248 temperature = 1.0341E-07 adjusted to 2.5300E-08	mat 228	08/24/07
2004.74c	4826	2-He- 4 at 2500K from endf/b-vii.0 njoy99.248 temperature = 2.1543E-07 adjusted to 2.5300E-08	mat 228	08/24/07
particle-production data for ipt= 9 being expunged from 9019.70c				
particle-production data for ipt= 34 being expunged from 9019.70c				
9019.70c	84796	9-F - 19 at 293.6K from endf/b-vii.0 njoy99.248	mat 925	08/25/07
particle-production data for ipt= 9 being expunged from 9019.71c				
particle-production data for ipt= 34 being expunged from 9019.71c				
9019.71c	84824	9-F - 19 at 600K from endf/b-vii.0 njoy99.248 temperature = 5.1704E-08 adjusted to 2.5300E-08	mat 925	08/25/07
particle-production data for ipt= 9 being expunged from 9019.72c				
particle-production data for ipt= 34 being expunged from 9019.72c				
9019.72c	84844	9-F - 19 at 900K from endf/b-vii.0 njoy99.248 temperature = 7.7556E-08 adjusted to 2.5300E-08	mat 925	08/25/07
particle-production data for ipt= 9 being expunged from 9019.73c				
particle-production data for ipt= 34 being expunged from 9019.73c				
9019.73c	84888	9-F - 19 at 1200K from endf/b-vii.0 njoy99.248 temperature = 1.0341E-07 adjusted to 2.5300E-08	mat 925	08/25/07
particle-production data for ipt= 9 being expunged from 9019.74c				
particle-production data for ipt= 34 being expunged from 9019.74c				
9019.74c	84888	9-F - 19 at 2500K from endf/b-vii.0 njoy99.248 temperature = 2.1543E-07 adjusted to 2.5300E-08	mat 925	08/25/07
tables from file endf70j				
92235.70c	675995	92-U -235 at 293.6K from endf/b-vii.0 njoy99.248 total nu probability tables used from 2.2500E-03 to 2.5000E-02 mev.	mat9228	08/25/07
92235.71c	564807	92-U -235 at 600K from endf/b-vii.0 njoy99.248 total nu probability tables used from 2.2500E-03 to 2.5000E-02 mev. temperature = 5.1704E-08 adjusted to 2.5300E-08	mat9228	08/25/07
warning. 1 coincident energy grid points in 92235.72c				
92235.72c	517930	92-U -235 at 900K from endf/b-vii.0 njoy99.248 total nu	mat9228	08/25/07

probability tables used from 2.2500E-03 to 2.5000E-02 mev.
 temperature = 7.7556E-08 adjusted to 2.5300E-08
 92235.73c 491125 92-U -235 at 1200K from endf/b-vii.0 njoy99.248 total nu mat9228 08/25/07
 probability tables used from 2.2500E-03 to 2.5000E-02 mev.
 temperature = 1.0341E-07 adjusted to 2.5300E-08

warning. 1 coincident energy grid points in 92235.74c
 92235.74c 444234 92-U -235 at 2500K from endf/b-vii.0 njoy99.248 total nu mat9228 08/25/07
 probability tables used from 2.2500E-03 to 2.5000E-02 mev.
 temperature = 2.1543E-07 adjusted to 2.5300E-08

92238.70c 1318483 92-U -238 at 293.6K from endf/b-vii.0 njoy99.248 total nu mat9237 08/25/07
 probability tables used from 2.0000E-02 to 1.4903E-01 mev.

92238.71c 1151953 92-U -238 at 600K from endf/b-vii.0 njoy99.248 total nu mat9237 08/25/07
 probability tables used from 2.0000E-02 to 1.4903E-01 mev.
 temperature = 5.1704E-08 adjusted to 2.5300E-08

92238.72c 1072272 92-U -238 at 900K from endf/b-vii.0 njoy99.248 total nu mat9237 08/25/07
 probability tables used from 2.0000E-02 to 1.4903E-01 mev.
 temperature = 7.7556E-08 adjusted to 2.5300E-08

92238.73c 1021732 92-U -238 at 1200K from endf/b-vii.0 njoy99.248 total nu mat9237 08/25/07
 probability tables used from 2.0000E-02 to 1.4903E-01 mev.
 temperature = 1.0341E-07 adjusted to 2.5300E-08

92238.74c 911622 92-U -238 at 2500K from endf/b-vii.0 njoy99.248 total nu mat9237 08/25/07
 probability tables used from 2.0000E-02 to 1.4903E-01 mev.
 temperature = 2.1543E-07 adjusted to 2.5300E-08

warning. multi-temperature treatment used for neutron unresolved.

total 8618019

warning. 16 cross sections modified by free gas thermal treatment.

lparticles and energy limits print table 101

particle type	particle cutoff	maximum energy	smallest table maximum	largest table maximum	always use table	always use model
1 n neutron	0.0000E+00	1.0000E+37	2.0000E+01	3.0000E+01	2.0000E+01	3.0000E+01

ldecimal words of dynamically allocated storage

general 0
 tallies 14338
 bank 581633
 cross sections 8618020

total 0 = 0 bytes

 dump no. 1 on file runtp nps = 0 coll = 0 ctm = 0.00 nrm = 0

25 warning messages so far.
 1 starting mcrun. dynamic storage = 0 words, 0 bytes. cp0 = 0.08 print table 110

UF6 Shockwave Reactor 10cm wave

nps	x	y	z	cell	surf	u	v	w	energy	weight	time
1	5.080E+00	4.728E+00	7.186E+00	10	0	2.566E-01	6.731E-01	6.936E-01	2.000E+00	1.000E+00	0.000E+00
2	8.943E+00	-4.442E+00	-2.942E-01	10	0	9.530E-01	1.832E-01	-2.413E-01	2.000E+00	1.000E+00	0.000E+00
3	-6.178E+00	-4.490E+00	6.440E+00	10	0	-7.618E-01	-6.038E-01	-2.346E-01	2.000E+00	1.000E+00	0.000E+00
4	9.700E+00	-5.660E-01	-2.320E+00	10	0	-8.276E-01	-1.542E-01	-5.398E-01	2.000E+00	1.000E+00	0.000E+00
5	5.855E+00	1.495E+00	-7.955E+00	10	0	7.831E-01	-1.660E-01	-5.994E-01	2.000E+00	1.000E+00	0.000E+00
6	-6.482E-01	-1.625E+00	9.836E+00	10	0	-8.262E-01	4.814E-01	2.925E-01	2.000E+00	1.000E+00	0.000E+00
7	-7.061E-01	3.260E-01	-9.960E+00	10	0	3.703E-02	9.959E-01	8.298E-02	2.000E+00	1.000E+00	0.000E+00
8	-3.911E+00	4.659E+00	-7.924E+00	10	0	-4.714E-01	-6.124E-01	-6.346E-01	2.000E+00	1.000E+00	0.000E+00
9	-2.366E+00	9.206E+00	-3.075E+00	10	0	4.995E-01	-1.108E-01	8.592E-01	2.000E+00	1.000E+00	0.000E+00
10	1.944E+00	-3.200E+00	9.262E+00	10	0	-4.993E-01	-5.038E-01	-7.050E-01	2.000E+00	1.000E+00	0.000E+00
11	-6.692E+00	-7.169E+00	-1.903E+00	10	0	-4.723E-01	5.705E-01	6.719E-01	2.000E+00	1.000E+00	0.000E+00
12	-8.390E+00	-4.125E+00	3.520E+00	10	0	-8.354E-03	9.954E-01	9.552E-02	2.000E+00	1.000E+00	0.000E+00
13	-1.712E+00	-8.563E+00	4.852E+00	10	0	1.374E-01	3.418E-02	9.899E-01	2.000E+00	1.000E+00	0.000E+00
14	-2.486E+00	-5.113E+00	-8.214E+00	10	0	5.151E-01	-8.011E-02	8.534E-01	2.000E+00	1.000E+00	0.000E+00
15	-2.956E+00	2.117E+00	9.305E+00	10	0	3.734E-01	-8.859E-01	2.752E-01	2.000E+00	1.000E+00	0.000E+00
16	1.393E+00	-9.819E+00	1.201E+00	10	0	-1.418E-01	9.037E-01	-4.040E-01	2.000E+00	1.000E+00	0.000E+00
17	6.902E+00	-7.103E+00	1.306E+00	10	0	-5.034E-01	-6.179E-01	6.040E-01	2.000E+00	1.000E+00	0.000E+00
18	-6.574E+00	5.315E+00	-5.324E+00	10	0	-4.506E-01	5.114E-01	7.317E-01	2.000E+00	1.000E+00	0.000E+00
19	-9.894E+00	-1.378E+00	1.351E-01	10	0	-1.838E-02	-6.229E-01	7.821E-01	2.000E+00	1.000E+00	0.000E+00
20	7.455E+00	4.854E+00	-4.546E+00	10	0	-5.347E-01	-8.270E-01	1.736E-01	2.000E+00	1.000E+00	0.000E+00
21	-1.975E+00	9.787E+00	3.356E-01	10	0	-5.539E-01	6.585E-01	-5.094E-01	2.000E+00	1.000E+00	0.000E+00
22	-9.108E+00	-3.643E+00	-1.889E+00	10	0	9.244E-01	3.642E-01	-1.131E-01	2.000E+00	1.000E+00	0.000E+00
23	-4.282E+00	8.353E+00	-3.419E+00	10	0	-6.813E-01	-5.866E-01	-4.379E-01	2.000E+00	1.000E+00	0.000E+00
24	1.079E+00	3.408E+00	-9.328E+00	10	0	8.710E-01	1.299E-01	4.739E-01	2.000E+00	1.000E+00	0.000E+00
25	-9.101E+00	-9.003E-02	-4.118E+00	10	0	2.531E-01	-9.243E-01	2.858E-01	2.000E+00	1.000E+00	0.000E+00
26	-2.566E+00	-6.385E+00	-7.242E+00	10	0	2.244E-01	9.723E-01	6.497E-02	2.000E+00	1.000E+00	0.000E+00
27	-2.909E+00	8.078E+00	5.108E+00	10	0	-3.163E-01	-9.343E-01	-1.645E-01	2.000E+00	1.000E+00	0.000E+00
28	1.471E+00	-9.505E+00	2.702E+00	10	0	-3.078E-01	9.120E-01	2.711E-01	2.000E+00	1.000E+00	0.000E+00
29	-6.129E+00	-7.637E+00	-1.976E+00	10	0	-3.449E-01	-7.183E-01	-6.043E-01	2.000E+00	1.000E+00	0.000E+00
30	-5.696E+00	5.646E+00	-5.957E+00	10	0	-7.427E-01	4.420E-01	-5.031E-01	2.000E+00	1.000E+00	0.000E+00
31	-6.601E+00	5.367E+00	-5.237E+00	10	0	5.991E-01	2.347E-02	8.003E-01	2.000E+00	1.000E+00	0.000E+00
32	-9.733E-01	-3.636E+00	-9.254E+00	10	0	5.141E-01	-6.626E-01	5.447E-01	2.000E+00	1.000E+00	0.000E+00
33	-1.963E+00	-3.142E+00	-9.278E+00	10	0	9.767E-01	-2.074E-01	5.564E-02	2.000E+00	1.000E+00	0.000E+00

```

34 4.093E+00 8.457E+00 -3.395E+00 10 0 4.302E-01 2.974E-01 -8.523E-01 2.000E+00 1.000E+00 0.000E+00
35 -4.044E-01 8.822E+00 4.670E+00 10 0 8.995E-01 4.352E-01 -3.994E-02 2.000E+00 1.000E+00 0.000E+00
36 3.368E+00 -9.259E+00 -1.650E+00 10 0 9.302E-01 -2.691E-02 3.660E-01 2.000E+00 1.000E+00 0.000E+00
37 -1.865E+00 9.746E+00 -1.154E+00 10 0 -2.562E-01 -6.974E-01 6.693E-01 2.000E+00 1.000E+00 0.000E+00
38 -2.614E+00 2.333E+00 -9.356E+00 10 0 1.134E-01 -8.691E-01 4.815E-01 2.000E+00 1.000E+00 0.000E+00
39 9.771E+00 -7.633E-01 -1.937E+00 10 0 -1.946E-01 -9.777E-01 -7.886E-02 2.000E+00 1.000E+00 0.000E+00
40 2.577E+00 -7.069E+00 6.572E+00 10 0 1.886E-01 -9.701E-01 1.529E-01 2.000E+00 1.000E+00 0.000E+00
41 -3.209E+00 -7.670E+00 -5.538E+00 10 0 8.902E-01 -2.416E-01 3.863E-01 2.000E+00 1.000E+00 0.000E+00
42 5.034E+00 -1.459E+00 8.505E+00 10 0 -2.972E-01 -8.971E-01 3.268E-01 2.000E+00 1.000E+00 0.000E+00
43 6.074E+00 5.482E+00 5.732E+00 10 0 -9.159E-01 -3.466E-01 -2.023E-01 2.000E+00 1.000E+00 0.000E+00
44 -2.930E+00 9.295E+00 -2.197E+00 10 0 7.015E-01 5.832E-01 4.096E-01 2.000E+00 1.000E+00 0.000E+00
45 -8.466E+00 -3.989E+00 -3.494E+00 10 0 1.309E-02 -7.521E-01 -6.589E-01 2.000E+00 1.000E+00 0.000E+00
46 1.199E+00 -9.186E+00 -3.739E+00 10 0 -5.343E-01 -2.166E-01 8.171E-01 2.000E+00 1.000E+00 0.000E+00
47 7.078E+00 5.873E+00 3.900E+00 10 0 2.044E-01 4.559E-01 -8.662E-01 2.000E+00 1.000E+00 0.000E+00
48 4.257E+00 9.037E+00 9.245E-02 10 0 -5.783E-01 5.842E-01 5.694E-01 2.000E+00 1.000E+00 0.000E+00
49 5.425E+00 4.266E+00 -7.223E+00 10 0 1.459E-01 -7.580E-01 -6.357E-01 2.000E+00 1.000E+00 0.000E+00
50 -1.052E+00 -9.795E+00 1.656E+00 10 0 4.058E-01 -5.934E-01 -6.951E-01 2.000E+00 1.000E+00 0.000E+00

```

```

*****
dump no. 2 on file runtp  nps = 46609455  coll = 348534  ctm = 15.00  nrm = 626884616

```

```

*****
dump no. 3 on file runtp  nps = 93218957  coll = 697389  ctm = 30.00  nrm = 1253835571

```

Problem summary

```

run terminated when 100000000 particle histories were done.
+ 10/05/13 03:08:19
UF6 Shockwave Reactor 10cm wave  prohibid = 10/05/13 02:36:03

```

neutron creation	tracks	weight	energy	neutron loss	tracks	weight	energy
	(per source particle)				(per source particle)		
source	100000000	1.000E+00	2.000E+00	escape	100031760	1.0003E+00	1.9979E+00
nucl. interaction	0	0.	0.	energy cutoff	0	0.	0.
particle decay	0	0.	0.	time cutoff	404	4.0077E-06	2.0333E-06
weight window	0	0.	0.	weight window	0	0.	0.
cell importance	0	0.	0.	cell importance	0	0.	0.
weight cutoff	0	0.	0.	weight cutoff	0	0.	0.
energy importance	0	0.	0.	energy importance	0	0.	0.
dxtran	0	0.	0.	dxtran	0	0.	0.
forced collisions	0	0.	0.	forced collisions	0	0.	0.
exp. transform	0	0.	0.	exp. transform	0	0.	0.
upscattering	0	0.	0.	downscattering	0	0.	2.7461E-03
*photonuclear	0	0.	0.	capture	0	9.8435E-06	1.9640E-05
(n,xn)	0	0.	0.	loss to (n,xn)	0	0.	0.
prompt fission	51189	5.0770E-04	1.0406E-03	loss to fission	19429	1.9270E-04	3.8483E-04
delayed fission	404	4.0077E-06	2.0333E-06	nucl. interaction	0	0.	0.
*prompt photofiss	0	0.	0.	particle decay	0	0.	0.
tabular boundary	0	0.	0.	tabular boundary	0	0.	0.
tabular sampling	0	0.	0.				
total	100051593	1.0005E+00	2.0010E+00	total	100051593	1.0005E+00	2.0010E+00

number of neutrons banked	31902	average time of (shakes)	cutoffs
neutron tracks per source particle	1.0005E+00	escape	2.5891E-01
neutron collisions per source particle	7.4825E-03	capture	2.7081E-01
total neutron collisions	748253	capture or escape	2.5891E-01
net multiplication	1.0003E+00 0.0000	any termination	1.3168E+03
			wc1 -5.0000E-01
			wc2 -2.5000E-01

```

computer time so far in this run 32.27 minutes maximum number ever in bank 4
computer time in mcrun 32.19 minutes bank overflows to backup file 0
source particles per minute 3.1070E+06 dynamic storage 0 words, 0 bytes.
random numbers generated 1345043567 most random numbers used was 137 in history 10137130

```

range of sampled source weights = 1.0000E+00 to 1.0000E+00

source efficiency = 1.0000 in cell 10

Induced fission multiplicity and moments. print table 117

	----- by number -----			----- by weight -----			error
	fissions	neutrons	fraction	fissions	neutrons	fraction	
nu = 2	6694	13388	3.44537E-01	6.63918E-05	1.32784E-04	3.44533E-01	0.0122
nu = 3	12735	38205	6.55463E-01	1.26309E-04	3.78927E-04	6.55467E-01	0.0089
total	19429	51593	1.00000E+00	1.92701E-04	5.11711E-04	1.00000E+00	0.0072

factorial moments	by number	by weight
nu	2.65546E+00 0.0013	2.65547E+00 0.0013
nu(nu-1)/2!	2.31093E+00 0.0030	2.31093E+00 0.0030
nu(nu-1)(nu-2)/3!	6.55463E-01 0.0052	6.55467E-01 0.0052

1neutron activity in each cell print table 126

cell entering	tracks	population	collisions	collisions	number	flux	average	average
							track weight	track mfp
			* weight	weighted	weighted	track weight	track weight	track mfp
		(per history)	energy	energy	energy	(relative)	(cm)	

```

2 10 147808100 100031902 34835 3.4835E-04 1.9976E+00 1.9986E+00 9.9999E-01 2.4724E+02
3 11 93355248 47803123 39359 3.9359E-04 1.9969E+00 1.9982E+00 9.9999E-01 2.5687E+02
4 12 88901080 45568140 53540 5.3539E-04 1.9964E+00 1.9979E+00 9.9999E-01 2.6625E+02
5 13 83677102 43337694 85500 8.5499E-04 1.9957E+00 1.9976E+00 9.9999E-01 2.8664E+02
6 14 72138322 40330068 280708 2.8070E-03 1.9946E+00 1.9969E+00 9.9999E-01 3.2961E+02
7 15 59159084 31777056 90991 9.0990E-04 1.9940E+00 1.9966E+00 9.9998E-01 6.1526E+02
8 16 51146995 27332185 49617 4.9616E-04 1.9938E+00 1.9965E+00 9.9998E-01 9.4171E+02
9 17 44581826 23771661 28984 2.8984E-04 1.9939E+00 1.9965E+00 9.9998E-01 1.3843E+03
10 18 38987094 20775255 17259 1.7259E-04 1.9939E+00 1.9965E+00 9.9998E-01 1.9776E+03
11 19 34111962 18184365 10372 1.0372E-04 1.9940E+00 1.9965E+00 9.9998E-01 2.8251E+03
12 20 29803478 15906525 6398 6.3979E-05 1.9940E+00 1.9965E+00 9.9998E-01 3.9551E+03
13 21 25958515 13881096 3887 3.8869E-05 1.9939E+00 1.9965E+00 9.9998E-01 5.5371E+03
14 22 22509194 12065839 2257 2.2570E-05 1.9938E+00 1.9964E+00 9.9998E-01 8.1427E+03
15 23 19407118 10435069 1399 1.3990E-05 1.9938E+00 1.9964E+00 9.9998E-01 1.1536E+04
16 24 12741569 8966319 2767 2.7669E-05 1.9933E+00 1.9962E+00 9.9998E-01 1.7303E+04
17 25 4689717 3773281 35528 3.5527E-04 1.9910E+00 1.9949E+00 9.9998E-01 4.6917E+02
18 26 917362 917051 4852 4.8519E-05 1.9901E+00 1.9942E+00 9.9997E-01 4.6914E+02

total 829893766 464856629 748253 7.4824E-03
Neutron weight balance in each cell print table 130

cell index 2 3 4 5 6 7 8 9 10
cell number 10 11 12 13 14 15 16 17 18

external events:
entering 4.7807E-01 9.3354E-01 8.8900E-01 8.3676E-01 7.2137E-01 5.9158E-01 5.1146E-01 4.4581E-01 3.8986E-01
source 1.0000E+00 0.0000E+00 0.0000E+00 0.0000E+00 0.0000E+00 0.0000E+00 0.0000E+00 0.0000E+00 0.0000E+00
energy cutoff 0.0000E+00 0.0000E+00 0.0000E+00 0.0000E+00 0.0000E+00 0.0000E+00 0.0000E+00 0.0000E+00 0.0000E+00
time cutoff -2.0833E-07 -1.3892E-07 -2.1823E-07 -5.1586E-07 -1.5277E-06 -4.4632E-07 -2.5793E-07 -1.9844E-07 -8.9270E-08
exiting -1.4781E+00 -9.3356E-01 -8.8902E-01 -8.3679E-01 -7.2149E-01 -5.9162E-01 -5.1148E-01 -4.4582E-01 -3.8987E-01
-----
total -1.4006E-05 -1.6217E-05 -2.2673E-05 -3.5216E-05 -1.1574E-04 -3.7454E-05 -2.0074E-05 -1.2873E-05 -7.3176E-06

variance reduction events:
weight window 0.0000E+00 0.0000E+00 0.0000E+00 0.0000E+00 0.0000E+00 0.0000E+00 0.0000E+00 0.0000E+00 0.0000E+00
cell importance 0.0000E+00 0.0000E+00 0.0000E+00 0.0000E+00 0.0000E+00 0.0000E+00 0.0000E+00 0.0000E+00 0.0000E+00
weight cutoff 0.0000E+00 0.0000E+00 0.0000E+00 0.0000E+00 0.0000E+00 0.0000E+00 0.0000E+00 0.0000E+00 0.0000E+00
energy importance 0.0000E+00 0.0000E+00 0.0000E+00 0.0000E+00 0.0000E+00 0.0000E+00 0.0000E+00 0.0000E+00 0.0000E+00
dxtan 0.0000E+00 0.0000E+00 0.0000E+00 0.0000E+00 0.0000E+00 0.0000E+00 0.0000E+00 0.0000E+00 0.0000E+00
forced collisions 0.0000E+00 0.0000E+00 0.0000E+00 0.0000E+00 0.0000E+00 0.0000E+00 0.0000E+00 0.0000E+00 0.0000E+00
exp. transform 0.0000E+00 0.0000E+00 0.0000E+00 0.0000E+00 0.0000E+00 0.0000E+00 0.0000E+00 0.0000E+00 0.0000E+00
-----
total 0.0000E+00 0.0000E+00 0.0000E+00 0.0000E+00 0.0000E+00 0.0000E+00 0.0000E+00 0.0000E+00 0.0000E+00

physical events:
capture -4.5513E-07 -5.1566E-07 -7.0384E-07 -1.1245E-06 -3.6961E-06 -1.2070E-06 -6.4567E-07 -3.8758E-07 -2.3028E-07
(n,xn) 0.0000E+00 0.0000E+00 0.0000E+00 0.0000E+00 0.0000E+00 0.0000E+00 0.0000E+00 0.0000E+00 0.0000E+00
loss to (n,xn) 0.0000E+00 0.0000E+00 0.0000E+00 0.0000E+00 0.0000E+00 0.0000E+00 0.0000E+00 0.0000E+00 0.0000E+00
fission 2.3219E-05 2.6691E-05 3.7352E-05 5.8488E-05 1.9158E-04 6.2197E-05 3.3325E-05 1.2656E-05 1.2071E-05
loss to fission -8.7578E-06 -9.9582E-06 -1.3975E-05 -2.2148E-05 -7.2145E-05 -2.3536E-05 -1.2606E-05 -8.0041E-06 -4.5227E-06
phonuclear 0.0000E+00 0.0000E+00 0.0000E+00 0.0000E+00 0.0000E+00 0.0000E+00 0.0000E+00 0.0000E+00 0.0000E+00
nucl. interaction 0.0000E+00 0.0000E+00 0.0000E+00 0.0000E+00 0.0000E+00 0.0000E+00 0.0000E+00 0.0000E+00 0.0000E+00
tabular boundary 0.0000E+00 0.0000E+00 0.0000E+00 0.0000E+00 0.0000E+00 0.0000E+00 0.0000E+00 0.0000E+00 0.0000E+00
particle decay 0.0000E+00 0.0000E+00 0.0000E+00 0.0000E+00 0.0000E+00 0.0000E+00 0.0000E+00 0.0000E+00 0.0000E+00
tabular sampling 0.0000E+00 0.0000E+00 0.0000E+00 0.0000E+00 0.0000E+00 0.0000E+00 0.0000E+00 0.0000E+00 0.0000E+00
photofission 0.0000E+00 0.0000E+00 0.0000E+00 0.0000E+00 0.0000E+00 0.0000E+00 0.0000E+00 0.0000E+00 0.0000E+00
-----
total 1.4006E-05 1.6217E-05 2.2673E-05 3.5216E-05 1.1574E-04 3.7454E-05 2.0074E-05 1.2873E-05 7.3176E-06

-----
total 1.1377E-11 4.8392E-13 6.2094E-13 9.0770E-13 2.2162E-12 4.8832E-13 2.0056E-13 7.2632E-14 1.3066E-14

cell index 11 12 13 14 15 16 17 18
cell number 19 20 21 22 23 24 25 26 total

external events:
entering 3.4111E-01 2.9803E-01 2.5958E-01 2.2509E-01 1.9407E-01 1.2741E-01 4.6896E-02 9.1734E-03 7.2988E+00
source 0.0000E+00 0.0000E+00 0.0000E+00 0.0000E+00 0.0000E+00 0.0000E+00 0.0000E+00 0.0000E+00 1.0000E+00
energy cutoff 0.0000E+00 0.0000E+00 0.0000E+00 0.0000E+00 0.0000E+00 0.0000E+00 0.0000E+00 0.0000E+00 0.0000E+00
time cutoff -6.9471E-08 -2.9751E-08 -1.9834E-08 -9.9170E-09 -9.9342E-09 0.0000E+00 -2.0829E-07 -5.9536E-08 -4.0077E-06
exiting -3.4112E-01 -2.9803E-01 -2.5958E-01 -2.2509E-01 -1.9407E-01 -1.2741E-01 -4.6911E-02 -9.1753E-03 -8.2991E+00
-----
total -4.5290E-06 -2.2883E-06 -1.5338E-06 -9.9284E-07 -7.1445E-07 -1.2213E-06 -1.4361E-05 -1.9562E-06 -3.0917E-04

variance reduction events:
weight window 0.0000E+00 0.0000E+00 0.0000E+00 0.0000E+00 0.0000E+00 0.0000E+00 0.0000E+00 0.0000E+00 0.0000E+00
cell importance 0.0000E+00 0.0000E+00 0.0000E+00 0.0000E+00 0.0000E+00 0.0000E+00 0.0000E+00 0.0000E+00 0.0000E+00
weight cutoff 0.0000E+00 0.0000E+00 0.0000E+00 0.0000E+00 0.0000E+00 0.0000E+00 0.0000E+00 0.0000E+00 0.0000E+00
energy importance 0.0000E+00 0.0000E+00 0.0000E+00 0.0000E+00 0.0000E+00 0.0000E+00 0.0000E+00 0.0000E+00 0.0000E+00
dxtan 0.0000E+00 0.0000E+00 0.0000E+00 0.0000E+00 0.0000E+00 0.0000E+00 0.0000E+00 0.0000E+00 0.0000E+00
forced collisions 0.0000E+00 0.0000E+00 0.0000E+00 0.0000E+00 0.0000E+00 0.0000E+00 0.0000E+00 0.0000E+00 0.0000E+00
exp. transform 0.0000E+00 0.0000E+00 0.0000E+00 0.0000E+00 0.0000E+00 0.0000E+00 0.0000E+00 0.0000E+00 0.0000E+00
-----
total 0.0000E+00 0.0000E+00 0.0000E+00 0.0000E+00 0.0000E+00 0.0000E+00 0.0000E+00 0.0000E+00 0.0000E+00

physical events:
capture -1.3250E-07 -8.2237E-08 -5.3061E-08 -2.8851E-08 -1.9508E-08 -3.8235E-08 -4.5651E-07 -6.6933E-08 -9.8435E-06
(n,xn) 0.0000E+00 0.0000E+00 0.0000E+00 0.0000E+00 0.0000E+00 0.0000E+00 0.0000E+00 0.0000E+00 0.0000E+00
loss to (n,xn) 0.0000E+00 0.0000E+00 0.0000E+00 0.0000E+00 0.0000E+00 0.0000E+00 0.0000E+00 0.0000E+00 0.0000E+00
fission 7.4288E-06 3.8088E-06 2.5489E-06 1.6168E-06 1.1704E-06 2.0233E-06 2.3693E-05 3.2331E-06 5.1171E-04
loss to fission -2.7672E-06 -1.4382E-06 -9.6202E-07 -5.9514E-07 -4.3642E-07 -7.6368E-07 -8.8763E-06 -1.2099E-06 -1.9270E-04

```

photonuclear 0.0000E+00 0.0000E+00 0.0000E+00 0.0000E+00 0.0000E+00 0.0000E+00 0.0000E+00 0.0000E+00 0.0000E+00 0.0000E+00
 nucl. interaction 0.0000E+00 0.0000E+00 0.0000E+00 0.0000E+00 0.0000E+00 0.0000E+00 0.0000E+00 0.0000E+00 0.0000E+00 0.0000E+00
 tabular boundary 0.0000E+00 0.0000E+00 0.0000E+00 0.0000E+00 0.0000E+00 0.0000E+00 0.0000E+00 0.0000E+00 0.0000E+00 0.0000E+00
 particle decay 0.0000E+00 0.0000E+00 0.0000E+00 0.0000E+00 0.0000E+00 0.0000E+00 0.0000E+00 0.0000E+00 0.0000E+00 0.0000E+00
 tabular sampling 0.0000E+00 0.0000E+00 0.0000E+00 0.0000E+00 0.0000E+00 0.0000E+00 0.0000E+00 0.0000E+00 0.0000E+00 0.0000E+00
 photofission 0.0000E+00 0.0000E+00 0.0000E+00 0.0000E+00 0.0000E+00 0.0000E+00 0.0000E+00 0.0000E+00 0.0000E+00 0.0000E+00

total 4.5290E-06 2.2883E-06 1.5338E-06 9.9284E-07 7.1445E-07 1.2213E-06 1.4361E-05 1.9562E-06 3.0917E-04

total -1.2568E-14 -8.4132E-15 -5.0679E-15 -2.8355E-15 -1.6105E-15 -2.3732E-15 -1.4181E-14 0.0000E+00 1.6337E-11

Ineutron activity of each nuclide in each cell, per source particle print table 140

cell index	cell name	nuclides	atom fraction	total collisions	wgt. lost * weight to capture	wgt. gain by fission	wgt. gain by (n,xn)	photons produced	photon produced	wgt avg photon energy	
2	10	92235.70c	7.27E-02	4508	4.5080E-05	3.7487E-07	1.2971E-05	0.0000E+00	0	0.0000E+00 0.0000E+00	
			92238.70c	1.82E-02	1155	1.1550E-05	7.5979E-08	1.4901E-06	0.0000E+00	0	0.0000E+00 0.0000E+00
			9019.70c	5.45E-01	16611	1.6611E-04	4.2797E-09	0.0000E+00	0.0000E+00	0	0.0000E+00 0.0000E+00
			2004.70c	3.64E-01	12561	1.2561E-04	0.0000E+00	0.0000E+00	0.0000E+00	0	0.0000E+00 0.0000E+00
3	11	92235.70c	7.27E-02	5088	5.0880E-05	4.2335E-07	1.5014E-05	0.0000E+00	0	0.0000E+00 0.0000E+00	
			92238.70c	1.82E-02	1313	1.3130E-05	8.6564E-08	1.7186E-06	0.0000E+00	0	0.0000E+00 0.0000E+00
			9019.70c	5.45E-01	18817	1.8817E-04	5.7478E-09	0.0000E+00	0.0000E+00	0	0.0000E+00 0.0000E+00
			2004.70c	3.64E-01	14141	1.4141E-04	0.0000E+00	0.0000E+00	0.0000E+00	0	0.0000E+00 0.0000E+00
4	12	92235.70c	7.27E-02	6992	6.9919E-05	5.8116E-07	2.1390E-05	0.0000E+00	0	0.0000E+00 0.0000E+00	
			92238.70c	1.82E-02	1761	1.7610E-05	1.1590E-07	1.9868E-06	0.0000E+00	0	0.0000E+00 0.0000E+00
			9019.70c	5.45E-01	25659	2.5659E-04	6.7720E-09	0.0000E+00	0.0000E+00	0	0.0000E+00 0.0000E+00
			2004.70c	3.64E-01	19128	1.9128E-04	0.0000E+00	0.0000E+00	0.0000E+00	0	0.0000E+00 0.0000E+00
5	13	92235.70c	7.27E-02	11145	1.1145E-04	9.2733E-07	3.2933E-05	0.0000E+00	0	0.0000E+00 0.0000E+00	
			92238.70c	1.82E-02	2816	2.8160E-05	1.8594E-07	3.4074E-06	0.0000E+00	0	0.0000E+00 0.0000E+00
			9019.70c	5.45E-01	40848	4.0848E-04	1.1200E-08	0.0000E+00	0.0000E+00	0	0.0000E+00 0.0000E+00
			2004.70c	3.64E-01	30691	3.0691E-04	0.0000E+00	0.0000E+00	0.0000E+00	0	0.0000E+00 0.0000E+00
6	14	92235.70c	7.27E-02	36468	3.6467E-04	3.0391E-06	1.0845E-04	0.0000E+00	0	0.0000E+00 0.0000E+00	
			92238.70c	1.82E-02	9390	9.3898E-05	6.1982E-07	1.0987E-05	0.0000E+00	0	0.0000E+00 0.0000E+00
			9019.70c	5.45E-01	133513	1.3351E-03	3.7141E-08	0.0000E+00	0.0000E+00	0	0.0000E+00 0.0000E+00
			2004.70c	3.64E-01	101337	1.0134E-03	0.0000E+00	0.0000E+00	0.0000E+00	0	0.0000E+00 0.0000E+00
7	15	92235.70c	7.27E-02	12001	1.2001E-04	9.9961E-07	3.5323E-05	0.0000E+00	0	0.0000E+00 0.0000E+00	
			92238.70c	1.82E-02	2971	2.9710E-05	1.9609E-07	3.3379E-06	0.0000E+00	0	0.0000E+00 0.0000E+00
			9019.70c	5.45E-01	43333	4.3332E-04	1.1271E-08	0.0000E+00	0.0000E+00	0	0.0000E+00 0.0000E+00
			2004.70c	3.64E-01	32686	3.2686E-04	0.0000E+00	0.0000E+00	0.0000E+00	0	0.0000E+00 0.0000E+00
8	16	92235.71c	7.27E-02	6325	6.3248E-05	5.2742E-07	1.8633E-05	0.0000E+00	0	0.0000E+00 0.0000E+00	
			92238.71c	1.82E-02	1696	1.6960E-05	1.1201E-07	2.0861E-06	0.0000E+00	0	0.0000E+00 0.0000E+00
			9019.71c	5.45E-01	23731	2.3731E-04	6.2316E-09	0.0000E+00	0.0000E+00	0	0.0000E+00 0.0000E+00
			2004.71c	3.64E-01	17865	1.7865E-04	0.0000E+00	0.0000E+00	0.0000E+00	0	0.0000E+00 0.0000E+00
9	17	92235.71c	7.27E-02	3819	3.8190E-05	3.1809E-07	1.2049E-05	0.0000E+00	0	0.0000E+00 0.0000E+00	
			92238.71c	1.82E-02	972	9.7198E-06	6.4148E-08	1.2120E-06	0.0000E+00	0	0.0000E+00 0.0000E+00
			9019.71c	5.45E-01	13723	1.3723E-04	5.3441E-09	0.0000E+00	0.0000E+00	0	0.0000E+00 0.0000E+00
			2004.71c	3.64E-01	10470	1.0470E-04	0.0000E+00	0.0000E+00	0.0000E+00	0	0.0000E+00 0.0000E+00
10	18	92235.72c	7.27E-02	2295	2.2950E-05	1.9092E-07	6.7730E-06	0.0000E+00	0	0.0000E+00 0.0000E+00	
			92238.72c	1.82E-02	562	5.6199E-06	3.7231E-08	7.7487E-07	0.0000E+00	0	0.0000E+00 0.0000E+00
			9019.72c	5.45E-01	8285	8.2848E-05	2.1355E-09	0.0000E+00	0.0000E+00	0	0.0000E+00 0.0000E+00
			2004.72c	3.64E-01	6117	6.1170E-05	0.0000E+00	0.0000E+00	0.0000E+00	0	0.0000E+00 0.0000E+00
11	19	92235.73c	7.27E-02	1304	1.3039E-05	1.0868E-07	4.2642E-06	0.0000E+00	0	0.0000E+00 0.0000E+00	
			92238.73c	1.82E-02	343	3.4299E-06	2.2564E-08	3.9737E-07	0.0000E+00	0	0.0000E+00 0.0000E+00
			9019.73c	5.45E-01	4883	4.8829E-05	1.2581E-09	0.0000E+00	0.0000E+00	0	0.0000E+00 0.0000E+00
			2004.73c	3.64E-01	3842	3.8420E-05	0.0000E+00	0.0000E+00	0.0000E+00	0	0.0000E+00 0.0000E+00
12	20	92235.73c	7.27E-02	819	8.1899E-06	6.8097E-08	2.1322E-06	0.0000E+00	0	0.0000E+00 0.0000E+00	
			92238.73c	1.82E-02	203	2.0300E-06	1.3365E-08	2.3842E-07	0.0000E+00	0	0.0000E+00 0.0000E+00
			9019.73c	5.45E-01	3012	3.0119E-05	7.7489E-10	0.0000E+00	0.0000E+00	0	0.0000E+00 0.0000E+00
			2004.73c	3.64E-01	2364	2.3640E-05	0.0000E+00	0.0000E+00	0.0000E+00	0	0.0000E+00 0.0000E+00
13	21	92235.74c	7.27E-02	531	5.3097E-06	4.4501E-08	1.4379E-06	0.0000E+00	0	0.0000E+00 0.0000E+00	
			92238.74c	1.82E-02	123	1.2300E-06	8.0900E-09	1.4901E-07	0.0000E+00	0	0.0000E+00 0.0000E+00
			9019.74c	5.45E-01	1819	1.8190E-05	4.7040E-10	0.0000E+00	0.0000E+00	0	0.0000E+00 0.0000E+00
			2004.74c	3.64E-01	1414	1.4140E-05	0.0000E+00	0.0000E+00	0.0000E+00	0	0.0000E+00 0.0000E+00
14	22	92235.74c	7.27E-02	281	2.8099E-06	2.3248E-08	8.8261E-07	0.0000E+00	0	0.0000E+00 0.0000E+00	
			92238.74c	1.82E-02	81	8.1000E-07	5.3275E-09	1.3908E-07	0.0000E+00	0	0.0000E+00 0.0000E+00
			9019.74c	5.45E-01	1065	1.0650E-05	2.7602E-10	0.0000E+00	0.0000E+00	0	0.0000E+00 0.0000E+00
			2004.74c	3.64E-01	830	8.2998E-06	0.0000E+00	0.0000E+00	0.0000E+00	0	0.0000E+00 0.0000E+00
15	23	92235.74c	7.27E-02	195	1.9499E-06	1.6278E-08	6.7436E-07	0.0000E+00	0	0.0000E+00 0.0000E+00	
			92238.74c	1.82E-02	47	4.6992E-07	3.0579E-09	5.9605E-08	0.0000E+00	0	0.0000E+00 0.0000E+00
			9019.74c	5.45E-01	667	6.6699E-06	1.7153E-10	0.0000E+00	0.0000E+00	0	0.0000E+00 0.0000E+00
			2004.74c	3.64E-01	490	4.8998E-06	0.0000E+00	0.0000E+00	0.0000E+00	0	0.0000E+00 0.0000E+00
16	24	92235.74c	7.27E-02	389	3.8900E-06	3.2312E-08	1.1900E-06	0.0000E+00	0	0.0000E+00 0.0000E+00	
			92238.74c	1.82E-02	84	8.4000E-07	5.5911E-09	6.9540E-08	0.0000E+00	0	0.0000E+00 0.0000E+00
			9019.74c	5.45E-01	1277	1.2770E-05	3.3187E-10	0.0000E+00	0.0000E+00	0	0.0000E+00 0.0000E+00
			2004.74c	3.64E-01	1017	1.0170E-05	0.0000E+00	0.0000E+00	0.0000E+00	0	0.0000E+00 0.0000E+00
17	25	92235.74c	7.27E-02	4550	4.5499E-05	3.7946E-07	1.3645E-05	0.0000E+00	0	0.0000E+00 0.0000E+00	

	92238.74c	1.82E-02	1082	1.0820E-05	7.1409E-08	1.1722E-06	0.0000E+00	0	0.0000E+00	0.0000E+00
	9019.74c	5.45E-01	16824	1.6824E-04	5.6353E-09	0.0000E+00	0.0000E+00	0	0.0000E+00	0.0000E+00
	2004.74c	3.64E-01	13072	1.3072E-04	0.0000E+00	0.0000E+00	0.0000E+00	0	0.0000E+00	0.0000E+00
18	26	92235.74c	7.27E-02	665	6.6498E-06	5.5945E-08	1.9338E-06	0.0000E+00	0	0.0000E+00
		92238.74c	1.82E-02	155	1.5499E-06	1.0399E-08	8.9408E-08	0.0000E+00	0	0.0000E+00
		9019.74c	5.45E-01	2280	2.2799E-05	5.8912E-10	0.0000E+00	0.0000E+00	0	0.0000E+00
		2004.74c	3.64E-01	1752	1.7520E-05	0.0000E+00	0.0000E+00	0.0000E+00	0	0.0000E+00

total 748253 7.4824E-03 9.8435E-06 3.1901E-04 0.0000E+00 0 0.0000E+00 0.0000E+00

total over all cells by nuclide	total collisions	wgt. lost	wgt. gain	wgt. gain	photons produced	photon produced	wgt avg photon energy
	* weight to capture	by fission	by (n,xn)	produced	produced		
2004.70c	210544	2.1054E-03	0.0000E+00	0.0000E+00	0.0000E+00	0	0.0000E+00
2004.71c	28335	2.8335E-04	0.0000E+00	0.0000E+00	0.0000E+00	0	0.0000E+00
2004.72c	6117	6.1170E-05	0.0000E+00	0.0000E+00	0.0000E+00	0	0.0000E+00
2004.73c	6206	6.2059E-05	0.0000E+00	0.0000E+00	0.0000E+00	0	0.0000E+00
2004.74c	18575	1.8575E-04	0.0000E+00	0.0000E+00	0.0000E+00	0	0.0000E+00
9019.70c	278781	2.7878E-03	7.6411E-08	0.0000E+00	0.0000E+00	0	0.0000E+00
9019.71c	37454	3.7453E-04	1.1576E-08	0.0000E+00	0.0000E+00	0	0.0000E+00
9019.72c	8285	8.2848E-05	2.1355E-09	0.0000E+00	0.0000E+00	0	0.0000E+00
9019.73c	7895	7.8948E-05	2.0330E-09	0.0000E+00	0.0000E+00	0	0.0000E+00
9019.74c	23932	2.3931E-04	7.4742E-09	0.0000E+00	0.0000E+00	0	0.0000E+00
92235.70c	76202	7.6201E-04	6.3454E-06	2.2608E-04	0.0000E+00	0	0.0000E+00
92235.71c	10144	1.0144E-04	8.4551E-07	3.0682E-05	0.0000E+00	0	0.0000E+00
92235.72c	2295	2.2950E-05	1.9092E-07	6.7730E-06	0.0000E+00	0	0.0000E+00
92235.73c	2123	2.1229E-05	1.7677E-07	6.3963E-06	0.0000E+00	0	0.0000E+00
92235.74c	6611	6.6108E-05	5.5175E-07	1.9764E-05	0.0000E+00	0	0.0000E+00
92238.70c	19406	1.9406E-04	1.2803E-06	2.2928E-05	0.0000E+00	0	0.0000E+00
92238.71c	2668	2.6679E-05	1.7616E-07	3.2981E-06	0.0000E+00	0	0.0000E+00
92238.72c	562	5.6199E-06	3.7231E-08	7.7487E-07	0.0000E+00	0	0.0000E+00
92238.73c	546	5.4599E-06	3.5929E-08	6.3579E-07	0.0000E+00	0	0.0000E+00
92238.74c	1572	1.5720E-05	1.0387E-07	1.6789E-06	0.0000E+00	0	0.0000E+00

Itally 2 nps=10000000

tally type 2 particle flux averaged over a surface.
particle(s): neutron

areas

surface:	10	11	12	13	14	15	16		
	1.25664E+03	1.25162E+03	1.24410E+03	1.23163E+03	1.20687E+03	1.08687E+03	9.95382E+02		
surface:	17	18	19	20	21	22	23		
	9.07920E+02	8.24480E+02	7.45060E+02	6.69662E+02	5.98285E+02	5.30929E+02	4.67595E+02		
surface:	24	25	26						
	4.08281E+02	1.81458E+02	4.53646E+01						

surface 10

multiplier bin: 1.0000E+00

energy

5.0000E-01	6.75732E-07	0.0068
1.0000E+00	1.18363E-06	0.0052
2.0000E+00	3.29596E-03	0.0001
4.0000E+00	2.54700E-07	0.0124
2.0000E+01	9.58960E-08	0.0181
total	3.29817E-03	0.0001

surface 11

multiplier bin: 1.0000E+00

energy

5.0000E-01	6.95000E-07	0.0077
1.0000E+00	1.21252E-06	0.0059
2.0000E+00	2.83055E-03	0.0002
4.0000E+00	2.60811E-07	0.0135
2.0000E+01	1.01065E-07	0.0208
total	2.83282E-03	0.0002

surface 12

multiplier bin: 1.0000E+00

energy

5.0000E-01	7.05942E-07	0.0081
1.0000E+00	1.24013E-06	0.0064
2.0000E+00	2.42841E-03	0.0002
4.0000E+00	2.64845E-07	0.0141
2.0000E+01	1.03343E-07	0.0224
total	2.43073E-03	0.0002

surface 13

multiplier bin: 1.0000E+00

energy

5.0000E-01	7.21603E-07	0.0087
1.0000E+00	1.25010E-06	0.0066
2.0000E+00	2.14676E-03	0.0002
4.0000E+00	2.73271E-07	0.0157
2.0000E+01	1.05417E-07	0.0240
total	2.14911E-03	0.0002

surface 14

multiplier bin: 1.0000E+00

energy

5.0000E-01	7.37003E-07	0.0094
1.0000E+00	1.26382E-06	0.0071
2.0000E+00	1.87714E-03	0.0002

```

4.0000E+00 2.75471E-07 0.0162
2.0000E+01 1.07500E-07 0.0266
total 1.87953E-03 0.0002

surface 15
multiplier bin: 1.0000E+00
energy
5.0000E-01 7.01503E-07 0.0111
1.0000E+00 1.21939E-06 0.0086
2.0000E+00 1.42417E-03 0.0002
4.0000E+00 2.65751E-07 0.0190
2.0000E+01 1.01333E-07 0.0297
total 1.42645E-03 0.0002

surface 16
multiplier bin: 1.0000E+00
energy
5.0000E-01 6.63415E-07 0.0120
1.0000E+00 1.12950E-06 0.0094
2.0000E+00 1.27612E-03 0.0003
4.0000E+00 2.45244E-07 0.0205
2.0000E+01 9.25300E-08 0.0313
total 1.27825E-03 0.0003

surface 17
multiplier bin: 1.0000E+00
energy
5.0000E-01 6.22772E-07 0.0133
1.0000E+00 1.03311E-06 0.0100
2.0000E+00 1.18004E-03 0.0003
4.0000E+00 2.28332E-07 0.0223
2.0000E+01 8.29590E-08 0.0335
total 1.18201E-03 0.0003

surface 18
multiplier bin: 1.0000E+00
energy
5.0000E-01 5.88539E-07 0.0143
1.0000E+00 9.56843E-07 0.0109
2.0000E+00 1.11097E-03 0.0003
4.0000E+00 2.18377E-07 0.0237
2.0000E+01 8.08347E-08 0.0373
total 1.11282E-03 0.0003

surface 19
multiplier bin: 1.0000E+00
energy
5.0000E-01 5.55805E-07 0.0151
1.0000E+00 8.94360E-07 0.0115
2.0000E+00 1.05827E-03 0.0003
4.0000E+00 2.07897E-07 0.0254
2.0000E+01 7.51513E-08 0.0397
total 1.06001E-03 0.0003

surface 20
multiplier bin: 1.0000E+00
energy
5.0000E-01 5.32028E-07 0.0159
1.0000E+00 8.63526E-07 0.0126
2.0000E+00 1.01586E-03 0.0004
4.0000E+00 1.96164E-07 0.0257
2.0000E+01 7.22084E-08 0.0404
total 1.01753E-03 0.0004

surface 21
multiplier bin: 1.0000E+00
energy
5.0000E-01 5.18174E-07 0.0172
1.0000E+00 8.29744E-07 0.0134
2.0000E+00 9.81959E-04 0.0004
4.0000E+00 1.92342E-07 0.0278
2.0000E+01 7.45788E-08 0.0483
total 9.83573E-04 0.0004

surface 22
multiplier bin: 1.0000E+00
energy
5.0000E-01 5.00674E-07 0.0180
1.0000E+00 8.36711E-07 0.0146
2.0000E+00 9.52901E-04 0.0004
4.0000E+00 1.90899E-07 0.0312
2.0000E+01 7.08862E-08 0.0480
total 9.54501E-04 0.0004

surface 23
multiplier bin: 1.0000E+00
energy
5.0000E-01 4.92476E-07 0.0189
1.0000E+00 7.92477E-07 0.0152
2.0000E+00 9.28302E-04 0.0004
4.0000E+00 1.81023E-07 0.0317
2.0000E+01 6.87933E-08 0.0498
total 9.29836E-04 0.0004

```



```

2.00+00 1.3+07 3.18-01 -0.498 *****|*****|*****|*****|*****|*****|*****|*****
2.51+00 1.0+07 2.01-01 -0.698 *****|*****|*****|*****|*****|*****|*****|*****
3.16+00 8.2+06 1.27-01 -0.897 *****|*****|*****|*****|*****|*****|*****|*****
3.98+00 6.6+06 8.03-02 -1.095 *****|*****|*****|*****|*****|*****|*****|*****
5.01+00 5.3+06 5.11-02 -1.291 *****|*****|*****|*****|*****|*****|*****|*****
mmmmmmmmmmmmmm|mmmmmmmmmmmm|mmmmmmmmmmmm|mmmmmmmmmmmm|mmmmmmmmmmmm|mmmmmmmmmmmm|mmmmmmmmmmmm|
6.31+00 4.2+06 3.26-02 -1.487 *****|*****|*****|*****|*****|*****|*****|*****
7.94+00 3.4+06 2.10-02 -1.677 *****|*****|*****|*****|*****|*****|*****|*****
1.00+01 2.8+06 1.37-02 -1.862 *****|*****|*****|*****|*****|*****|*****|*****
1.26+01 643 2.48-06 -5.605 *****|*****|*****|*****|*****|*****|*****|*****
1.58+01 240 7.36-07 -6.133 *****|*****|*****|*****|*****|*****|*****|*****
2.00+01 972 2.37-06 -5.626 *****|*****|*****|*****|*****|*****|*****|*****
2.51+01 8.9+06 1.73-02 -1.762 *****|*****|*****|*****|*****|*****|*****|***** s|
3.16+01 81 1.25-07 -6.905 *****|*****|*****|*****|*****|*****|*****|***** s|
3.98+01 10 1.22-08 -7.913 * *****|*****|*****|*****|*****|*****|*****|***** s
5.01+01 16 1.55-08 -7.809 ** *****|*****|*****|*****|*****|*****|*****|***** s|
total 1.00+08 1.00+00 d-----d-----d-----d-----d-----d-----d-----d-----d-----

```

cumulative tally number for tally 2 8.9+06 nonzero tally mean(m) = 4.145E+00 nps = 100000000 print table 162

```

abscissa cum ordinate plot of the cumulative number of tallies in the tally fluctuation chart bin from 0 to 100 percent
tally number cum pct:-----10-----20-----30-----40-----50-----60-----70-----80-----90-----100
1.0000E+00 1667 0.002| | | | | | | | | | | | | | | | | | | | | | | | | | | | | | | | | | | | | | | | | | | | |
1.25893E+00 2.07+07 20.665| | | | | | | | | | | | | | | | | | | | | | | | | | | | | | | | | | | | | | | | | | | | | |
1.58490E+00 3.71+07 37.078| | | | | | | | | | | | | | | | | | | | | | | | | | | | | | | | | | | | | | | | | | | | |
1.99527E+00 5.01+07 50.115| | | | | | | | | | | | | | | | | | | | | | | | | | | | | | | | | | | | | | | | | | | | |
2.51188E+00 6.05+07 60.479| | | | | | | | | | | | | | | | | | | | | | | | | | | | | | | | | | | | | | | | | | | | |
3.16228E+00 6.87+07 68.723| | | | | | | | | | | | | | | | | | | | | | | | | | | | | | | | | | | | | | | | | | | | |
3.98108E+00 7.53+07 75.301| | | | | | | | | | | | | | | | | | | | | | | | | | | | | | | | | | | | | | | | | | | | |
5.01188E+00 8.06+07 80.570| | | | | | | | | | | | | | | | | | | | | | | | | | | | | | | | | | | | | | | | | | | | |
| | | | | | | | | | | | | | | | | | | | | | | | | | | | | | | | | | | | | | | | | | | | | | | | | | | | | | | |
6.30959E+00 8.48+07 84.801| | | | | | | | | | | | | | | | | | | | | | | | | | | | | | | | | | | | | | | | | | | | |
7.94328E+00 8.82+07 88.237| | | | | | | | | | | | | | | | | | | | | | | | | | | | | | | | | | | | | | | | | | | | |
1.00000E+01 9.11+07 91.061| | | | | | | | | | | | | | | | | | | | | | | | | | | | | | | | | | | | | | | | | | | | |
1.25893E+01 9.11+07 91.061| | | | | | | | | | | | | | | | | | | | | | | | | | | | | | | | | | | | | | | | | | | | |
1.58490E+01 9.11+07 91.061| | | | | | | | | | | | | | | | | | | | | | | | | | | | | | | | | | | | | | | | | | | | |
1.99527E+01 9.11+07 91.062| | | | | | | | | | | | | | | | | | | | | | | | | | | | | | | | | | | | | | | | | | | | |
2.51188E+01 1.00+08 100.000| | | | | | | | | | | | | | | | | | | | | | | | | | | | | | | | | | | | | | | | | | | | |
3.16228E+01 1.00+08 100.000| | | | | | | | | | | | | | | | | | | | | | | | | | | | | | | | | | | | | | | | | | | | |
3.98108E+01 1.00+08 100.000| | | | | | | | | | | | | | | | | | | | | | | | | | | | | | | | | | | | | | | | | | | | |
5.01188E+01 1.00+08 100.000| | | | | | | | | | | | | | | | | | | | | | | | | | | | | | | | | | | | | | | | | | | | |
total 100000000 100.000| | | | | | | | | | | | | | | | | | | | | | | | | | | | | | | | | | | | | | | | | | | | |
|cumulative unormed tally for tally 2 8.9+06 nonzero tally mean(m) = 4.145E+00 nps = 100000000 print table 162

```

```

abscissa cum ordinate plot of the cumulative tally in the tally fluctuation chart bin from 0 to 100 percent
tally tally/nps cum pct:-----10-----20-----30-----40-----50-----60-----70-----80-----90-----100
1.000E+00 1.660E-05 0.000| | | | | | | | | | | | | | | | | | | | | | | | | | | | | | | | | | | | | | | | | | | | |
1.259E+00 2.314E-01 5.582| | | | | | | | | | | | | | | | | | | | | | | | | | | | | | | | | | | | | | | | | | | | |
1.585E+00 4.627E-01 11.163| | | | | | | | | | | | | | | | | | | | | | | | | | | | | | | | | | | | | | | | | | | | |
1.995E+00 6.940E-01 16.745| | | | | | | | | | | | | | | | | | | | | | | | | | | | | | | | | | | | | | | | | | | | |
2.512E+00 9.255E-01 22.331| | | | | | | | | | | | | | | | | | | | | | | | | | | | | | | | | | | | | | | | | | | | |
3.162E+00 1.157E+00 27.925| | | | | | | | | | | | | | | | | | | | | | | | | | | | | | | | | | | | | | | | | | | | |
3.981E+00 1.390E+00 33.544| | | | | | | | | | | | | | | | | | | | | | | | | | | | | | | | | | | | | | | | | | | | |
5.012E+00 1.625E+00 39.211| | | | | | | | | | | | | | | | | | | | | | | | | | | | | | | | | | | | | | | | | | | | |
6.310E+00 1.863E+00 44.941| | | | | | | | | | | | | | | | | | | | | | | | | | | | | | | | | | | | | | | | | | | | |
7.943E+00 2.105E+00 50.799| | | | | | | | | | | | | | | | | | | | | | | | | | | | | | | | | | | | | | | | | | | | |
1.000E+01 2.357E+00 56.864| | | | | | | | | | | | | | | | | | | | | | | | | | | | | | | | | | | | | | | | | | | | |
1.259E+01 2.357E+00 56.866| | | | | | | | | | | | | | | | | | | | | | | | | | | | | | | | | | | | | | | | | | | | |
1.585E+01 2.357E+00 56.866| | | | | | | | | | | | | | | | | | | | | | | | | | | | | | | | | | | | | | | | | | | | |
1.995E+01 2.357E+00 56.871| | | | | | | | | | | | | | | | | | | | | | | | | | | | | | | | | | | | | | | | | | | | |
2.512E+01 4.145E+00 99.999| | | | | | | | | | | | | | | | | | | | | | | | | | | | | | | | | | | | | | | | | | | | |
3.162E+01 4.145E+00 100.000| | | | | | | | | | | | | | | | | | | | | | | | | | | | | | | | | | | | | | | | | | | | |
3.981E+01 4.145E+00 100.000| | | | | | | | | | | | | | | | | | | | | | | | | | | | | | | | | | | | | | | | | | | | |
5.012E+01 4.145E+00 100.000| | | | | | | | | | | | | | | | | | | | | | | | | | | | | | | | | | | | | | | | | | | | |
total 4.14461E+00 100.000| | | | | | | | | | | | | | | | | | | | | | | | | | | | | | | | | | | | | | | | | | | | |

```

l tally 4 nps = 100000000
tally type 4 track length estimate of particle flux.
particle(s): neutron
volumes
cell: 10 11 12 13 14 15 16
2.50825E+01 3.74357E+01 6.18930E+01 1.21923E+02 5.73173E+02 4.16315E+02 3.80526E+02
cell: 17 18 19 20 21 22 23
3.46346E+02 3.13774E+02 2.82810E+02 2.53455E+02 2.25709E+02 1.99571E+02 1.75041E+02
cell: 24 25 26
5.45887E+02 2.01116E+02 2.87309E+01

```

cell 10
multiplier bin: 1.00000E+00
energy
5.0000E-01 6.80363E-07 0.0070
1.0000E+00 1.19101E-06 0.0054
2.0000E+00 3.42407E-03 0.0002
4.0000E+00 2.55988E-07 0.0127
2.0000E+01 9.66473E-08 0.0182
total 3.42629E-03 0.0002

```

```

cell 11
multiplier bin: 1.00000E+00
energy
5.0000E-01 6.98364E-07 0.0077
1.0000E+00 1.22074E-06 0.0059

```

```

2.0000E+00 2.69368E-03 0.0002
4.0000E+00 2.61996E-07 0.0133
2.0000E+01 1.01070E-07 0.0205
total 2.69596E-03 0.0002

cell 12
multiplier bin: 1.0000E+00
energy
5.0000E-01 7.11980E-07 0.0077
1.0000E+00 1.24466E-06 0.0060
2.0000E+00 2.30383E-03 0.0002
4.0000E+00 2.68035E-07 0.0138
2.0000E+01 1.04872E-07 0.0219
total 2.30616E-03 0.0002

cell 13
multiplier bin: 1.0000E+00
energy
5.0000E-01 7.26456E-07 0.0077
1.0000E+00 1.26130E-06 0.0059
2.0000E+00 2.00805E-03 0.0002
4.0000E+00 2.75090E-07 0.0140
2.0000E+01 1.05980E-07 0.0218
total 2.01042E-03 0.0002

cell 14
multiplier bin: 1.0000E+00
energy
5.0000E-01 7.33728E-07 0.0073
1.0000E+00 1.26935E-06 0.0056
2.0000E+00 1.60681E-03 0.0002
4.0000E+00 2.71592E-07 0.0130
2.0000E+01 1.04008E-07 0.0199
total 1.60919E-03 0.0002

cell 15
multiplier bin: 1.0000E+00
energy
5.0000E-01 6.83851E-07 0.0086
1.0000E+00 1.16568E-06 0.0066
2.0000E+00 1.34572E-03 0.0002
4.0000E+00 2.57417E-07 0.0151
2.0000E+01 9.68213E-08 0.0233
total 1.34792E-03 0.0002

cell 16
multiplier bin: 1.0000E+00
energy
5.0000E-01 6.45941E-07 0.0094
1.0000E+00 1.08435E-06 0.0073
2.0000E+00 1.22665E-03 0.0002
4.0000E+00 2.36595E-07 0.0163
2.0000E+01 9.17915E-08 0.0253
total 1.22871E-03 0.0002

cell 17
multiplier bin: 1.0000E+00
energy
5.0000E-01 5.95979E-07 0.0101
1.0000E+00 1.01041E-06 0.0079
2.0000E+00 1.14494E-03 0.0002
4.0000E+00 2.19718E-07 0.0175
2.0000E+01 8.35442E-08 0.0276
total 1.14685E-03 0.0002

cell 18
multiplier bin: 1.0000E+00
energy
5.0000E-01 5.69528E-07 0.0109
1.0000E+00 9.37412E-07 0.0085
2.0000E+00 1.08424E-03 0.0002
4.0000E+00 2.09283E-07 0.0186
2.0000E+01 7.85668E-08 0.0297
total 1.08603E-03 0.0002

cell 19
multiplier bin: 1.0000E+00
energy
5.0000E-01 5.39492E-07 0.0116
1.0000E+00 8.85847E-07 0.0091
2.0000E+00 1.03668E-03 0.0003
4.0000E+00 2.01613E-07 0.0197
2.0000E+01 7.46326E-08 0.0314
total 1.03838E-03 0.0003

cell 20
multiplier bin: 1.0000E+00
energy
5.0000E-01 5.19603E-07 0.0123
1.0000E+00 8.43286E-07 0.0097
2.0000E+00 9.98868E-04 0.0003
4.0000E+00 1.98025E-07 0.0210
2.0000E+01 7.49056E-08 0.0334

```

```

total 1.00050E-03 0.0003

cell 21
multiplier bin: 1.00000E+00
energy
5.0000E-01 5.05759E-07 0.0131
1.0000E+00 8.20120E-07 0.0103
2.0000E+00 9.67270E-04 0.0003
4.0000E+00 1.90086E-07 0.0221
2.0000E+01 7.02430E-08 0.0352
total 9.68856E-04 0.0003

cell 22
multiplier bin: 1.00000E+00
energy
5.0000E-01 4.99558E-07 0.0139
1.0000E+00 8.04018E-07 0.0109
2.0000E+00 9.40520E-04 0.0003
4.0000E+00 1.83974E-07 0.0235
2.0000E+01 6.92301E-08 0.0373
total 9.42077E-04 0.0003

cell 23
multiplier bin: 1.00000E+00
energy
5.0000E-01 4.91125E-07 0.0147
1.0000E+00 7.87886E-07 0.0116
2.0000E+00 9.17938E-04 0.0003
4.0000E+00 1.80641E-07 0.0247
2.0000E+01 6.85843E-08 0.0392
total 9.19467E-04 0.0003

cell 24
multiplier bin: 1.00000E+00
energy
5.0000E-01 4.96752E-07 0.0139
1.0000E+00 7.93940E-07 0.0109
2.0000E+00 8.74822E-04 0.0003
4.0000E+00 1.85059E-07 0.0237
2.0000E+01 7.03420E-08 0.0372
total 8.76369E-04 0.0003

cell 25
multiplier bin: 1.00000E+00
energy
5.0000E-01 6.28751E-07 0.0183
1.0000E+00 1.00139E-06 0.0145
2.0000E+00 8.25921E-04 0.0005
4.0000E+00 2.34055E-07 0.0318
2.0000E+01 9.13108E-08 0.0489
total 8.27877E-04 0.0005

cell 26
multiplier bin: 1.00000E+00
energy
5.0000E-01 6.60303E-07 0.0376
1.0000E+00 1.08735E-06 0.0293
2.0000E+00 8.05529E-04 0.0011
4.0000E+00 2.66354E-07 0.0615
2.0000E+01 8.32491E-08 0.1065
total 8.07626E-04 0.0011

```

lanalysis of the results in the tally fluctuation chart bin (tfc) for tally 4 with nps = 100000000 print table 160

```

normed average tally per history = 3.42629E-03      unnormed average tally per history = 8.59401E-02
estimated tally relative error = 0.0002             estimated variance of the variance = 0.0000
relative error from zero tallies = 0.0000          relative error from nonzero scores = 0.0002

number of nonzero history tallies = 100000000      efficiency for the nonzero tallies = 1.0000
history number of largest tally = 27573958        largest unnormalized history tally = 2.03133E+00
(largest tally)/(average tally) = 2.36366E+01     (largest tally)/(avg nonzero tally) = 2.36366E+01

(confidence interval shift)/mean = 0.0000         shifted confidence interval center = 3.42630E-03

```

if the largest history score sampled so far were to occur on the next history, the tfc bin quantities would change as follows:

estimated quantities	value at nps	value at nps+1	value(nps+1)/value(nps)-1.
mean	3.42629E-03	3.42630E-03	0.000000
relative error	1.63016E-04	1.63016E-04	0.000001
variance of the variance	1.90408E-07	1.90411E-07	0.000015
shifted center	3.42630E-03	3.42630E-03	0.000000
figure of merit	1.16919E+06	1.16919E+06	-0.000001

the estimated slope of the 198 largest tallies starting at 1.19363E+00 appears to be decreasing at least exponentially. the large score tail of the empirical history score probability density function appears to have no unsampled regions.

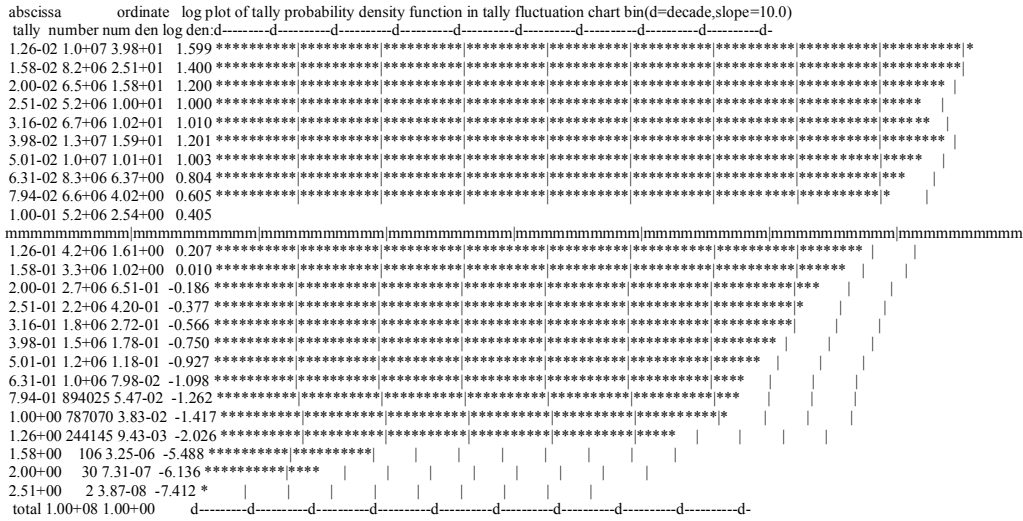
results of 10 statistical checks for the estimated answer for the tally fluctuation chart (tfc) bin of tally 4

tfc bin behavior	--mean-- behavior	-----relative error----- value	decrease	decrease rate	----variance of the variance---- value	decrease	decrease rate	--figure of merit-- value	--pdf-- behavior	-pdf- slope
desired	random	<0.10	yes	1/sqrt(nps)	<0.10	yes	1/nps	constant	random	>3.00
observed	random	0.00	yes	yes	0.00	yes	yes	constant	random	10.00
passed?	yes	yes	yes	yes	yes	yes	yes	yes	yes	yes

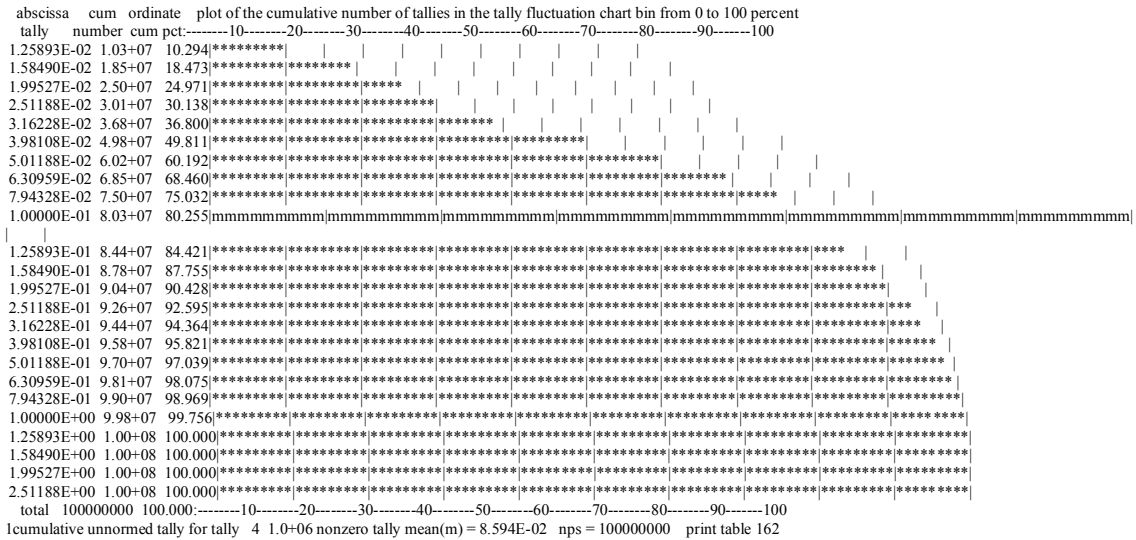
this tally meets the statistical criteria used to form confidence intervals: check the tally fluctuation chart to verify. the results in other bins associated with this tally may not meet these statistical criteria.

estimated asymmetric confidence interval(1,2,3 sigma): 3.4257E-03 to 3.4269E-03; 3.4252E-03 to 3.4274E-03; 3.4246E-03 to 3.4280E-03
 estimated symmetric confidence interval(1,2,3 sigma): 3.4257E-03 to 3.4269E-03; 3.4252E-03 to 3.4274E-03; 3.4246E-03 to 3.4280E-03

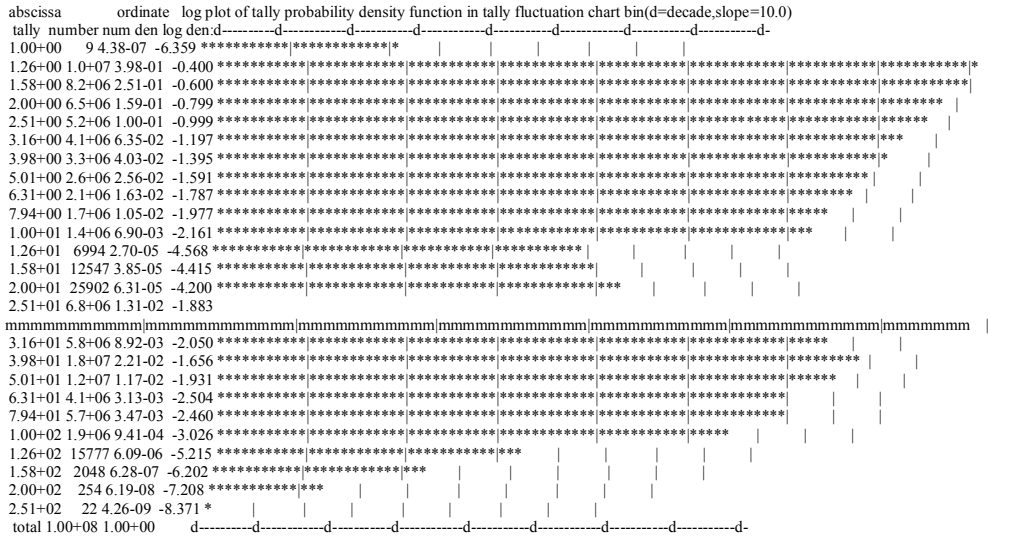
fom = (histories/minute)*(f(x) signal-to-noise ratio)**2 = (3.107E+06)*(6.134E-01)**2 = (3.107E+06)*(3.763E-01) = 1.169E+06
 lunnormed tally density for tally 4 nonzero tally mean(m) = 8.594E-02 nps = 10000000 print table 161



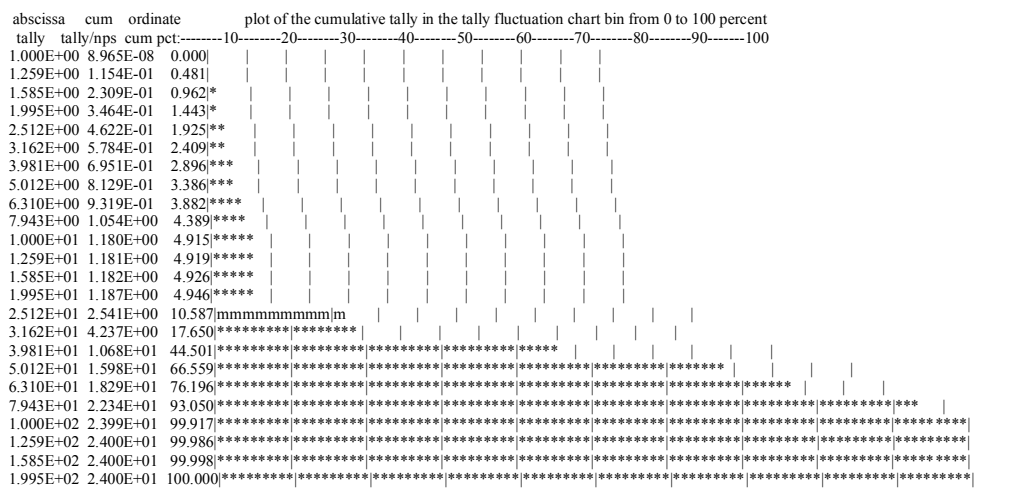
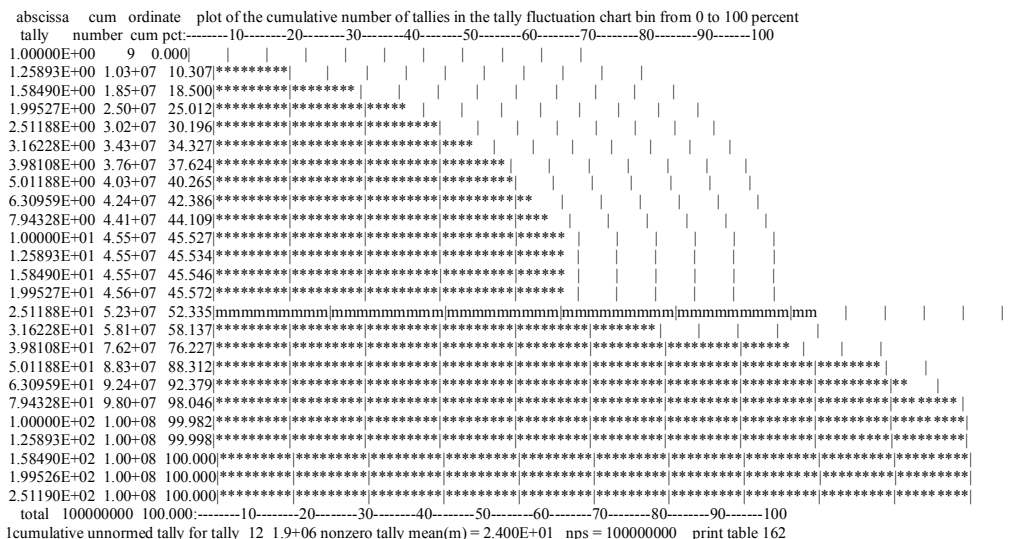
cumulative tally number for tally 4 1.0+06 nonzero tally mean(m) = 8.594E-02 nps = 10000000 print table 162



fom = (histories/minute)*(f(x) signal-to-noise ratio)**2 = (3.107E+06)*(5.673E+11)**2 = (3.107E+06)*(3.219E+23) = 1.000E+30
 lunnormed tally density for tally 12 nonzero tally mean(m) = 2.400E+01 nps = 100000000 print table 161



cumulative tally number for tally 12 1.9+06 nonzero tally mean(m) = 2.400E+01 nps = 100000000 print table 162



```
2.512E+02 2.400E+01 100.000*****|*****|*****|*****|*****|*****|*****|*****|*****|*****|*****|*****
total 2.40049E+01 100.000-----10-----20-----30-----40-----50-----60-----70-----80-----90-----100
tally 14 nps = 100000000
tally type 4 track length estimate of particle flux.
particle(s): neutron
cell a is (10 11 12 13 14 15 16 17 18 19 20 21 22 23 24 25 26)
```

```
volumes
cell: a
4.18879E+03
cell (10 11 12 13 14 15 16 17 18 19 20 21 22 23 24 25 26)
multiplier bin: 1.00000E+00
energy
```

```
5.0000E-01 5.99862E-07 0.0069
1.0000E+00 1.00023E-06 0.0053
2.0000E+00 1.20291E-03 0.0001
4.0000E+00 2.23259E-07 0.0126
2.0000E+01 8.47457E-08 0.0190
total 1.20482E-03 0.0001
```

lanalysis of the results in the tally fluctuation chart bin (tfc) for tally 14 with nps = 100000000 print table 160

```
normed average tally per history = 1.20482E-03 unnormed average tally per history = 5.04674E+00
estimated tally relative error = 0.0001 estimated variance of the variance = 0.0000
relative error from zero tallies = 0.0000 relative error from nonzero scores = 0.0001
```

```
number of nonzero history tallies = 100000000 efficiency for the nonzero tallies = 1.0000
history number of largest tally = 45413412 largest unnormalized history tally = 7.12051E+01
(largest tally)/(average tally) = 1.41091E+01 (largest tally)/(avg nonzero tally) = 1.41091E+01
(confidence interval shift)/mean = 0.0000 shifted confidence interval center = 1.20482E-03
```

if the largest history score sampled so far were to occur on the next history, the tfc bin quantities would change as follows:

estimated quantities	value at nps	value at nps+1	value(nps+1)/value(nps)-1.
mean	1.20482E-03	1.20482E-03	0.000000
relative error	1.27896E-04	1.27896E-04	0.000000
variance of the variance	1.44711E-08	1.44721E-08	0.000072
shifted center	1.20482E-03	1.20482E-03	0.000000
figure of merit	1.89946E+06	1.89946E+06	-0.000001

the estimated slope of the 200 largest tallies starting at 5.00015E+01 appears to be decreasing at least exponentially.
the large score tail of the empirical history score probability density function appears to have no unsampled regions.



```
results of 10 statistical checks for the estimated answer for the tally fluctuation chart (tfc) bin of tally 14

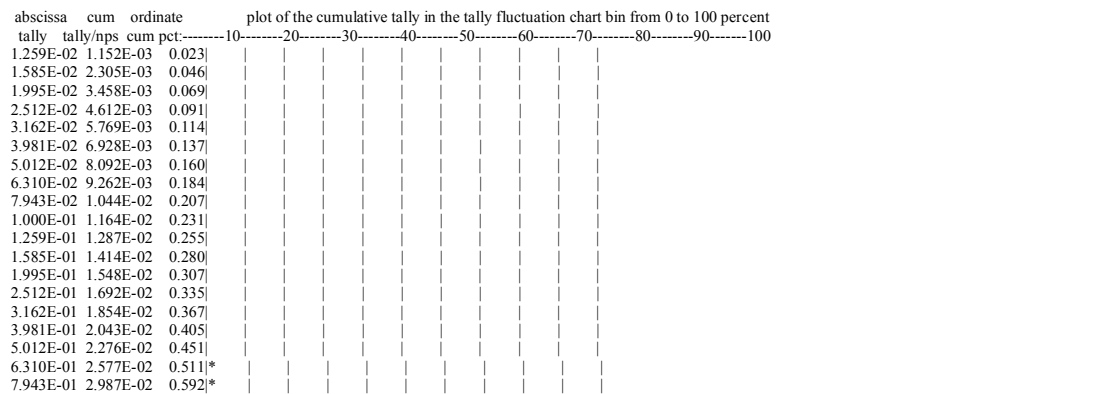
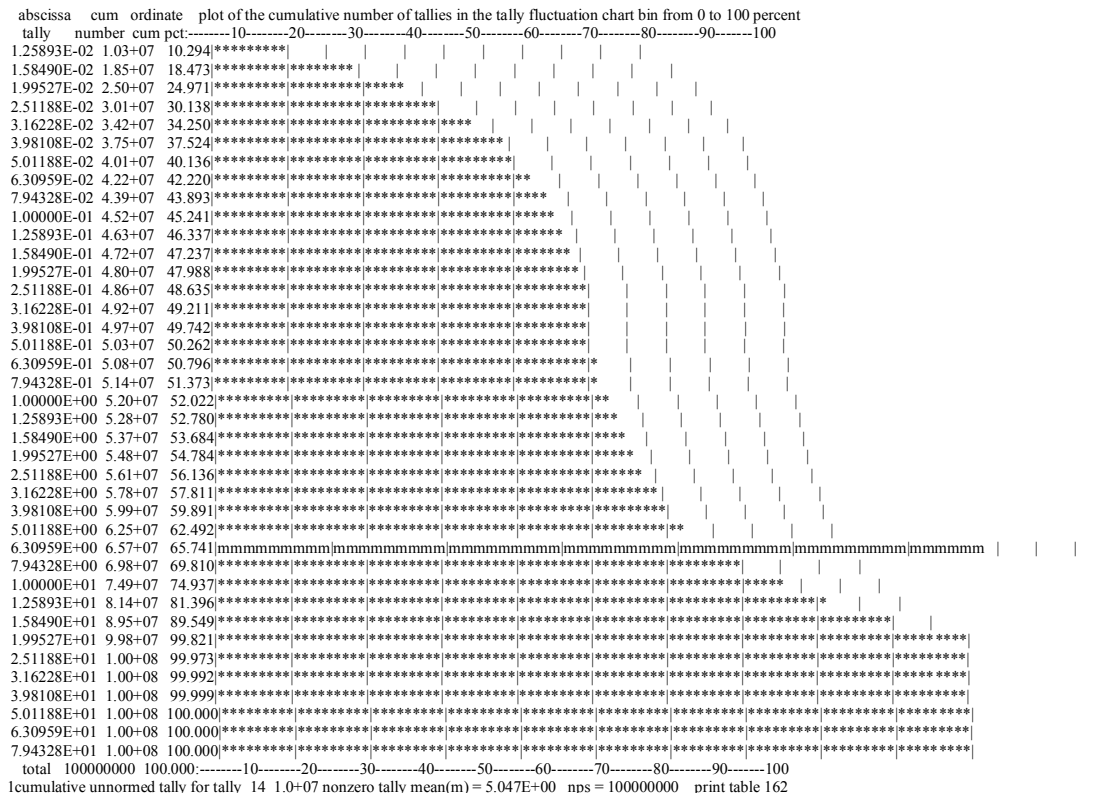
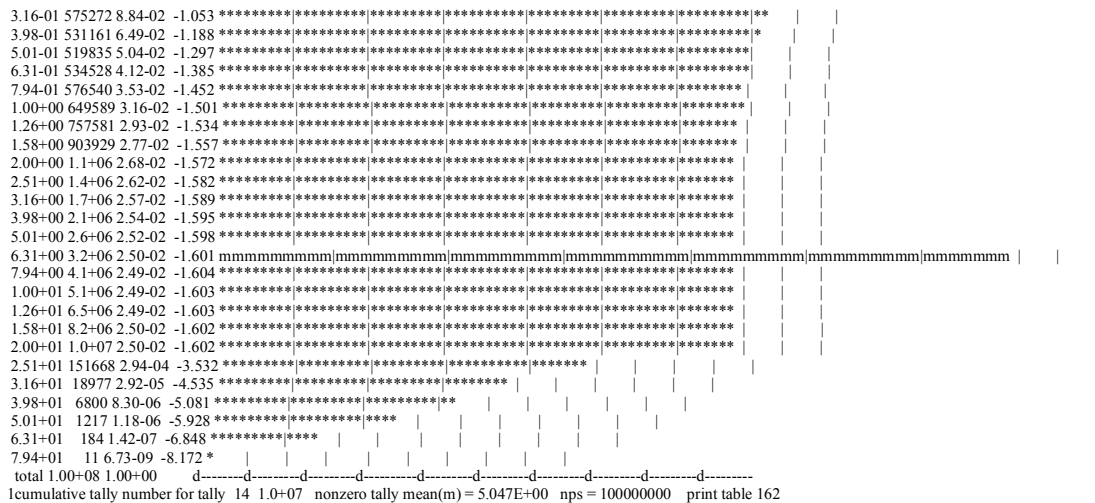
tfc bin --mean-- -----relative error----- ----variance of the variance---- --figure of merit-- -pdf-
behavior behavior value decrease decrease rate value decrease decrease rate value behavior slope
desired random <0.10 yes 1/sqrt(nps) <0.10 yes 1/nps constant random >3.00
observed random 0.00 yes yes 0.00 yes yes constant random 10.00
passed? yes yes yes yes yes yes yes yes yes yes yes
```



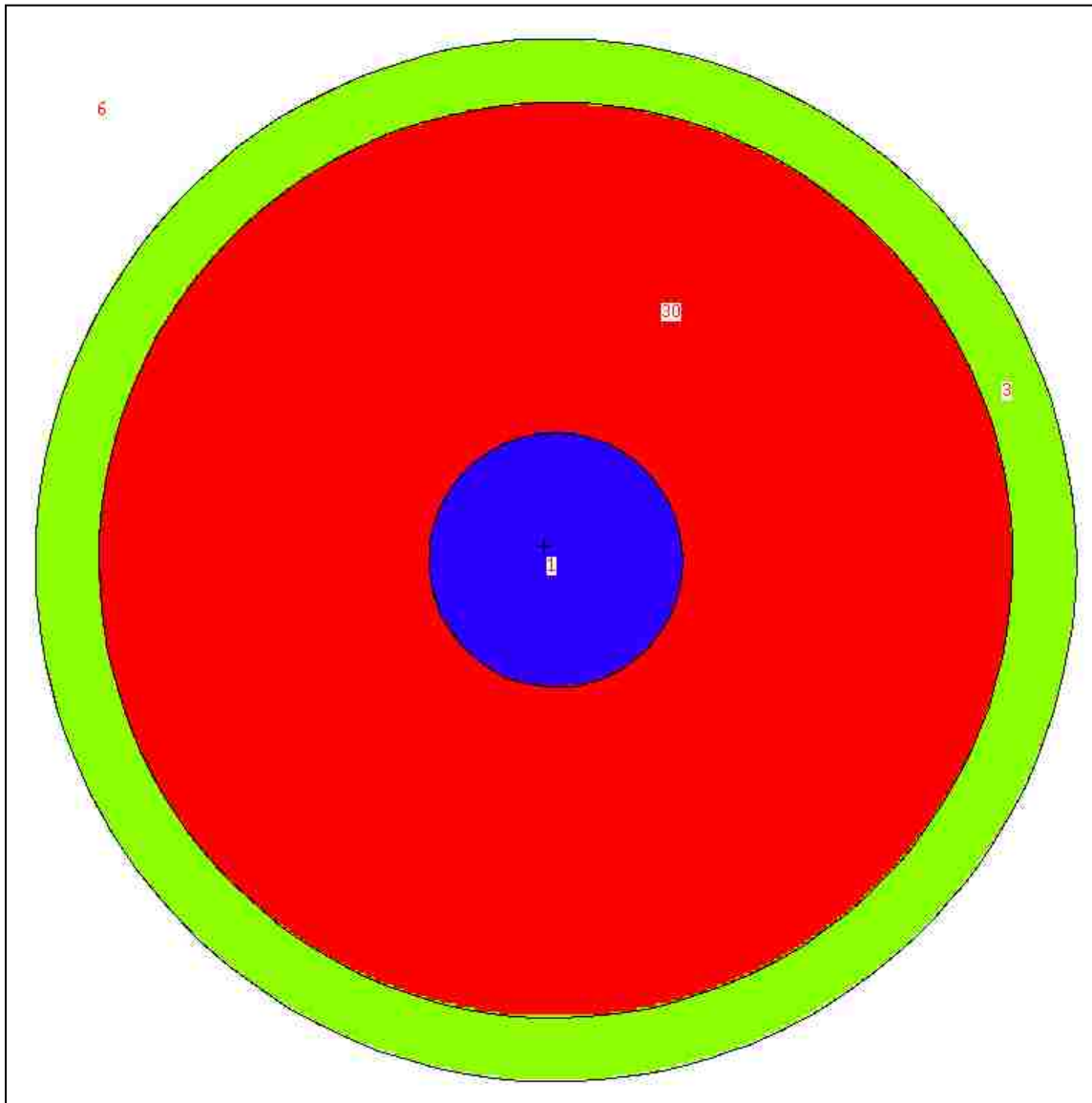
this tally meets the statistical criteria used to form confidence intervals: check the tally fluctuation chart to verify.
the results in other bins associated with this tally may not meet these statistical criteria.
estimated asymmetric confidence interval(1,2,3 sigma): 1.2047E-03 to 1.2050E-03; 1.2045E-03 to 1.2051E-03; 1.2044E-03 to 1.2053E-03
estimated symmetric confidence interval(1,2,3 sigma): 1.2047E-03 to 1.2050E-03; 1.2045E-03 to 1.2051E-03; 1.2044E-03 to 1.2053E-03

```
fom = (histories/minute)*(f(x) signal-to-noise ratio)**2 = (3.107E+06)*( 7.819E-01)**2 = (3.107E+06)*(6.113E-01) = 1.899E+06
lunnormed tally density for tally 14 nonzero tally mean(m) = 5.047E+00 nps = 100000000 print table 161
```

```
abscissa ordinate log plot of tally probability density function in tally fluctuation chart bin(d=decade,slope=10.0)
tally number num den log den d-----d-----d-----d-----d-----d-----d-----d-----d-----d-----d-----
1.26-02 1.0+07 3.98+01 1.599 *****|*****|*****|*****|*****|*****|*****|*****|*****|*****|*****
1.58-02 8.2+06 2.51+01 1.400 *****|*****|*****|*****|*****|*****|*****|*****|*****|*****|*****
2.00-02 6.5+06 1.58+01 1.200 *****|*****|*****|*****|*****|*****|*****|*****|*****|*****|*****
2.51-02 5.2+06 1.00+01 1.000 *****|*****|*****|*****|*****|*****|*****|*****|*****|*****|*****
3.16-02 4.1+06 6.32+00 0.801 *****|*****|*****|*****|*****|*****|*****|*****|*****|*****|*****
3.98-02 3.3+06 4.00+00 0.602 *****|*****|*****|*****|*****|*****|*****|*****|*****|*****|*****
5.01-02 2.6+06 2.53+00 0.404 *****|*****|*****|*****|*****|*****|*****|*****|*****|*****|*****
6.31-02 2.1+06 1.61+00 0.206 *****|*****|*****|*****|*****|*****|*****|*****|*****|*****|*****
7.94-02 1.7+06 1.02+00 0.010 *****|*****|*****|*****|*****|*****|*****|*****|*****|*****|*****
1.00-01 1.3+06 6.56-01 -0.183 *****|*****|*****|*****|*****|*****|*****|*****|*****|*****|*****
1.26-01 1.1+06 4.23-01 -0.374 *****|*****|*****|*****|*****|*****|*****|*****|*****|*****|*****
1.58-01 900138 2.76-01 -0.559 *****|*****|*****|*****|*****|*****|*****|*****|*****|*****|*****
2.00-01 751455 1.83-01 -0.737 *****|*****|*****|*****|*****|*****|*****|*****|*****|*****|*****
2.51-01 646958 1.25-01 -0.902 *****|*****|*****|*****|*****|*****|*****|*****|*****|*****|*****
```

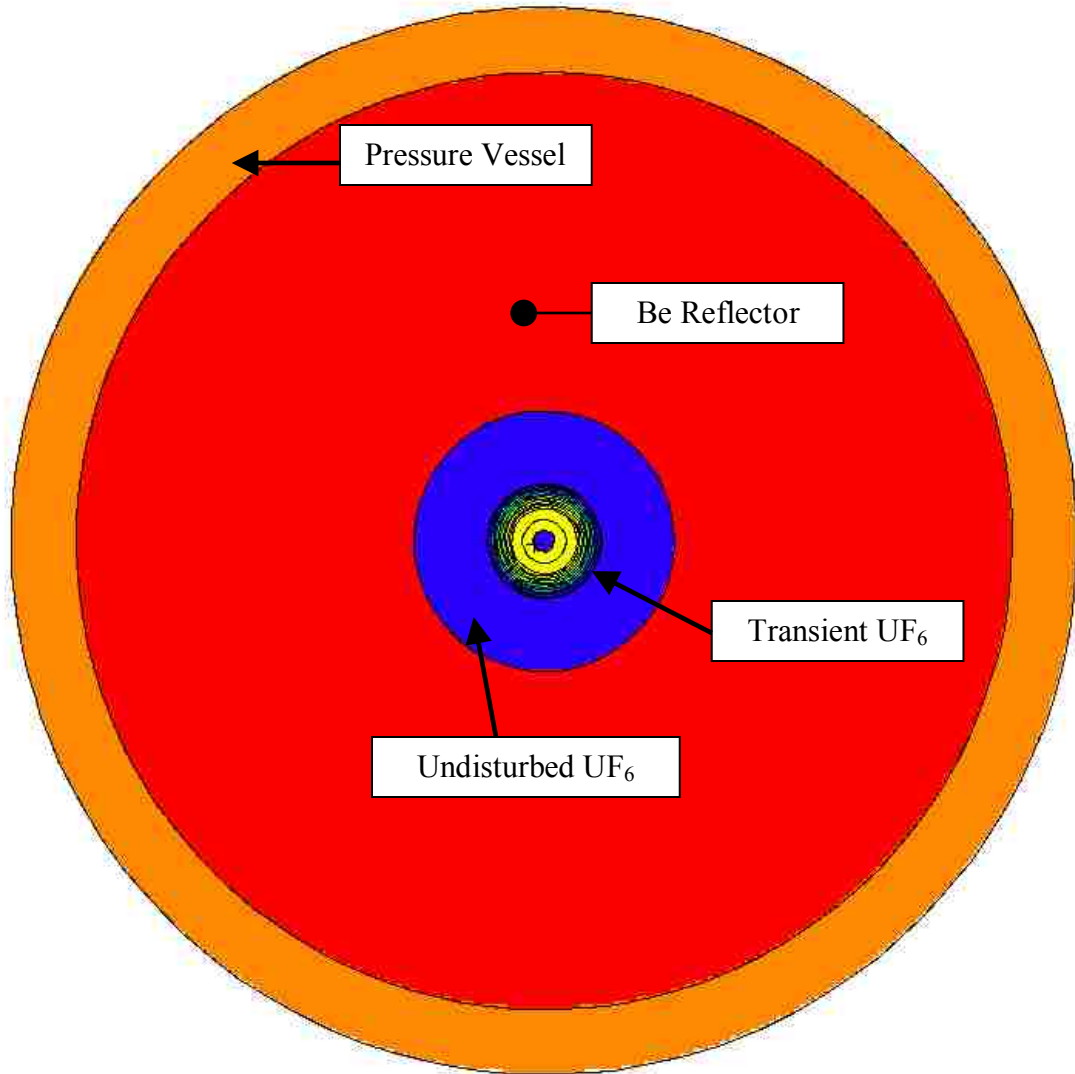
Schematics



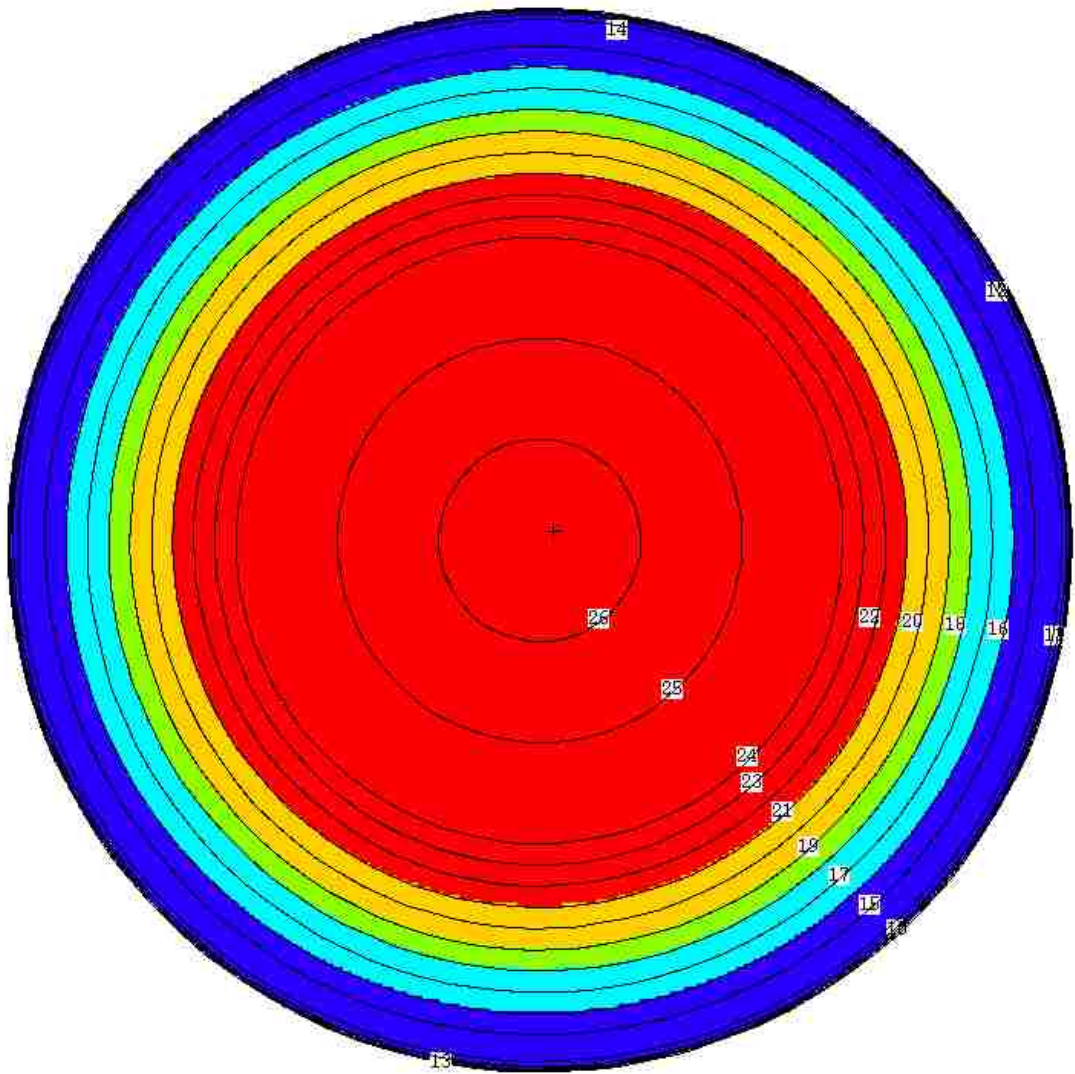
Schematic of Spherical Gaseous Shockwave Reactor

List of Materials and Functions in Spherical Gaseous Shockwave Reactor Design

<i>Numbered Location</i>	<i>Functions</i>	<i>Material</i>	<i>Dimensions</i>
1	Reactor Core	UF ₆ -He Mixture	25cm – Radius
30	Reflector	Beryllium	65cm – Thickness
3	Pressure Vessel	S. Steel AISI 302	12.5cm – Thick
6	Void	Edge of Analysis Area	Infinite



Final Design of the Transient-State Pulsed Spherical Uranium-Hexafluoride Reactor



MCNPX Shockwave Geometry Model Color Coded by Cell Temperature

WORKS CITED

- Anderson, John D. *Modern Compressible Flow: With Historical Perspective*. 3rd Edition. McGraw Hill, 2002.
- Beer, Ferdinand P., et al. *Mechanics of Materials*. Fifth Edition. McGraw Hill, 2009.
- Boles, Jeremiah. "Personal Photographic Record." Undisclosed Location, 2005.
- Brady, Phil, et al. *Assessment of UF₆ Equation of State*. Lawrence Livermore National Laboratory, 2009. Online Access: LLNL-TR-410694.
- Brookhaven National Laboratory. *National Nuclear Data Center*. Uphausen, n.d. 2013. <<http://www.nndc.bnl.gov/>>.
- Cengel, Yunus A. and Michael A. Boles. *Thermodynamics: An Engineering Approach*. Sixth Edition. McGraw Hill, 2008.
- D. B. Pelowitz, ed. *MCNPX User's Manual, Version 2.7.0*. Los Alamos National Laboratory (LA-CP-11-00438), 2011.
- Duderstadt, James J. and Louis J. Hamilton. *Nuclear Reactor Analysis*. John Wiley & Sons, Inc, 1976.
- J. T. Thomas, Ed. "Nuclear Safety Guide/TID-7016/Revision 2,." U.S. Nuclear Regulatory Commission, June 1978.
- Knief, Ronald Allen. *Nuclear Criticality Safety: Theory and Practice*. La Grange Park: American Nuclear Society, 2000.
- Korea Atomic Energy Research Institute (KAERI). *Table of Nuclides*. n.d. 2013. <<http://atom.kaeri.re.kr/index.html>>.
- Krane, Kenneth S. *Introductory Nuclear Physics*. John Wiley & Sons, Inc., 1988.

- Lamarsh, John R and Anthony J. Baratta. *Introduction to Nuclear Engineering*. 3rd Edition. Upper Saddle River: Prentice-Hall, 2001.
- Mourtos, Nikos J. *Moving Shocks*. San Jose State University, n.d.
<<http://www.engr.sjsu.edu/nikos/courses/ME223/pdf/Moving.Shocks.pdf>>.
- Parametric Technology Corporation. "Mathcad 14.0 M020." Massachusetts, 2013.
<www.ptc.com>.
- Podney, Walter N., Harold P. Smith and A. K. Oppenheim. "Generation of a Fissioning Plasma in a Shock Tube." *Physics of Fluids* 1969: I-68 to I-72.
- Taylor, Geoffrey. "The Formation of a Blast Wave by a Very Intense Explosion I. Theoretical Discussion." *Proceedings of the Royal Society of London. Series A. Mathematical and Physical Sciences* 201.1065 (1950): 159-174. Online Access: JSTOR.
- . "The Formation of a Blast Wave by a Very Intense Explosion II. The Atomic Explosion of 1945." *Proceedings of the Royal Society of London. Series A. Mathematical and Physical Sciences* 201.1065 (1950): 175-186. Online Access: JSTOR.
- The MathWorks, Inc. "MATLAB & SIMULINK: Student Version R2010a." 1984-2013.
<www.mathworks.com>.
- X-5 Monte Carlo Team. *MCNP—A General Monte Carlo N-Particle Transport Code, Version 5 - Vol. I: Overview and Theory*. Los Alamos National Laboratory (LA-UR-03-1987), 2003, Revised 2008.

- . *MCNP–A General Monte Carlo N-Particle Transport Code, Version 5 - Volume II: User’s Guide*. Los Alamos National Laboratory (LA-CP-03-0245), 2003, Revised 2008.
- . *MCNP–A General Monte Carlo N-Particle Transport Code, Version 5 - Volume III: Developer’s Guide*. Los Alamos National Laboratory (LA-CP-03-0284), 2003, Revised 2008.

CURRICULUM VITAE

Jeremiah Boles

Las Vegas, Nevada

Phone: 702-683-4141

Email: jeremiah.t.boles@gmail.com

Education:

- 2013 M.S. in Materials and Nuclear Engineering, University of Nevada, Las Vegas
- 2013 Nuclear Criticality Safety Engineering Certificate, Univ. of Nevada, Las Vegas
- 2012 B.S. in Mechanical Engineering, University of Nevada, Las Vegas (Honors)
- 2006 A.A.S. in Ecological Controls, Community College of the Air Force, Maxwell AFB, Al.

Professional and Academic Experience:

2013-Present: Engineer II, Nuclear Safety Associates, N. Carolina

- Nuclear Safety Analyst; Unreviewed Safety Question (USQ) Analyst
- Reviews client requests for changes to nuclear facilities against the DOE approved Facility Safety Basis documents
- Provides impact analysis of the requested changes, including potential impacts to: equipment important-to-safety; analyzed accident scenarios; potential inadequacies of safety analysis (PISA)
- DOE Q Clearance

2012-2013: Graduate Research Assistant, University of Nevada, Las Vegas

- Evaluated material inclusions to Advanced Test Reactor Critical located within Idaho National Laboratory (INL) using MCNPX 2.7.0 and MCNP5 with ENDF/B.VII cross-section data libraries
- Formal MCNPX training for proper modeling, convergence, and analysis of effective multiplication factor (k_{eff}) during 2-day training seminar in Eunice, NM, presented by Dr. John Hendricks (Los Alamos National Laboratory)
- Statistically determined theoretical changes in effective multiplication factors (Δk_{eff}) resulting from experimental configuration changes to reactor and Aluminum experiment apparatus
- Utilized SCALE 6.1 with KENO6 and TSUNAMI-3D modules with ENDF/B.VII cross-section data libraries for study of spent fuel cross-sections in HI-STAR 100 Storage Casks for verification of Nuclear Regulatory Commission/American Nuclear Society storage requirements
- Analyzed isotope variance and sensitivity data to determine biases and uncertainties in k_{eff} and Uranium cross-section data

2010-2011: Undergraduate Research Assistant, University of Nevada, Las Vegas

- Performed extensive research on the feasibility and hazards of long-term extra-planetary habitability as part of a multi-disciplinary team
- Proposed possible solutions to interstellar radiation hazards based on safety to personnel, cost, transport effectiveness, and currently available products

2000-2006: United States Air Force

- Squadron Safety Manager (Interim) for over 400 personnel. Duties included providing Command Staff with status briefings, personnel training sessions, filing incident reports, and official inspections
- Certified for Emergency Response to Hazardous Materials Incidents (2001). Successfully completed 40 hour US Environmental Protection Agency (165.15) Course (HAZWOPER) presented by Spectra Training
- Member of 820th RED HORSE Sq. Nuclear, Biological, and Chemical (NBC) Response Team. Duties included post-attack camp survey, identification, and quarantine of NBC-contaminated equipment/assets and unexploded ordnance hazards
- Served as point of contact for guidance and questions relating to proper operations and maintenance of hazardous waste disposal sites, which accumulated used oil, antifreeze, paints, and other petroleum product
- Top Secret (TS-SCI) security clearance

Publications:

- J. Boles, A. McGee, Q. Newell, and C. Sanders, "Uncertainty Evaluation of Reactivity for Long-term Dry Cask Storage," *Proceedings of the Nuclear Criticality Safety Division (NCS D) 2013*, Wilmington, NC, September 29-October 3, 2013.
- Denis Beller, John D. Bess, Darin Lords, Jeremiah Boles, Kimberly Clark, Anthony Santo Domingo, Alex Lui, Jacob Mills, Larry Lakeotes, Craig Jackson, Benjamin Chase, J. Blair Briggs, and Fred Hua, "The UNLV ATRC Criticality Benchmark Experiment Project," *Trans. of the ANS, Vol. 109*, American Nuclear Society, La Grange Park, Illinois, 2013, pp 838-841.
- J. Boles, A. McGee, C. Sanders, and D. Beller, "Uncertainty Evaluation of Reactivity for Long-term Dry Cask Storage," *Trans. of the ANS, Vol. 108*, American Nuclear Society, La Grange Park, Illinois, 2013.

Professional Certifications, Abilities:

- Certified Engineer Intern; State of Nevada – Board of Professional Engineers and Land Surveyors, 2011
- Familiar in MCNP5/MCNPX and SCALE 6.1 with KENO and TSUNAMI modules.
- Proficient with MATLAB, SolidWorks 2011, and MathCAD programs
- Active member of American Nuclear Society and American Society of Mechanical Engineers

Academic Awards and Honors:

- 2012 – Cum Laude; B.S. Mechanical Engineering
- 2010-2011 – Michael Patrick Keller Scholarship Recipient
- 2010 – Tau Beta Pi; Engineering Honor Society
- 2007-2011 – Dean’s Honor List